



March 2023
Report No. 23-038

Maura Healey
Governor

Kim Driscoll
Lieutenant Governor

Gina Fiandaca
MassDOT Secretary & CEO

Uncovering the Root Causes of Truck Rollover Crashes on Ramps

Principal Investigator (s)
Dr. Yuanchang Xie
Dr. Chengbo Ai
University of Massachusetts Lowell
University of Massachusetts Amherst



Research and Technology Transfer Section
MassDOT Office of Transportation Planning



Technical Report Document Page

1. Report No. 23-038	2. Government Accession No. n/a	3. Recipient's Catalog No. n/a	
4. Title and Subtitle Uncovering the Root Causes of Truck Rollover Crashes on Ramps		5. Report Date March 2023	
		6. Performing Organization Code 23-038	
7. Author(s) Yuanchang Xie, Benyuan Liu, Chengbo Ai, Qilei Chen, Zubin Bhuyan, and Vinay Kusupati		8. Performing Organization Report No.	
9. Performing Organization Name and Address University of Massachusetts Lowell 1 University Avenue Lowell, MA 01854		10. Work Unit No. (TRAIS) n/a	
		11. Contract or Grant No. 113772	
12. Sponsoring Agency Name and Address Massachusetts Department of Transportation Office of Transportation Planning 10 Park Plaza, Room 4150 Boston, MA 02116-3969		13. Type of Report and Period Covered Final Report - March 2023 (03/01/2021-03/31/2023)	
		14. Sponsoring Agency Code n/a	
15. Supplementary Notes Derek Krevat — Manager of MPO Activities, MassDOT			
16. Abstract Highway ramps are hotspots of truck rollover crashes. Such crashes often block the entire ramp and cause severe congestion. Understanding the major causes of ramp truck rollovers is critical for developing effective countermeasures. This research utilizes drones to collect ramp traffic videos at seven high-risk ramps and develops an Oriented Mask-RCNN model for vehicle detection and several other algorithms for tracking vehicles, extracting vehicle trajectories, and identifying high-risk events such as unsafe and last-minute lane changes. A thorough review of literature and best practices on reducing ramp truck rollovers is conducted. The narratives of all ramp truck rollovers between January 2015 and February 2022 in Massachusetts are reviewed. The locations and types of traffic signs, slopes, and curve radii of seven identified highway ramps are also obtained and carefully investigated together with the trajectory analysis results. It is found that over 95% of ramp truck rollovers are single-vehicle crashes and speeding is the predominant cause. Based on the analysis, some practical and specific safety improvement recommendations are provided. Drones are proven to be a useful and convenient tool for short-term traffic data collection. The developed vehicle detection and tracking algorithms work well to generate vehicle trajectories and detect high-risk events. The proposed suite of algorithms can also be applied to trajectories generated by other sensors such as radar. Overall, the proposed trajectory-based safety analysis approach provides important inputs for understanding driver behavior at/near highway ramps, and it can be used as an effective tool for road safety audits.			
17. Key Word Truck Rollover, Ramp, Highway, Image Processing, Deep Learning, Trajectory, Clustering		18. Distribution Statement Unrestricted	
19. Security Classif. (of this report) Unclassified	20. Security Classif. (of this page) Unclassified	21. No. of Pages 123	22. Price n/a

Uncovering the Root Causes of Truck Rollover Crashes on Ramps

Submitted by:

Yuanchang Xie¹, Ph.D., P.E., Professor
Vinay Kusupati¹, Graduate Research Assistant
Benyuan Liu², Ph.D., Professor
Qilei Chen², Postdoctoral Researcher
Zubin Bhuyan², Graduate Research Assistant

¹ Civil and Environmental Engineering

² Computer Science

University of Massachusetts Lowell
Lowell, MA 01854

Chengbo Ai, Ph.D., Assistant Professor
University of Massachusetts Amherst
Amherst, MA

Submitted to:

Massachusetts Department of Transportation
Office of Transportation Planning
Ten Park Plaza, Suite 4150
Boston, MA 02116

March 2023

Acknowledgments

Prepared in cooperation with the Massachusetts Department of Transportation (MassDOT), Office of Transportation Planning, and the United States Department of Transportation, Federal Highway Administration (FHWA).

The project team would like to thank the MassDOT for providing financial support to this research. Also, the team would like to thank Ed Gomez, Robin Grace, and Jason Benoit for providing support with the drone traffic video data collection and Dakota DelSignore for providing valuable comments on the draft report.

Finally, we would like to express our gratitude to Dr. Xiaopeng Li and Dr. Rachel James for sharing the drone videos collected through the Video-Based Intelligent Road Traffic Universal Analysis Tool (VIRTUAL) project.

Disclaimer

The contents of this report reflect the views of the authors, who are responsible for the facts and the accuracy of the data presented herein. The contents do not necessarily reflect the official views or policies of the MassDOT or the FHWA. This report does not constitute a standard, specification, or regulation. Also, mentions of trade names or commercial products do not constitute endorsement or recommendation for use.

Executive Summary

This study of Uncovering the Root Causes to Truck Rollover Crashes on Ramps, was undertaken as part of the Massachusetts Department of Transportation Research Program. This program is funded with Federal Highway Administration (FHWA) State Planning and Research (SPR) funds. Through this program, applied research is conducted on topics of importance to the Commonwealth of Massachusetts transportation agencies.

Rollover crashes involving heavy trucks usually occur on highways and tend to have significant and large-scale impacts on traffic operations. The sharp horizontal curves of highway ramps make them hotspots of truck rollover crashes. Such crashes often block the entire ramp and cause severe congestion. Understanding the major causes of ramp truck rollover crashes is critical for developing effective crash risk mitigation strategies and improving highway safety and system reliability.

This research takes both theoretical and applied approaches to address the ramp heavy truck rollover problem. It utilizes drones to collect ramp traffic video data and develops advanced deep learning-based computer vision algorithms to extract vehicle trajectories from the videos. Specifically, an Oriented Mask-RCNN model is developed for vehicle detection, and the Savitzky–Golay filter is adopted for vehicle tracking. Additional algorithms are developed to analyze the extracted vehicle trajectories to identify high-risk events (and use them as surrogate safety measures) such as unsafe and last-minute lane changes, approaching too fast, and following other vehicles too closely. Clustering analysis has also been performed on the trajectory data aiming to automatically identify abnormal trajectories.

From the practical perspective, this study conducts a thorough review of literature and best practices, such as traffic signage and pavement markings, on reducing highway ramp truck rollovers. The narratives of all ramp truck rollover crashes between January 2015 and February 2022 in Massachusetts are manually reviewed. The locations and types of traffic signs, slopes, and curve radii of seven identified highway ramps are also obtained and carefully investigated together with the above trajectory analysis results. Based on the analysis, some practical and specific safety improvement recommendations are provided for each site to the Massachusetts Department of Transportation (MassDOT).

According to the crash data analyzed for the above-described period, it is found that over 95% of ramp heavy truck rollovers are single-vehicle crashes. Speeding is a predominant reason for such crashes and accounts for about 56% of all rollovers. Various pavement markings and dynamic traffic warning signs have been the two most widely used strategies for reducing vehicle speeds on horizontal curves (including ramps). However, there has been a lack of thorough investigation of the effectiveness of such strategies using field data. Many of the evaluation studies were based on driving simulation.

Drones are a very useful and handy tool for short-term traffic data collection. It can cover a larger area than roadside cameras due to its height and can be deployed quickly. For long-term

data collection to cover various weather and lighting conditions, emerging high-definition radar sensors might be a better choice.

The developed deep-learning-based vehicle detection and tracking algorithms work very well. Some high-risk events have been successfully detected based on the generated vehicle trajectories. The proposed trajectory analysis methods such as clustering and t-SNE diagrams can potentially be applied to trajectories generated by other sensors such as radar. Overall, the proposed trajectory-based safety analysis approach provides important inputs for understanding driver behavior at/near highway ramps, and it can be used as an effective tool for road safety audits.

Table of Contents

Technical Report Document Page	i
Acknowledgments.....	v
Disclaimer	v
Executive Summary	vii
Table of Contents.....	ix
List of Tables	xi
List of Figures	xiii
List of Acronyms	xvii
1.0 Introduction.....	1
2.0 Review of Literature and Best Practices	3
2.1. Rollover Warning Signs for Trucks	3
2.2. Other Warning Signs.....	5
2.3. Pavement Markings	9
2.4. Other Ramp Safety Improvement Strategies	19
2.5. Truck Rollover Crash Data and Risk Modeling	19
2.6. Discussion.....	20
3.0 Site Selection and Data Collection	21
3.1. Initial Data Collection Sites	21
3.2. Summary of Initial Data Collection Efforts.....	22
3.3. Discussion.....	25
3.4. New Data Collection Sites.....	26
3.4.1. Ramp 3: West Springfield.....	26
3.4.2. Ramp 4: New Bedford	27
3.4.3. Ramps 5 and 6: Freetown North and South	28
3.4.4. Ramp 7: Sturbridge	30
3.5. Summary of Additional Data Collection Efforts	31
4.0 Analysis of Truck Rollover Crashes	33
4.1. Query Ramp Truck Rollovers.....	33
4.2. Distributions of Ramp Truck Rollovers.....	34
4.3. Main Causes of Ramp Truck Rollovers.....	39
4.4. Discussion.....	40
5.0 Vehicle Detection and Tracking from Drone Videos	41

5.1 Vehicle Detection from Aerial Images	41
5.2 Related Work	42
5.2.1 Aerial Image Datasets	42
5.2.2 Rotated Object Detection	42
5.3 Methodology	43
5.4 Dataset.....	45
5.5 Evaluation	47
6.0 Vehicle Trajectory Processing and Analysis	51
6.1 Vehicle Tracking and Trajectory Smoothing.....	51
6.2 Speed Estimation	52
6.3 Validating the Estimated Speed Results	54
6.4 Detecting High-Risk Events	55
6.5 Visualizing Risky Events using t-SNE	60
6.6 Vehicle Speed Profile Clustering Analysis.....	64
7.0 Detailed Site Analysis and Recommendations	69
7.1 Andover Site	69
7.2 Auburn/Worcester Site.....	71
7.3 Freetown North and South.....	73
7.3.1 Freetown North	74
7.3.2 Freetown South	76
7.4 West Springfield	78
7.5 New Bedford.....	81
7.6 Sturbridge.....	82
8.0 Conclusions and Discussion	89
9.0 References.....	91
Appendix A: Average Speed Profile Results.....	97

List of Tables

Table 1. Innovative pavement markings for speed control.....	13
Table 2. Video data collection efforts at the 5 new ramps.....	32
Table 3. Heavy truck ramp rollover crashes between 1/1/2015 and 2/2/2022 on major routes	34
Table 4. Detailed locations of heavy truck ramp rollover crashes.....	34
Table 5. Rollover distribution based on hour and day	37
Table 6. Rollover distribution based on day and month	37
Table 7. Rollover distribution based on hour and month.....	38
Table 8. Video datasets collected from 9 locations in Massachusetts	46
Table 9. Vehicle types over training, validation, and testing sets after data augmentation.....	46
Table 10. Performance of models trained and evaluated with OBB ground truth.....	47
Table 11. Locations and the travel distance for average speed calculation	54
Table 12. Observed traffic volumes at the selected ramps	69
Table 13. Risky events observed at the Andover site	70
Table 14. Risky events observed at the Auburn/Worcester site	72
Table 15. Risky events observed at the Freetown North site.....	75
Table 16. Risky events observed at the Freetown South site.....	76
Table 17. Risky events observed at West Springfield North and South.....	80

This page left blank intentionally.

List of Figures

Figure 1. A speeding truck activates the sign	4
Figure 2. Proposed dual-advisory speed signs	5
Figure 3. Forward-mounted vs. side-mounted DSFS	6
Figure 4. Dynamic speed feedback signs tested	6
Figure 5. Dynamic speed feedback signs with advisory speed panel	7
Figure 6. Applications of DSFS in the US.....	7
Figure 7. Two types of DSFS	8
Figure 8. Application of DSFS in Oregon	8
Figure 9. Narrow-lane pavement markings for ramp entrance (a) old markings and (b) new markings.....	9
Figure 10. Slow-down pavement markings on two-lane rural highways in Pennsylvania.....	10
Figure 11. Converging Chevron pavement markings in Georgia	10
Figure 12. Reverse linear perspective markings in China	11
Figure 13. Peripheral transverse pavement marking treatment on I-690 in Syracuse, New York	11
Figure 14. New York site on I-690	12
Figure 15. First data collection site at the interchange of I-495 and I-93 in Andover, MA	21
Figure 16. Second data collection site on Massachusetts Turnpike Near Exit 10 in Auburn, MA	22
Figure 17. Comparison of slanted and top-down views in Andover, MA	23
Figure 18. Top-down view captured by thermal camera at 400 ft in Andover, MA	24
Figure 19. Sample of the Data Collected from Auburn, MA.....	24
Figure 20. Sample traffic videos from Mass511 website	25
Figure 21. Ramp 3 in West Springfield MA (Data collected on June 6, 2022).....	26
Figure 22. Ramp 3 connecting I90W to I91N.....	27
Figure 23. Ramp 4 in New Bedford MA (Data collected on June 14, 2022)	28
Figure 24. Ramp 4 connecting 140S to I195W.....	28
Figure 25. Ramps 5 and 6 in Freetown, MA (Data collected on June 13, 2022).....	29
Figure 26. Ramps 5 and 6 connecting Route 24 to Route 79	29
Figure 27. Ramp 4 in Sturbridge, MA (Data collected on June 21, 2022)	30
Figure 28. Ramp 4 connecting 140S to I195W.....	30
Figure 29. Sample images from the new ramps.....	31
Figure 30. Locations of heavy truck ramp rollover crashes between 1/1/2015 and 2/2/2022	33
Figure 31. Detailed locations of ramp truck rollover crashes	35
Figure 32. Distribution of ramp truck rollovers by day of week	35
Figure 33. Distribution of ramp truck rollovers by time of day.....	36
Figure 34. Distribution of ramp truck rollovers by month	36
Figure 35. Traffic volumes at counting station 6228 on I-95 southbound.....	38
Figure 36. Traffic volumes at counting station 5016 on I-495 for both directions.....	39
Figure 37. Main causes of heavy truck ramp rollover crashes	40
Figure 38. Two instances where OBBs are better suited than HBBs	41
Figure 39. High-level representation of the proposed pipeline.....	43
Figure 40. Overview of the Mask R-CNN model used for vehicle detection.....	44

Figure 41. Segmentation masks more accurately measure the distance between large vehicles...	45
Figure 42. Changes of loss function values over the training epochs.....	47
Figure 43. Overall classification accuracy improvements over time.....	48
Figure 44. Detection samples of the MassDOT aerial dataset using Oriented Mask-RCNN.....	48
Figure 45. Sample outputs of the vehicle detection and tracking modules	51
Figure 46. A small car is occluded by an overhead traffic sign at Freetown South	52
Figure 47. Visualization of the changing speed of a truck	53
Figure 48. Sturbridge (top) and West Springfield (bottom) locations	55
Figure 49. A medium-sized vehicle is seen to slow down so that a vehicle in front of it can safely merge onto the freeway.....	57
Figure 50. Weaving area at the West Springfield site (South drone)	58
Figure 51. Unsafe lane changes: (left) Freetown South, (right) West Springfield South.....	59
Figure 52. t-SNE for West Springfield North.....	60
Figure 53. t-SNE for West Springfield South.....	61
Figure 54. t-SNE for West Springfield, old toll gate	61
Figure 55. t-SNE for Freetown North drone	62
Figure 56. t-SNE for Freetown South drone.....	62
Figure 57. t-SNE for Auburn (or Worcester).....	63
Figure 58. t-SNE for Sturbridge.....	63
Figure 59. t-SNE for New Bedford.....	64
Figure 60. t-SNE for Andover	64
Figure 61. Speed profile clustering for West Springfield South.....	65
Figure 62. Clustering result of West Springfield-Old toll gate.....	66
Figure 63. Clustering result of West Springfield-North	66
Figure 64. Clustering result of New Bedford.....	66
Figure 65. Clustering result of Sturbridge	67
Figure 66. Clustering result of Freetown North.....	67
Figure 67. Clustering result of Freetown South.....	67
Figure 68. Clustering result of Andover	68
Figure 69. Clustering result of Auburn	68
Figure 70. Advisory speed sign locations: Andover.....	70
Figure 71. Risky events at the Andover site	71
Figure 72. Advisory Speed sign locations: Auburn/Worcester	72
Figure 73. Risky events at the Auburn/Worcester site	73
Figure 74. Advisory speed sign locations: Freetown North and South	74
Figure 75. Sample risky events at the Freetown North ramp	75
Figure 76. Sample risky events at the Freetown South ramp	76
Figure 77. Example of Advisory Speed Signing for an Exit Ramp.....	77
Figure 78. Horizontal Alignment Sign Selection.....	78
Figure 79. Advisory Speed sign location: West Springfield.....	79
Figure 80. Risky events at the West Springfield North and South sites	80
Figure 81. Advisory speed sign location: New Bedford.....	82
Figure 82. Advisory speed sign location: Sturbridge.....	83
Figure 83. Ramp elevation profile for Andover.....	85
Figure 84. Ramp elevation profile the Auburn/Worcester.....	85
Figure 85. Ramp elevation profile for Freetown North and South	86

Figure 86. Ramp elevation profile for West Springfield-North.....	86
Figure 87. Ramp elevation profile for New Bedford.....	87
Figure 88. Ramp elevation profile for Sturbridge.....	87
Figure 89. Radii for the selected ramps	88
Figure 90. Average speed by category for West Springfield North	97
Figure 91. Average speed by category for West Springfield South	97
Figure 92. Average speed by category for West Springfield Old toll gate.....	98
Figure 93. Average speed by category for Freetown North.....	99
Figure 94. Average speed by category for Freetown South.....	100
Figure 95. Average speed by category for New Bedford	101
Figure 96. Average speed by category for Sturbridge	102
Figure 97. Average speed by category for Andover	103
Figure 98. Average speed by category for Auburn.....	104

This page left blank intentionally.

List of Acronyms

AASHTO	American Association of State Highway and Transportation Officials
AI	Artificial Intelligence
ATRWS	Automated Truck Rollover Warning System
BBAV	Box boundary-aware vectors
CMF	Crash Modification Factors
CNN	Convolutional Neural Networks
DOT	Department of Transportation
DSFS	Dynamic speed feedback signs
FHWA	Federal Highway Administration
FPN	Feature Pyramid Network
GEE	General Estimates System
HBB	Horizontal bounding box
ITS	Intelligent Transportation Systems
LiDAR	Light Detection and Ranging
MAP	Mean Average Precision
MassDOT	Massachusetts Department of Transportation
MUTCD	Manual on Uniform Traffic Control Devices
NMS	Non-Maximum Suppression
NYDOT	New York Department of Transportation
OBB	Oriented bounding box
R-CNN	Region-based Convolutional Neural Networks
RPN	Region Proposal Network
t-SNE	T-Distributed Stochastic Neighbor Embedding
UAV	Unmanned Aerial Vehicle
UMTRI	University of Michigan Transportation Research Institute
USGS	United States Geological Survey
VIRTUAL	Video-Based Intelligent Road Traffic Universal Analysis Tool

This page left blank intentionally.

1.0 Introduction

This study of Uncovering the Root Causes to Truck Rollover Crashes on Ramps, was undertaken as part of the Massachusetts Department of Transportation Research Program. This program is funded with Federal Highway Administration (FHWA) State Planning and Research (SPR) funds. Through this program, applied research is conducted on topics of importance to the Commonwealth of Massachusetts transportation agencies.

In the United States, heavy truck-related crashes accounted for 7.9% of total crashes, but 12.4% of total fatal crashes [1,2] in 2020. Crashes involving heavy trucks usually occur on highways and tend to have significant and large-scale impacts on highway network performance. For example, each heavy truck rollover crash typically takes over 3 hours to clean up. In 2016 alone, truck-related crashes in Massachusetts resulted in losses of over \$22M in terms of delay time and \$1.7M due to emissions and wasted fuel consumption [3].

Nationwide, approximately 11% of total truck crashes were on highway ramps and 44~52% of them involved rollovers [47]. The sharp horizontal curves of highway ramps make them hotspots of truck rollover crashes. Such crashes can block the entire ramp and cause severe congestion. Understanding the major causes of ramp truck rollover crashes is important for developing effective crash risk mitigation strategies and improving highway safety and traffic operational reliability.

This research aims to (1) review literature and best practices on reducing highway ramp truck rollovers; (2) analyze historical ramp truck rollover data in Massachusetts; (3) utilize traffic cameras and advanced video analytics tools to uncover the causes of truck rollovers on highway ramps and derive surrogate safety performance measures; and (4) establish correlations between truck rollovers and Intelligent Transportation Systems (ITS) devices, signage and markings, and roadway design practices, so that the number of ramp truck rollovers can be minimized through the use of systemic low-cost countermeasures identified in this research.

The main innovation of this study is to use Artificial Intelligence (AI) methods to analyze traffic videos and derive surrogate safety measures for improving ramp truck safety. Using historical crash data such as police crash reports to study ramp truck rollovers has limitations, as they cannot cover near-crash events. Since crashes are relatively rare events, being able to include near-crash events is very significant, and this can potentially generate useful data and lead to additional insights into how to prevent ramp truck rollovers. In addition, from crash reports it is difficult to derive objective information such as how drivers behave on a ramp and when they start to decelerate.

The recent advancements in AI for computer vision have inspired many innovative transportation applications, including vehicle counting, tracking, and re-identification. These AI technologies are already very mature and have generated highly accurate results. Such technologies can be naturally applied to detecting near-crash events from traffic videos and further deriving surrogate safety measures. Traffic cameras are widely deployed on state highways. Drones are also getting increasingly popular among state DOTs and have generated a huge amount of video data. These

traffic videos, however, have not been effectively utilized and sometimes not archived. This research field tests the capability of using drones for collecting useful traffic videos to improve safety, particularly ramp truck safety. The developed algorithms can potentially be applied to traffic videos and vehicle trajectories obtained from other sources for safety analysis.

This report is organized as follows: Chapter 2 reviews existing studies and best practices to improve highway ramp truck safety; Chapter 3 describes the study site selection and field data collection efforts; Chapter 4 presents the truck rollover crash history data analysis results; Chapters 5 and 6 describe the developed vehicle detection and tracking algorithms, respectively. Chapter 6 also covers the modeling of the vehicle trajectory data derived from drone videos; Chapter 7 provides detailed and specific recommendations to improve truck safety at the identified highway ramps; and finally, Chapter 8 summarizes the entire study and provides recommendations for future work.

2.0 Review of Literature and Best Practices

Heavy truck rollovers on ramps can be affected by many factors such as drivers, vehicle design and control, roadway design and pavement conditions, traffic signage and control, weather, etc. Based on the review of literature and best practices, most strategies taken by state Departments of Transportation (DOTs) to prevent truck rollovers on ramps are related to speed management using traffic signage and pavement markings. This finding is consistent with the analysis results of truck rollover crash reports (see Chapter 4), which suggest that speeding is the most prevalent contributing factor to ramp truck rollovers. The review results are organized into the following subsections:

- Truck rollover warning signs that are activated by sensors
- Other warning signs such as dual-advisory speed signs and dynamic speed feedback signs (DSFS)
- Various pavement markings to reduce vehicle speeds
- Other ramp safety improvement strategies that mostly require constructions (e.g., realign road geometry, resurface pavement)
- Truck rollover crash data and risk modeling to derive safe operating speeds and estimate rollover risks

2.1. Rollover Warning Signs for Trucks

Several studies [4,5,6,7,8] recommended using dynamic warning signs activated by risk behaviors to prevent heavy truck rollovers. These signs are equipped with sensors to detect vehicle classification and speed. They are activated only when a fast-moving truck is approaching the sign.

Freedman et al. [7] field tested a speed actuated rollover warning sign for heavy trucks at three highway exit ramps. There were standard speed advisory signs at these ramps. At each ramp, they also installed a rollover warning sign with yellow beacons that flash if an approaching heavy truck is traveling faster than the safe speed. They found that the additional sign with flashing beacons significantly reduced the frequencies of heavy trucks traveling more than 5 mph above the safe speed. Bergan et al. [8] also evaluated a prototype Automated Truck Rollover Warning System (ATRWS) installed at three ramps in the Washington DC area. The system consisted of a static truck rollover warning sign with an advisory speed and a dynamic message sign. The dynamic message sign will display “TRUCKS REDUCE SPEED” when activated (i.e., a speeding truck is detected). A sample sign is provided in Figure 1 [5]. It used piezoelectric sensors (weigh-in-motion detectors) and inductive loops to generate vehicle weight and speed information and a radar sensor to detect vehicle height. Based on data collected over a three-year period, they concluded that this ATRWS could effectively reduce truck speeds and rollover accidents. The results of the same study are also reported in [9,10].



Figure 1. A speeding truck activates the sign

Baker et al. [11] compared different truck rollover warning systems. They found that speed-based warning systems generated over 44% more false rollover warnings than weight-based warning systems. Although this finding is interesting, it is expensive and difficult to accurately measure truck weight. Therefore, most truck rollover signs are based on vehicle speeds.

California [12] also tested the ATRWS at a high-risk ramp around 2000. The beacons of the ATRWS were supposed to flash only when heavy vehicles were detected. Due to system maintenance issues, the beacons were flashing continuously for most of the time during the 2-year evaluation period. Therefore, they were unable to conclude whether ATRWS is more effective than continuously flashing beacons. However, they did find that continuously flashing beacons were effective in reducing truck rollover crashes.

In a 1993 FHWA report, Knoblauch and Nitzburg [13] field evaluated a dynamic truck rollover warning sign in Virginia and Maryland. The dynamic sign used continuously flashing beacons. Different from the conclusions in the above studies, they found that the speeds of heavy trucks were not affected by the dynamic warning sign.

Middleton [14] field tested static and dynamic “truck tipping” warning signs. The dynamic warning sign added two flashing lights to the static sign with one above it and one below it. These flashing lights were activated by speeding trucks. These dynamic signs were found to be more effective in reducing truck speeds.

Stevens and Richards [15] proposed that future truck rollover warning systems could be classified into three categories: infrastructure-based, vehicle-based, and integrated vehicle/infrastructure systems. Infrastructure-based systems such as those in [7,8] cannot precisely measure vehicle loads and load distributions to estimate truck rollover risks. Therefore, a conservative speed threshold is often used to activate the warning system. Vehicle-based systems with advanced onboard sensors can better estimate truck rollover risk under different driving conditions. To maximize the benefits of such systems, it is important to provide roadway information (e.g., horizontal curve, pavement conditions) ahead of time so that the systems [16] can generate warnings proactively. Therefore, an integrated system would work the best. The infrastructure subsystem estimates and broadcasts real-time roadway condition data, and the

vehicle subsystem predicts rollover risks and allows drivers sufficient time to react. In a later study [17], Stevens et al. conducted field data collection to demonstrate that such an integrated system is feasible.

2.2. Other Warning Signs

Most of the studies referenced in Section 2.1 were conducted in the 1990s and early 2000s. In 2008, et al. [18] introduced dual-advisory speed signing for freeway-to-freeway connectors to improve safety. They proposed several dual-advisory speed signs as shown in Figure 2 [18] and tested them at five curves in Texas. They found that dual-advisory signs were able to increase the percentages of driver speed compliance for both passenger cars and heavy trucks measured at the middle of a curve.

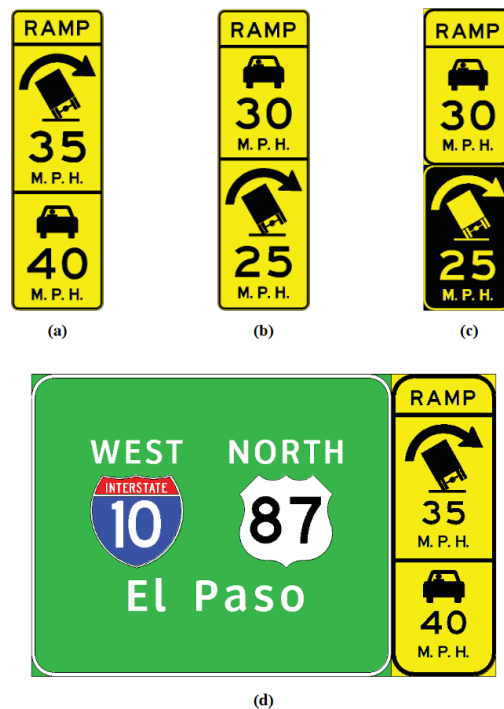


Figure 2. Proposed dual-advisory speed signs

More recently, Gates et al. [19] field tested the impacts of DSFS on driver behavior at six freeway ramps. The evaluated several DSFS configuration factors, including displaying different messages, distance between DSFS and the beginning of the ramp, lateral distance between DSFS and pavement edge, sign dimensions and other physical characteristics, radar activation range, and temporal changes in driver behavior. Overall, they found that:

- DSFS can effectively reduce vehicle speeds. This finding is consistent with what [20] reported.

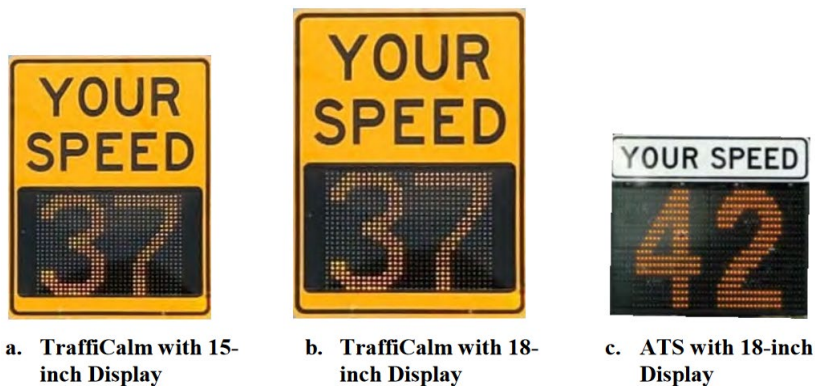
- It is better to activate the DSFS sign when vehicles are within 250 to 400 ft of the beginning of the ramp.
- Side-mounted and forward-mounted signs (Figure 3) [19] gave similar speed reduction results.
- 15-inch and 18-inch display panels (Figure 4) [19] generated similar speed reduction results. Including an advisory speed panel (Figure 5) [19] did not result in any differences.
- Displaying the measured speed and a “SLOW DOWN” message alternately appeared to be the most effective.
- The impacts of DSFS on driver behavior appeared to be consistent during the 14-month evaluation period (did not reduce over time).



(a) forward mounted

(b) side mounted

Figure 3. Forward-mounted vs. side-mounted DSFS



a. TrafficCalm with 15-inch Display

b. TrafficCalm with 18-inch Display

c. ATS with 18-inch Display

Figure 4. Dynamic speed feedback signs tested



Figure 5. Dynamic speed feedback signs with advisory speed panel

Gates et al. also surveyed state DOTs regarding their practices of using DSFS for highway curves and the results are shown in Figure 6 [19].

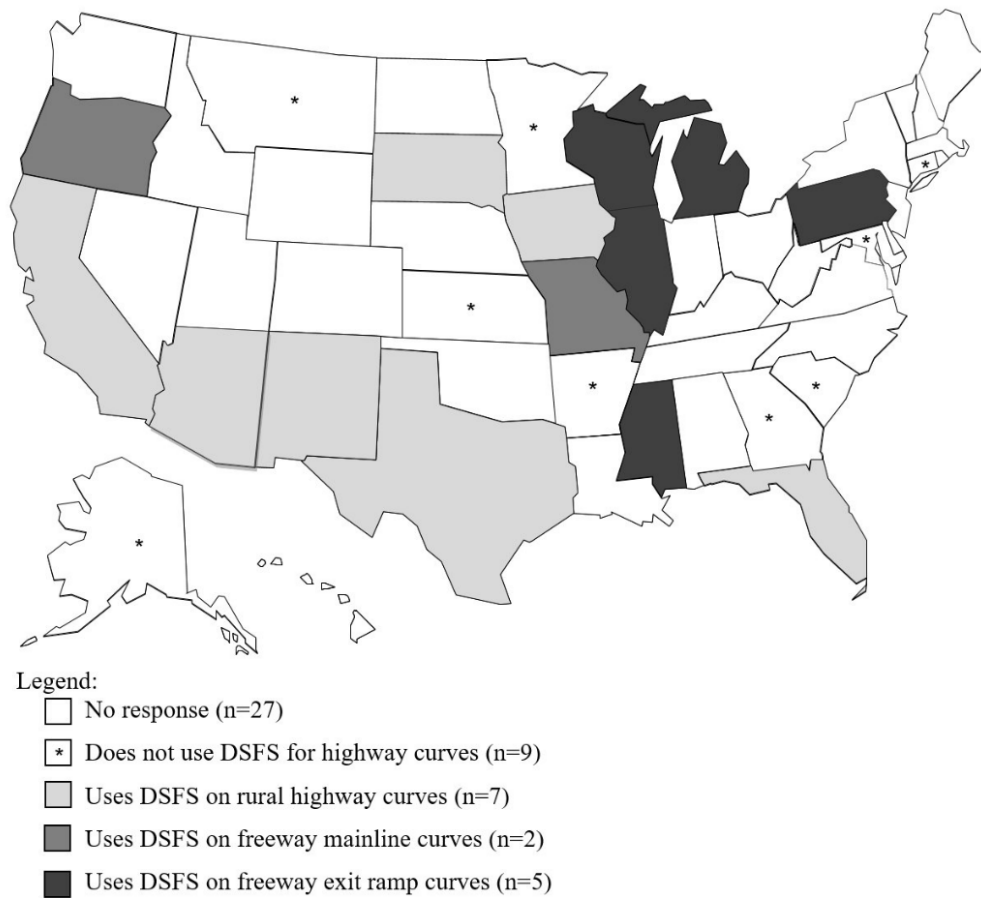


Figure 6. Applications of DSFS in the US

Hallmark et al. [21] evaluated DSFS on rural horizontal curves and developed crash modification factors for DSFS. Although this study is not specifically for ramps and heavy truck rollovers, the results are still relevant and are thus included in our literature review. They evaluated the following two signs shown in Figure 7 [21] at 22 sites in 7 states. The signs were activated (i.e., flashing yellow light or displaying speed) only when a vehicle's speed was greater than the 50th percentile speed for the site. They concluded that installing DSFS can reduce crashes by 5~7%.



Figure 7. Two types of DSFS

Monsere et al. [22] also evaluated DSFS at two highway horizontal curves in Oregon. Prior to installing the DSFS, the two sites had an advisory speed sign with four continuously flashing beacons (Figure 8a) [22]. They added a speed feedback sign, which was activated by speeds measured using a radar sensor (Figure 8b) [22]. The DSFS was found to reduce vehicle speed by 2~3 mph. This seems to suggest that continuous flashing beacons are not as effective as speed activated message signs. It would be interesting to further compare continuous flashing beacons and beacons activated by speed at more sites. A limitation of this study was that data was collected over only 7 days (4 before the installation and 3 after).



Figure 8. Application of DSFS in Oregon

2.3. Pavement Markings

Retting et al. [23] proposed narrow-lane pavement markings for ramp entrance, which make the entrance look narrower than it actually is. Figure 9(b) is an example of the proposed pavement markings. The “narrow” impression may prompt drivers to slow down. The painted area provides a buffer zone or safety margin to drivers in case they could not strictly follow the narrowed travel lane. These narrow-lane pavement markings were tested at four locations in New York and Virginia. Data from the New York site (Figure 9 [23]) and two Virginia sites showed statistically significant decreases in speed. However, the speed reductions were considered minor (less than 2 mph). The third Virginia site showed no difference. Unlike most other pavement markings, in this case faster vehicles did not slow down more than the slower vehicles and the standard deviation was unchanged or increased depending on the location.

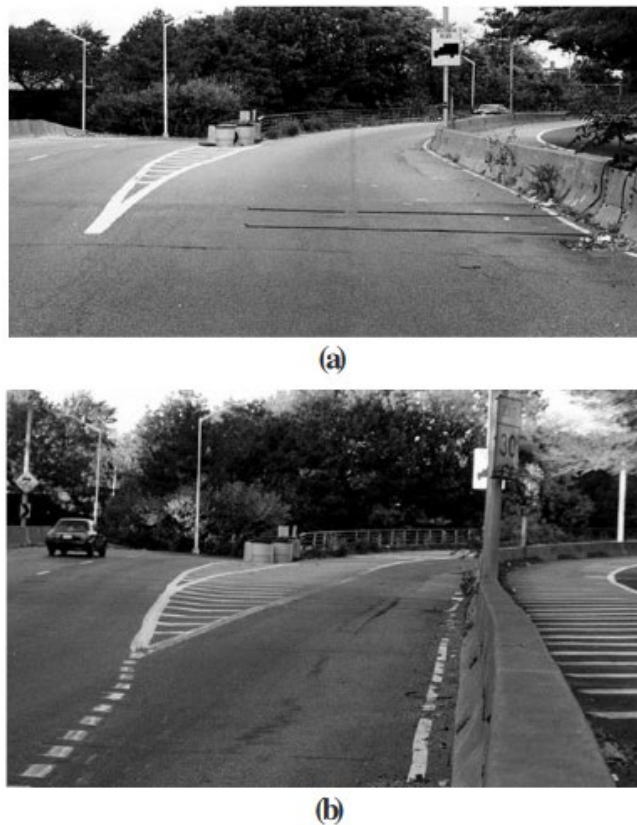


Figure 9. Narrow-lane pavement markings for ramp entrance (a) old markings and (b) new markings

Wood and Donnell [24] evaluated slow-down horizontal curve pavement markings (as shown in Figure 10 [24]) based on the data from 263 treatment sites on two-lane rural highways in Pennsylvania. They derived crash modification factors for total, fatal plus injury, run-off-road, nighttime, nighttime run-off-road, and nighttime fatal plus injury crashes. These CMFs were in the range of 0.65 to 0.77.



Figure 10. Slow-down pavement markings on two-lane rural highways in Pennsylvania

Hunter et al. [25] tested the converging Chevron markings (see Figure 11 [25]) at two freeway ramps in Georgia. They concluded that the speed reduction effect reduced over time. Nine months after the installation, the speed reduction benefit was less than 1~2 mph. Drakopoulos and Vergou [26] also evaluated Chevron markings at a ramp in Wisconsin. Based on the data collected 20 months after the markings were installed, they found the 85th percentile speed of this ramp to be 17 mph lower. Out of the 17 mph reduction, they estimated that approximately 3 mph were due to an increase in traffic volume. This finding is very different from what the Georgia study [25] suggested.



Figure 11. Converging Chevron pavement markings in Georgia

Ding and Jiao [27] evaluated the reverse linear perspective markings at two freeway sites in China, with one of the sites on a horizontal curve as shown in Figure 12 [27]. They collected speed and time and distance headways one day, four months, one year, two years, and three years after the installation. It was found that within one year the speed reduction effect was less than 1.5 mph, which is consistent with what Hunter et al. [25] reported. It is unclear whether the decreased effects were caused by the reduced reflectivity of pavement markings over time.

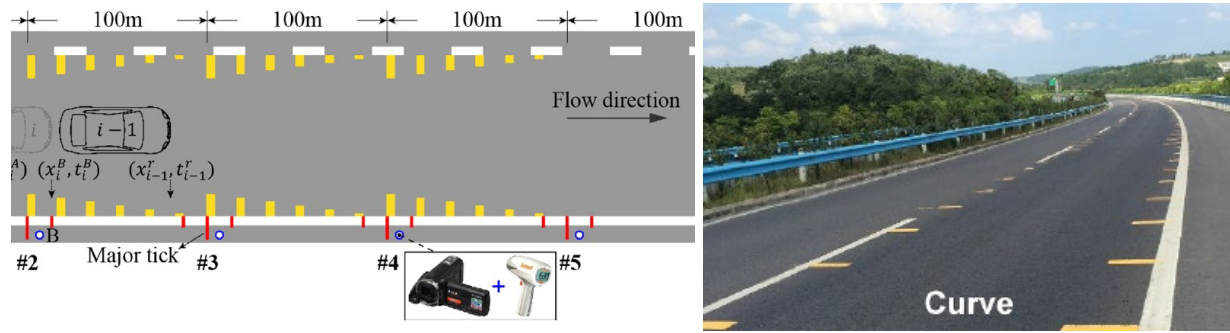


Figure 12. Reverse linear perspective markings in China

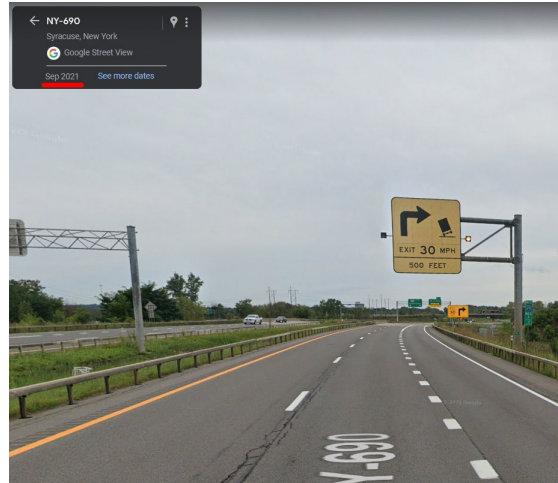
Katz [28] evaluated peripheral transverse pavement markings at three sites in New York (Figure 13 [28]), Texas, and Mississippi. Inconsistent results were obtained from the three sites, suggesting that other factors such as pavement color and driver familiarity with the site may affect the performance of pavement markings. Interestingly, Katz's study [28] was published in 2004. Google Street View (Figure 14) shows that the same New York site has been using a warning sign with flashing yellow beacons since 2007. It is difficult to tell from Google Street View whether the yellow beacons are continuously flashing or activated only by speeding trucks. However, Figure 14 may suggest that NYDOT favors the overhead warning sign over the peripheral transverse pavement marking treatment.



Figure 13. Peripheral transverse pavement marking treatment on I-690 in Syracuse, New York



(a) October 2007





(b) September 2021

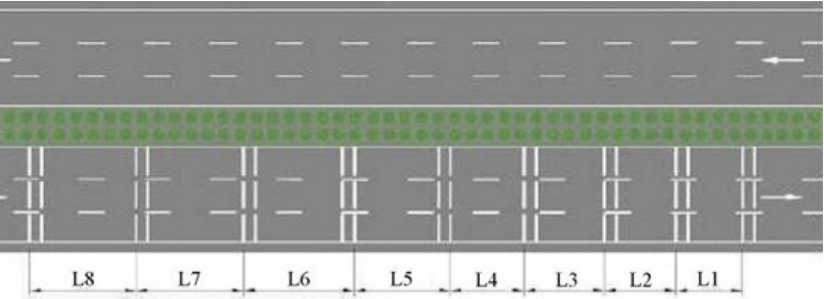
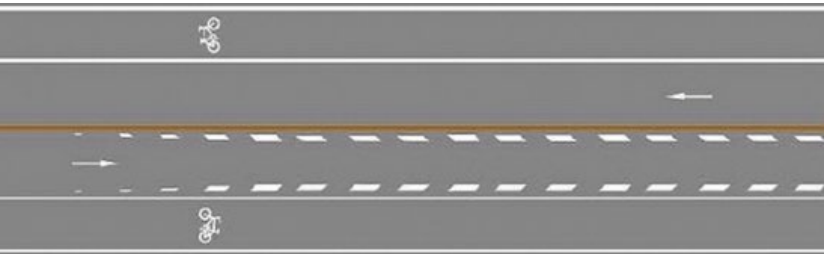
Figure 14. New York site on I-690


Source: I-690W Exit #2, Syracuse, New York; digital image, October 2007 and September 2021, “Street View,” Google Maps (<http://www.googlemaps.com>: accessed 1 January 2023)

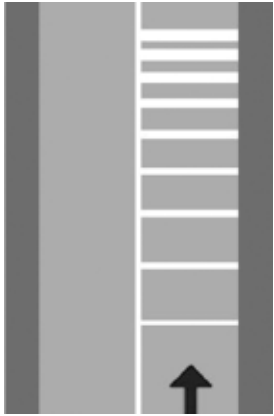
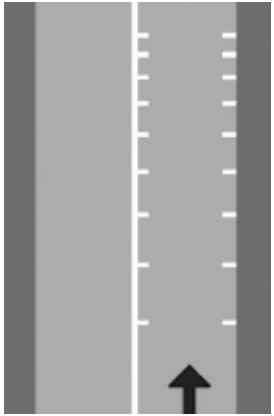
Many other pavement markings have been either field tested or evaluated using a driving simulator. These markings are summarized in Table 1. Much of the information in this table is based on the study by Hussain et al. [29].

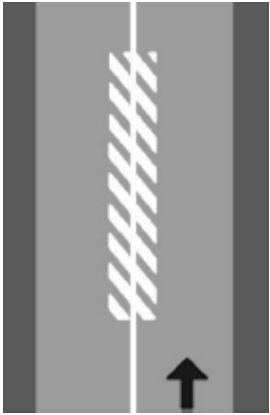
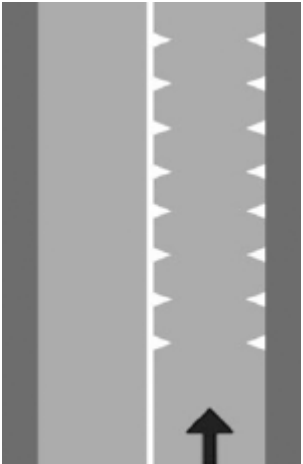
Table 1. Innovative pavement markings for speed control

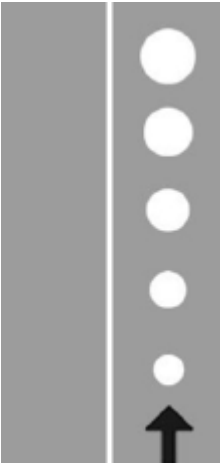
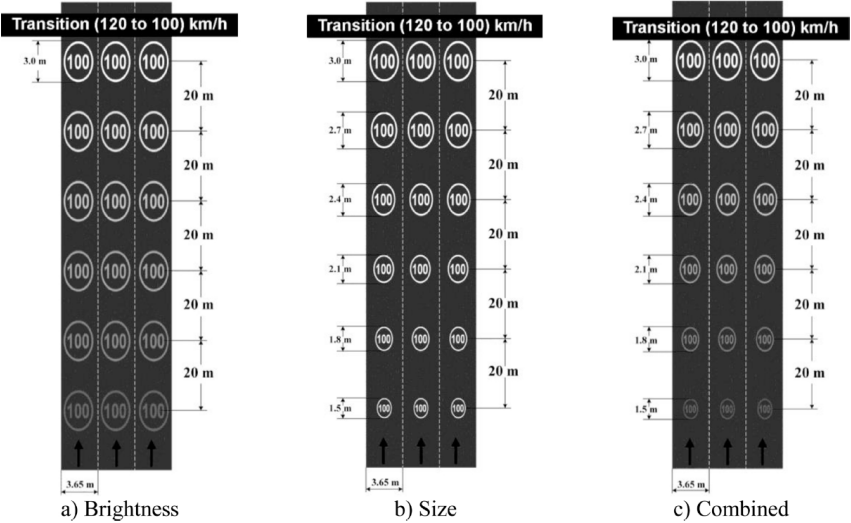
ID	Pavement markings evaluated	Studies	Findings
1	 <p>Herringbone Pattern 1 [30]</p>	<p>Zhao et al. [30] used a driving simulator</p> <p>Guo et al. [31] used field data</p>	<p>Speed reduction results depended on the radius of a curve and were inconsistent.</p> <p>Significantly reduced vehicle speed and speed violations before pedestrian crosswalks.</p>
2	 <p>Herringbone Pattern 2 [32]</p>	<p>Ariën et al. [32] used a driving simulator</p>	<p>Resulted in significant speed reductions into the curve, but not at the beginning of the curve. They compared this marking with marking #5 and recommended marking #5.</p>

ID	Pavement markings evaluated	Studies	Findings
3	 <p data-bbox="394 649 1003 682">Double transverse optical bars with equal width [33]</p>	Ding et al. [33] used a driving simulator	Significantly reduced speed.
4	 <p data-bbox="394 1128 1003 1161">Herringbone Pattern 3 (Gradually increasing size) [33]</p>	Ding et al. [33] used a driving simulator	Had minor and insignificant impacts on speed and driver behavior.

ID	Pavement markings evaluated	Studies	Findings
5	 <p>Transverse optical bars with equal width [29,32]</p>	<p>Ariën et al. [32] used a driving simulator</p> <p>Godley et al [34] used a driving simulator</p> <p>Maroney and Dewar [35] used field data</p> <p>Matírnez et al. [36] based on field data</p>	<p>Resulted in earlier and more stable speed reduction than the herringbone pattern 2 markings shown above.</p> <p>Considered constant and reducing space between bars and found no difference in effect. Found #5 to be more effective than #7.</p> <p>Significantly reduced speed violations but the effect disappeared after 3 weeks.</p> <p>Also considered other measures such as roadside delineators. The speed reductions cannot be attributed to pavement markings alone.</p>

ID	Pavement markings evaluated	Studies	Findings
6	 <p>Transverse optical bars with varying width [29]</p>	<p>Hussain et al. [37] used a driving simulator</p>	<p>Compared #6 with #10 and found both to be effective in reducing speeds. #10 was more effective.</p>
7	 <p>Peripheral transverse optical bars [29]</p>	<p>Arnold and Lantz [38] used field data</p> <p>Galante et al. [39] used a driving simulator</p> <p>Gates et al. [40] used field data</p>	<p>Considered both #5 and # 7. Found #5 to be more effective in reducing speed. This could be attributed to the slight bumping effect of the optical bar.</p> <p>Considered several other strategies such as transverse rumble strips, transverse optical bars, roadside fences, Gantry, colored brick strip, and dragon's teeth marking (see #9). It is hard to separate their individual impacts.</p> <p>Reduced mean curve speeds by 3-5 mph. The reduction effects sustained 6 months after the installation.</p>

ID	Pavement markings evaluated	Studies	Findings
8	 <p data-bbox="430 678 968 711">Wide painted hatched centerline marking [29]</p>	<p data-bbox="1152 253 1310 383">Godley et al. [41] used a driving simulator</p>	<p data-bbox="1369 253 1875 383">Narrowing lane width below 3.0 meters by a wide painted hatched centerline marking led to higher speed estimation and slowed vehicles down.</p>
9	 <p data-bbox="531 1203 865 1235">Dragon's teeth marking [29]</p>	<p data-bbox="1152 745 1348 842">Rossi et al. [42] used a driving simulator</p>	<p data-bbox="1369 745 1862 911">Tested roadside delineators and dragon's teeth. Found that regular and tall delineators were able to significantly reduce vehicle speeds. Dragon's teeth did not lead to significant speed reductions.</p>

ID	Pavement markings evaluated	Studies	Findings
10	 <p data-bbox="541 711 854 743">Gradual size marking [29]</p>	<p data-bbox="1152 256 1316 386">Hussain et al. [37] used a driving simulator</p> <p data-bbox="1152 423 1291 553">Awan et al. [43] used a driving simulator</p>	<p data-bbox="1369 256 1856 354">Compared #6 with #10 and found both to be effective in reducing speeds. #10 was more effective.</p> <p data-bbox="1369 423 1856 553">Compared #10 with #2. Found both to be effective. #2 resulted in more gradual speed reductions, while #10 helped drivers better maintain lateral positions.</p>
11	 <p data-bbox="331 1260 453 1284">a) Brightness</p> <p data-bbox="663 1260 730 1284">b) Size</p> <p data-bbox="940 1260 1062 1284">c) Combined</p> <p data-bbox="443 1292 953 1325">Gradual size and transparency marking [29]</p>	<p data-bbox="1152 764 1316 894">Hussain et al. [29] used a driving simulator</p>	<p data-bbox="1369 764 1856 927">Compared three marking configurations shown in the figure on the left. Configuration c (i.e., combining size and brightness) was the most effective strategy.</p>

2.4. Other Ramp Safety Improvement Strategies

Firestine et al. [44] identified the following contributing factors to ramp truck crashes:

- poor transitions to superelevation,
- abrupt changes in compound curves,
- short deceleration lanes preceding tight-radius exits,
- curbs placed on the outside of ramp curves,
- lowered friction levels on high-speed ramps, and
- substantial downgrades leading to tight ramp curves.

Based on their findings, they proposed countermeasures such as:

- incorporating a greater safety margin into formulations for side friction factors,
- reviewing and modifying posted speed limits,
- improving curve condition and downgrade signs at interchanges,
- increasing deceleration lane length,
- overlaying curbs with wedges of pavement or eliminating curbs altogether,
- resurfacing ramps with high-friction overlays, and
- redesigning sites where crashes are common.

The findings in Firestine et al. [44] were partially based on an earlier study by the University of Michigan Transportation Research Institute (UMTRI) published 1985 [45], which utilized a computer program to simulate heavy truck dynamics on highway ramps. The UMTRI study concluded that the AASHTO policy on geometric design standards at that time resulted in little safety margin for heavy trucks on highway exit ramps.

2.5. Truck Rollover Crash Data and Risk Modeling

McKnight and Bahouth [46] found that about 50% of all large truck rollover crashes (not only those on highway ramps) were speed related. This percentage is similar to what the Massachusetts ramp truck rollover crash data suggests (see Section 4.3 of this report). Using data from five states and the General Estimates System (GEE), Wang and Council [47] estimated that approximately 4,700 ramp truck rollovers occur each year and result in \$433 million losses.

Isaacs et al. [48] developed a rating system based on fuzzy math and expert surveys to evaluate the rollover crash risks of different highway ramps. This method can potentially be used to proactively identify problematic highway ramps.

Tarko et al. [49] proposed a model to evaluate a truck's rollover proximity using trajectories, which were extracted from videos. They tested the model at a roundabout. Although the proposed model is appealing, it is difficult to evaluate its accuracy.

Perera et al. [50] developed a PHASE-4 computer model that can estimate the safe operating speeds for heavy trucks on ramps. Compared to the popular ball bank indicator method, this PHASE-4 model seems to be a more appropriate approach since it is specifically designed for heavy vehicles. This PHASE-4 computer model may be used in conjunction with the simulation tool in [45] or CarSIM/TruckSim [51,52] to generate advisory speeds for trucks on highway ramps.

2.6. Discussion

The initial costs of deploying pavement markings are low, making them a very appealing choice for curve speed management. However, several issues regarding pavement markings need to be carefully considered:

- There are no MUTCD guidance for most of the pavement markings presented in Table 1,
- Maintenance can be challenging, particularly in northern states like Massachusetts with frequent snowstorms,
- Markings may reduce pavement friction,
- Depending on the materials used, markings may generate significant noise affecting surrounding residents,
- Drivers unfamiliar with the markings may be confused, which could lead to safety risks, and
- Many of the studies in Table 1 were based on driving simulation. It is important to conduct extensive field tests and evaluate their long-term effects.

A combination of pavement markings, roadside delineators, and warning signs can be considered. Mixed results for roadside delineators have been reported in the literature. Some [42,53] found them to be very effective in reducing speed, while others concluded that delineators were not very useful [54] and may even [55] increase vehicle speeds during the night, although the nighttime speeds were significantly lower than the corresponding daytime speeds.

3.0 Site Selection and Data Collection

3.1. Initial Data Collection Sites

With the support from the MassDOT Aeronautics Division, the research team first collected vehicle trajectory data from two ramps using drone to evaluate the quality of the collected data. The two ramps are shown in Figure 15 and Figure 16. The first ramp in Figure 15 was selected because it is next to a parking lot that can be used to easily launch the drone. The second ramp in Figure 16 had several heavy truck-related rollover crashes between 2015 and 2019. These crashes are marked in Figure 15 and Figure 16. The red dots and lines in these two figures show where the drone was launched and the ramps covered, respectively.

MassDOT has a facility with paved parking spaces at the first site near the red dot in Figure 15. This site is directly connected to the off-ramp by a driveway and is easy to access. While the second drone launching site was set up on a front slope with limited space and accessing the site was challenging. MassDOT District 3 helped the team with safely entering and exiting the site.

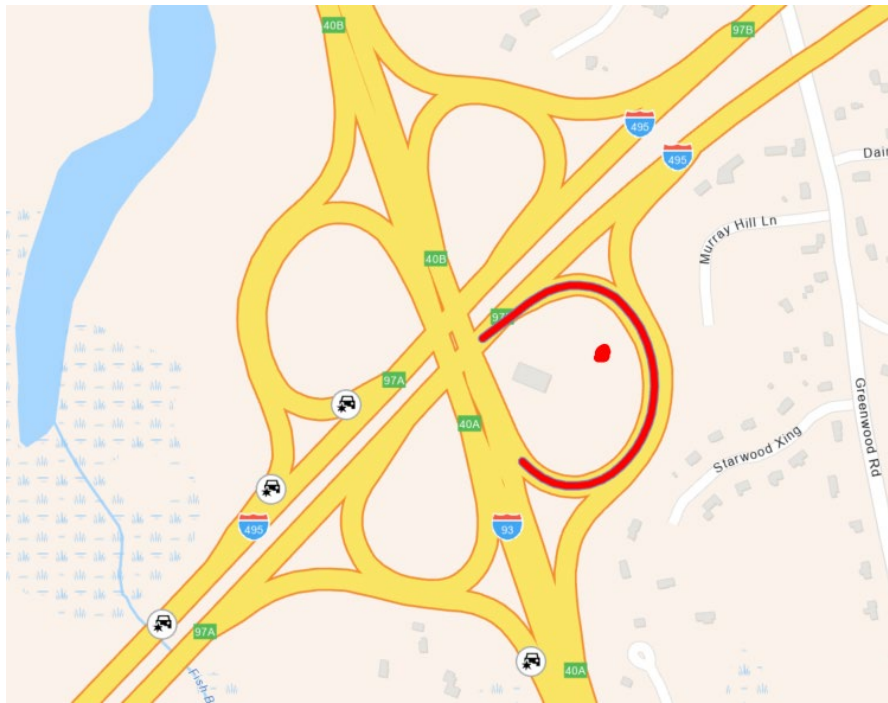


Figure 15. First data collection site at the interchange of I-495 and I-93 in Andover, MA

Source: Data collected on June 3, 2021. Google Maps Link <https://goo.gl/maps/d8mebw4sqXC5EAwU9>



Figure 16. Second data collection site on Massachusetts Turnpike Near Exit 10 in Auburn, MA

Source: Data collected on October 12, 2021. Google Maps Link <https://goo.gl/maps/mdpiCUqUxMgjims58>

3.2. Summary of Initial Data Collection Efforts

For the first site in Andover, MA, we started the data collection around 9 AM to capture as much heavy truck traffic as possible. The following factors were evaluated in the first data collection: camera angle, height, and type of camera. For camera angle, we experimented with a slanted view and the top-down view. The results are illustrated in Figure 17. Clearly, the slanted view covers larger areas than the top-down view, but also introduces more distortion. Pixels further away from the camera represent larger areas than those closer to the camera. This distortion makes it challenging to accurately estimate vehicle speeds. Therefore, we decided to use the top-down view.

For camera height, we tested 300 ft, 350 ft, and 400 ft. Higher positions allow us to see larger areas. The results in Figure 17 show that the images captured at 400 ft are clear enough for the purpose of this study. Ideally, we would like to fly the drone even higher to cover the entire ramp. However, the maximum height we are allowed to fly per current federal regulations is 400 ft.

In addition to a regular RGB camera, a thermal camera was tested during the first data collection in Andover, MA. A top-down view captured by the thermal camera at 400 ft is shown in Figure 18. The quality of the thermal camera image is good, clearly showing pavement markings, paved and unpaved surfaces, and vehicles. For nighttime data collection, this thermal camera is strongly recommended. However, compared to the captured RGB images in Figure 17(f), the thermal image covers a relatively smaller area. Given that our data collection was during the daytime, we decided to use the RGB camera due to its larger coverage.



(a) 300 ft slanted view



(d) 300 ft top-down view



(b) 350 ft slanted view



(e) 350 ft top-down view



(c) 400 ft slanted view



(f) 400 ft top-down view

Figure 17. Comparison of slanted and top-down views in Andover, MA



Figure 18. Top-down view captured by thermal camera at 400 ft in Andover, MA

Based on what we learned during the first data collection trip in Andover, MA, we considered top-down view, 400 ft altitude, and RGB camera for the second data collection in Auburn, MA. A sample of the collected data is shown in Figure 19.



Figure 19. Sample of the Data Collected from Auburn, MA

3.3. Discussion



Road SSCN-NB-S. Boston-S. Sta. Conn a



Ramp X-SB-Boston-Kneeland to HOV-E a



Ramp TC-SB-Charlestown-Tobin to 93S/Storrow d



Ramp TC-SB-Charlestown-Tobin to 93S/Storrow e



I-90-EB-Weston-before Exit 15



I-90-EB-Westfield-Exit 3 Rt 10



I-90-EB-Chicopee-Exit 6 Rt 291



I-495-NB-Marlborough-Ex 23

Figure 20. Sample traffic videos from Mass511 website

We also evaluated the feasibility of using roadside cameras mounted on tripods or guardrails spaced roughly 200 ft apart to provide a horizontal rear view of trucks in addition to the top-down view supplied by drones. Given the difficulty in accessing the Auburn site and the limited time allowed for data collection, the benefits of this approach appear to be outweighed by the challenges. Also, doing this will require precise knowledge of ramp superelevation and correlating the roadside camera data with the drone camera data, which are both very challenging. Therefore, only drone data was collected in subsequent data collection trips.

We obtained some traffic videos from the MassDOT website (<https://mass511.com/>). A few examples from the mass511 website are provided in Figure 20. Images extracted from these traffic videos are similar to those taken by the drone using a slanted view [Figure 17(a)–(c)]. Although they are helpful, it is difficult to derive accurate vehicle speed and potentially lateral position information from such videos. Also, traffic cameras are available at limited locations. Their views are often blocked by trees and bridges. Therefore, drone videos appear to be the best data collection option for this study given that drones are relatively easy to deploy and the quality of the collected videos is good.

3.4. New Data Collection Sites

With the gracious support of the MassDOT Aeronautics Division, additional ramp traffic videos were collected using drones. To avoid confusion, we use Ramps 3–7 to represent the 5 new data collection sites and Ramps 1–2 to refer to the previous two sites (1 for Andover and 2 for Auburn). These new sites are determined based on crash history and are described below.

3.4.1. Ramp 3: West Springfield

Ramp 3 is located in West Springfield (GPS 42.15905084 -72.63722185) and the Google Maps link is <https://goo.gl/maps/vrMdw9mj4BiVr9PM9>. Its location is shown in Figure 21 and a detailed layout is provided in Figure 22. Between 1/1/2015 and 2/2/2022, 4 heavy truck rollover crashes occurred here and were all due to speeding. Therefore, this ramp is selected for a detailed investigation.

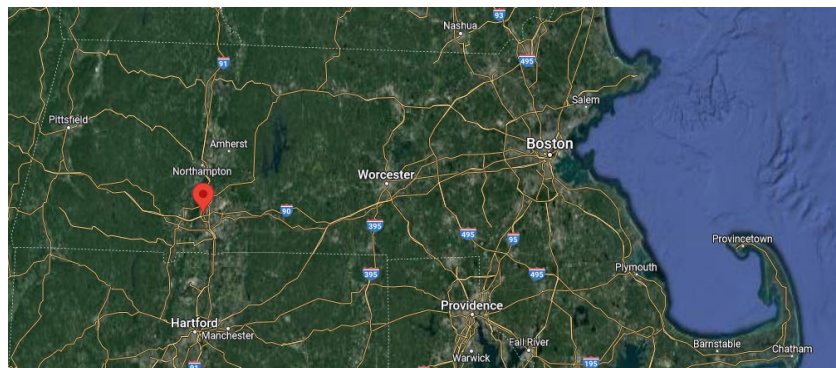


Figure 21. Ramp 3 in West Springfield MA (Data collected on June 6, 2022)

Google. (n.d.). [Google map of Ramp 3 in West Springfield, MA]. Retrieved January 1, 2023, from <https://goo.gl/maps/vrMdw9mj4BiVr9PM9>.

The locations of the four rollovers are marked in Figure 22. The ramp (Segment 1 in Figure 22) was downstream of a toll plaza (Segment 3 in Figure 22), which was removed in 2016. We also checked the rollover crash history at this location before 2015 and found no truck rollovers on this ramp between 1/1/2008 and 12/31/2014. Note that the 4 rollovers mentioned above occurred all after the removal of the toll plaza (1 in 2017, 2 in 2020, and 1 in 2021). This seems to suggest that removing the toll plaza played an important role in those four truck rollovers. With the toll plaza (Segment 3 in Figure 22), vehicles need to slow down first and then accelerate, this significantly reduces the chance for them to travel too fast on the downstream ramp (i.e., Segment 1 in Figure 22) and the risk of truck rollover crashes. Note that all four rollovers occurred after the removal of the toll plaza were attributed to speeding.

For this site, two drones were used to collect the data, since one drone was not enough to capture the entire site using the top-down view. As shown in Figure 22, the entire site was divided into three segments. Two drones were used simultaneously to collect data from Segments 1 and 2. Later, the drone covering Segment 1 was moved down to cover Segment 3.

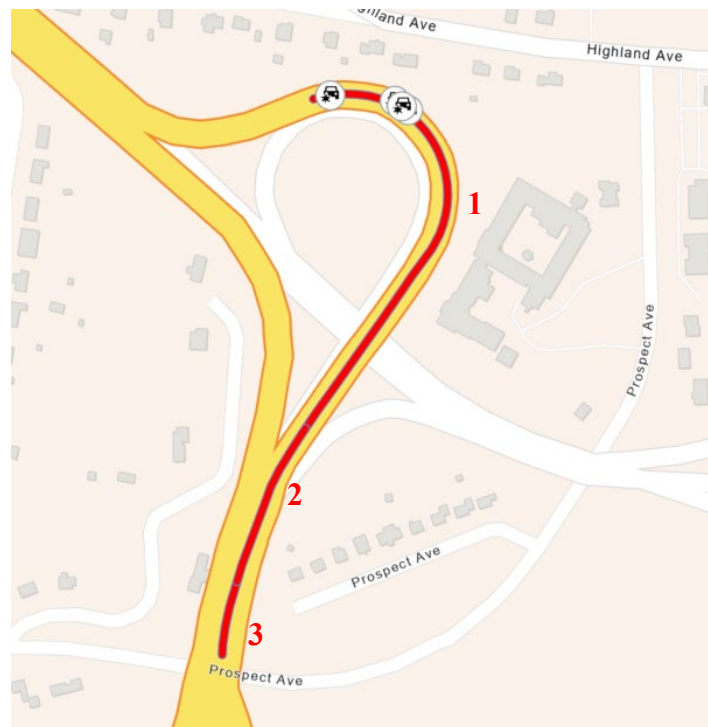


Figure 22. Ramp 3 connecting I90W to I91

3.4.2. Ramp 4: New Bedford

Ramp 4 is located in New Bedford as shown in Figure 23 (GPS 41.65315303 -70.95980417) and the Google Maps link is <https://goo.gl/maps/rzD3bCyijnQuDLJF7>. Two truck rollover crashes occurred here between 1/1/2015 and 2/2/2022. To cover the entire segment highlighted in Figure 24 using the top-down view, multiple drones would be needed. For this site, we experimented with a slightly slanted view to reduce the efforts needed and the amount of videos to be collected.

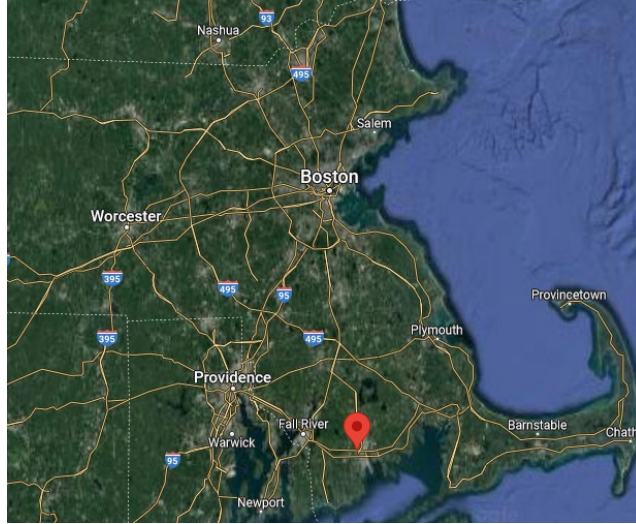


Figure 23. Ramp 4 in New Bedford MA (Data collected on June 14, 2022)

Source: Google. (n.d.). [Google map of Ramp 4 in New Bedford, MA]. Retrieved January 1, 2023, from <https://goo.gl/maps/rzD3bCyijnQuDLJF7>.

This site was selected because of the relatively straight segment between the exit and entrance ramps, which may create an opportunity for ramp vehicles to accelerate and exceed the speed limit. Again, both rollovers which occurred here were due to speeding.

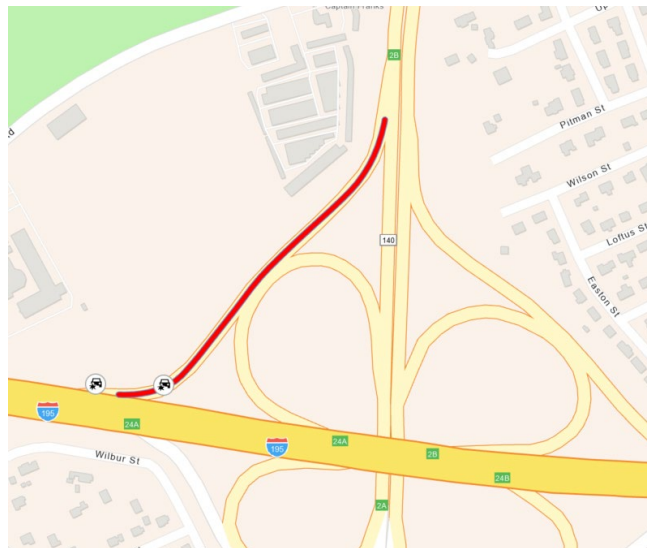


Figure 24. Ramp 4 connecting 140S to I195W

3.4.3. Ramps 5 and 6: Freetown North and South

Ramps 5 and 6 are located in Freetown, MA, as shown in Figure 25 (GPS 41.78380889 - 71.08031751) and the Google Maps link is <https://goo.gl/maps/G5QK1zUbo9Q23LQ86>. Both the southbound and northbound ramps are selected since they are very similar. The Freetown

North ramp had two truck rollovers during the study period, while the Freetown South one had 1 rollover (Figure 26). Two of the crashes were caused by speeding and the other one was due to fatigued driving. A top-down view was taken for both ramps at this location.

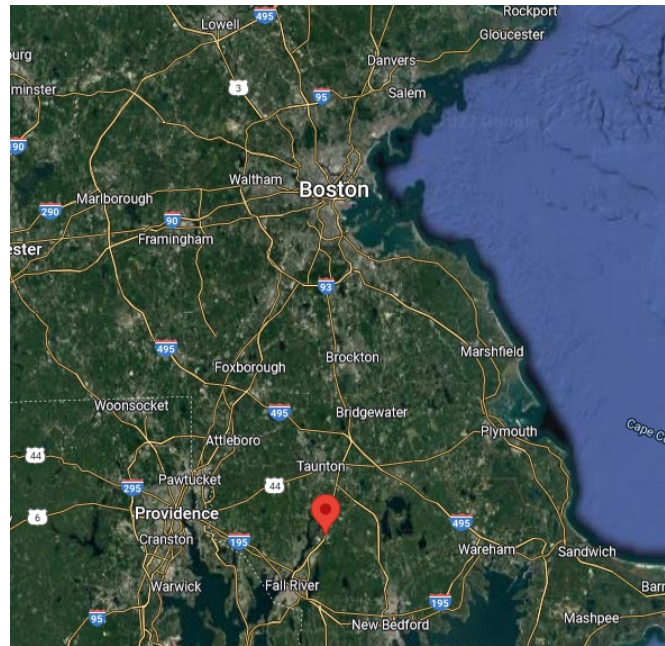


Figure 25. Ramps 5 and 6 in Freetown, MA (Data collected on June 13, 2022)

Source: Google. (n.d.). [Google map of Ramps 5 and 6 in Freetown, MA]. Retrieved January 1, 2023, from <https://goo.gl/maps/G5QK1zUbo9Q23LQ86>.

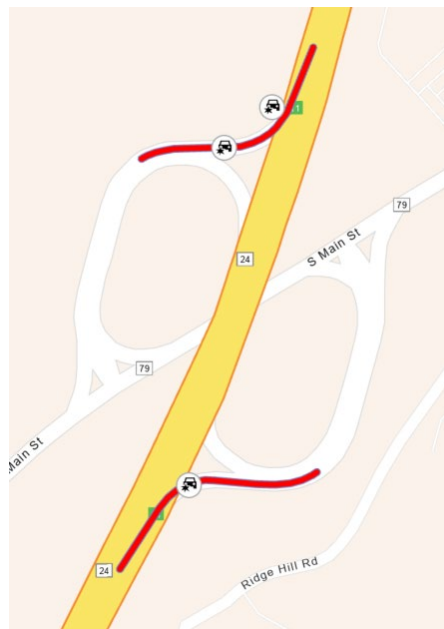


Figure 26. Ramps 5 and 6 connecting Route 24 to Route 79

3.4.4. Ramp 7: Sturbridge

Ramp 7 is located in Sturbridge MA as in Figure 27 (GPS 42.06756915 -72.10875083) and the Google Maps link is <https://goo.gl/maps/ngMbpHGM3czSFX4F8>. Three rollovers occurred toward the end of the ramp /1/2015 and 2/2/2022 (Figure 28)

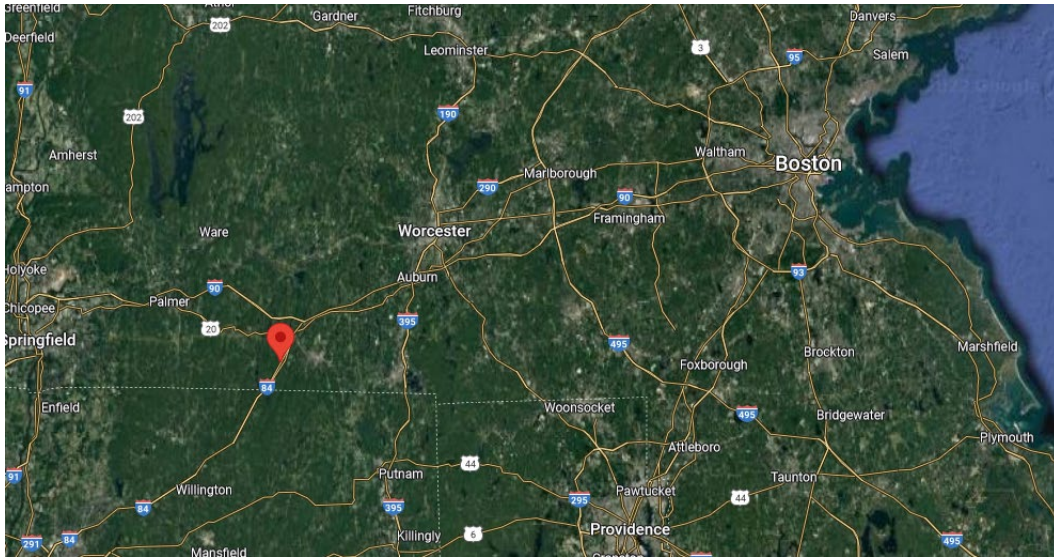


Figure 27. Ramp 4 in Sturbridge, MA (Data collected on June 21, 2022)

Source: Google. (n.d.). [Google map of Ramp 7 in Sturbridge, MA]. Retrieved January 1, 2023, from <https://goo.gl/maps/ngMbpHGM3czSFX4F8>.

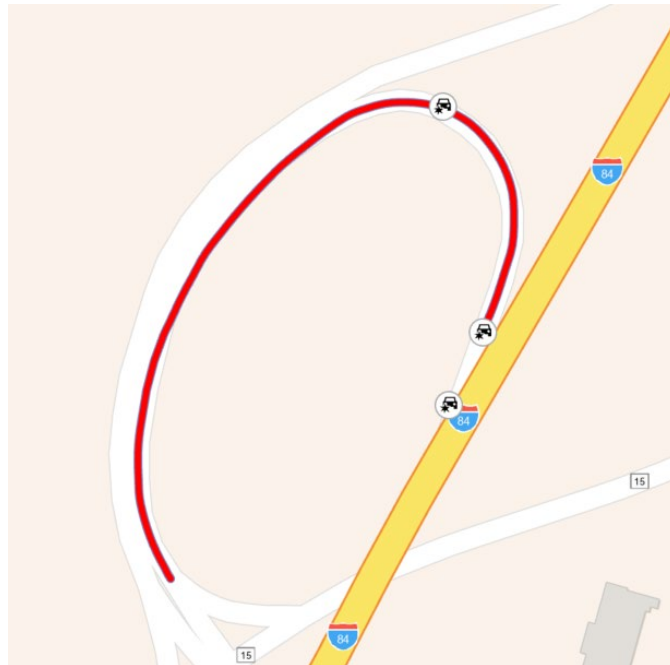


Figure 28. Ramp 4 connecting 140S to I195W

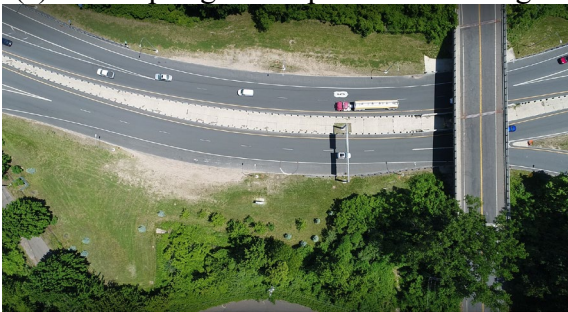
3.5. Summary of Additional Data Collection Efforts



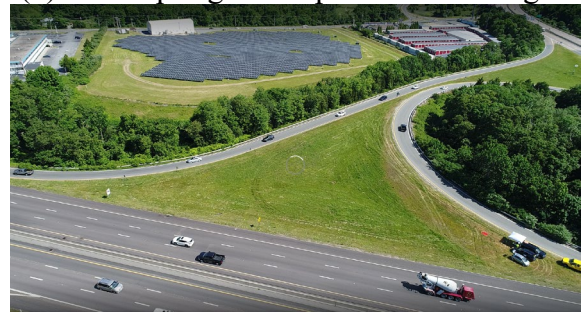
(a) West Springfield top-down view Seg. 1



(b) West Springfield top-down view Seg. 2



(c) West Springfield top-down view Seg. 3



(d) New Bedford slanted view



(e) Freetown North top-down view



(f) Freetown South top-down view



(g) Sturbridge slanted view

Figure 29. Sample images from the new ramps

For each of the 5 new ramps, videos were captured at the 400 ft altitude. The top-down view was considered at three sites and a slightly slanted view was used at the remaining two sites.

Table 2 summarizes when and how the videos were captured. Some sample images are provided in Figure 29.

Table 2. Video data collection efforts at the 5 new ramps

Location	View angle	Time and date
West Springfield	Top down	6/6/2022
Freetown South	Top down	6/13/2022
Freetown North	Top down	6/13/2022
New Bedford	Slightly Slanted	6/14/2022
Sturbridge	Slightly Slanted	6/21/2022

Although using a slightly slanted view reduced the efforts needed to collect data and the amount of data to be collected, it poses some challenges to video data processing. Drone movements (e.g., vibration, tilt, turn) due to wind and other effects also introduce some challenges to data processing, but the impacts are manageable. Overall, drones are proven to be very useful for short-term traffic data collection. They can be quickly deployed. The overall quality of the collected data is good.

4.0 Analysis of Truck Rollover Crashes

4.1. Query Ramp Truck Rollovers

The following SQL expression was used to query heavy truck-related rollover crashes on highway ramps from the MassDOT IMPACT database. This resulted in about 350 crash records. These records were double checked to remove crashes that were not on ramps or not related to heavy trucks. We finally ended up with 105 crashes. The locations of these crashes are illustrated in Figure 30 and Table 3.

```
SELECT * FROM tableName WHERE crash_date BETWEEN '1/1/2015' AND '2/2/2022'  
AND ( vehc_seq_events_cl LIKE('%ollover%') OR vehc_seq_events_cl  
LIKE('%verturn%') ) AND ( vehc_config_cl LIKE('%railer%') OR vehc_config_cl  
LIKE('%ractor%') )
```

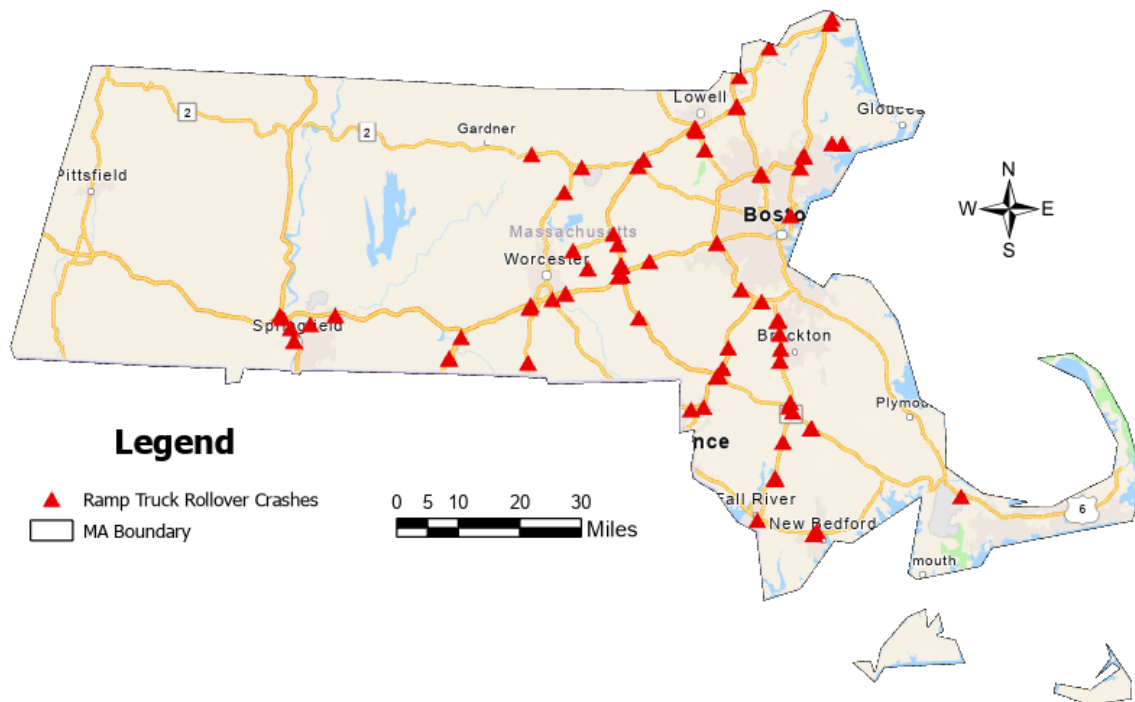


Figure 30. Locations of heavy truck ramp rollover crashes between 1/1/2015 and 2/2/2022

As shown in Table 3, most of the crashes occurred on I-90, I-95, I-495, and RT 24. It is surprising to see that RT 24 had 14 ramp truck rollover crashes between 1/1/2015 and 2/2/2022 given that it is not a major interstate highway.

Table 3. Heavy truck ramp rollover crashes between 1/1/2015 and 2/2/2022 on major routes

Route Number	Number of Truck Rollovers
RT 24	14
I-84	5
I-90	21
I-91	4
I-495	32
I-95	22

4.2. Distributions of Ramp Truck Rollovers

The narratives of each crash were carefully reviewed. It was found that some crashes' GPS coordinates did not match the corresponding narratives. The exact locations of these crashes were then determined manually based on the crash narratives and crash diagrams. Most of the 105 crashes occurred on ramps similar to the outer loop or inner loop of a typical cloverleaf interchange in Figure 31. Therefore, Figure 31 and Table 4 are used to illustrate the locations of 93 (out of 105) crashes. For the exact locations of the remaining 12 crashes, 4 were unknown due to a lack of information, 6 were on a ramp that functions as the mainline, and 2 were very different from a cloverleaf interchange.

As shown in Figure 31 and Table 4, the beginning and end of the outer ramp appear to be more dangerous than the middle. While for the inner ramp, the middle and end appear to be more dangerous than the beginning.

Table 4. Detailed locations of heavy truck ramp rollover crashes

Location	Beginning of Ramp	Middle of Ramp	End of Ramp	Total
Outer Ramp	20	8	25	53
Inner Ramp	9	14	17	40
Total	29	22	42	93

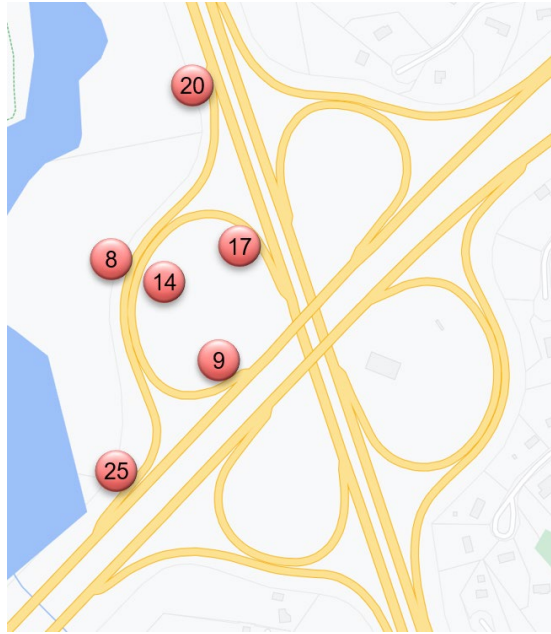


Figure 31. Detailed locations of ramp truck rollover crashes

Figure 32 suggests that most ramp truck rollovers occurred during weekdays, which probably is because of higher truck and passenger vehicle traffic during weekdays. Figure 33 shows that 1-2 PM is the most dangerous period during a day. Figure 34 suggests that ramp truck rollovers are more likely to happen in January through May and September. Although these are very interesting observations, at this moment we do not have enough information to derive a reasonable explanation for them.

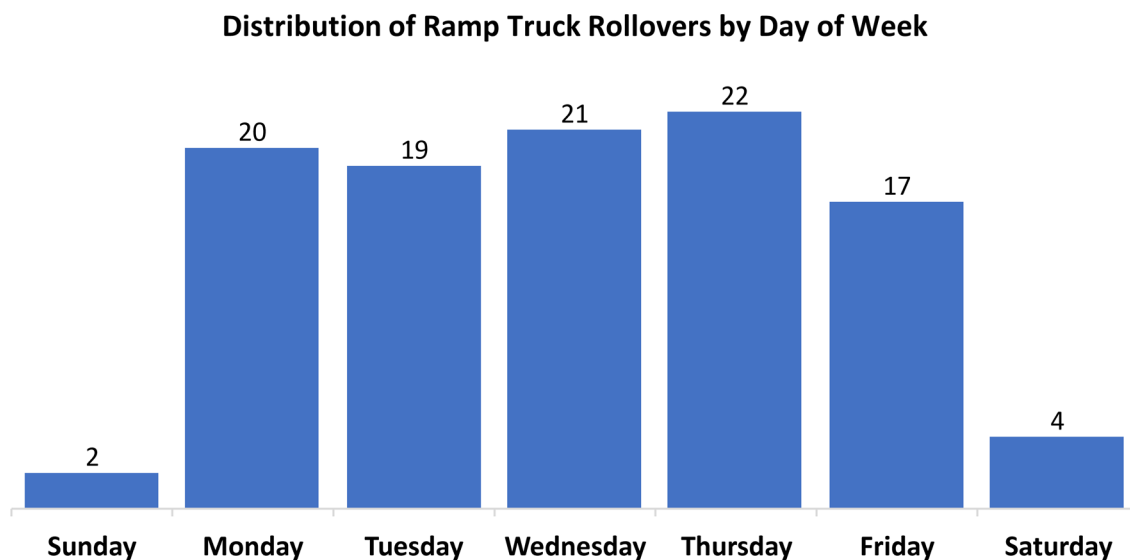


Figure 32. Distribution of ramp truck rollovers by day of week

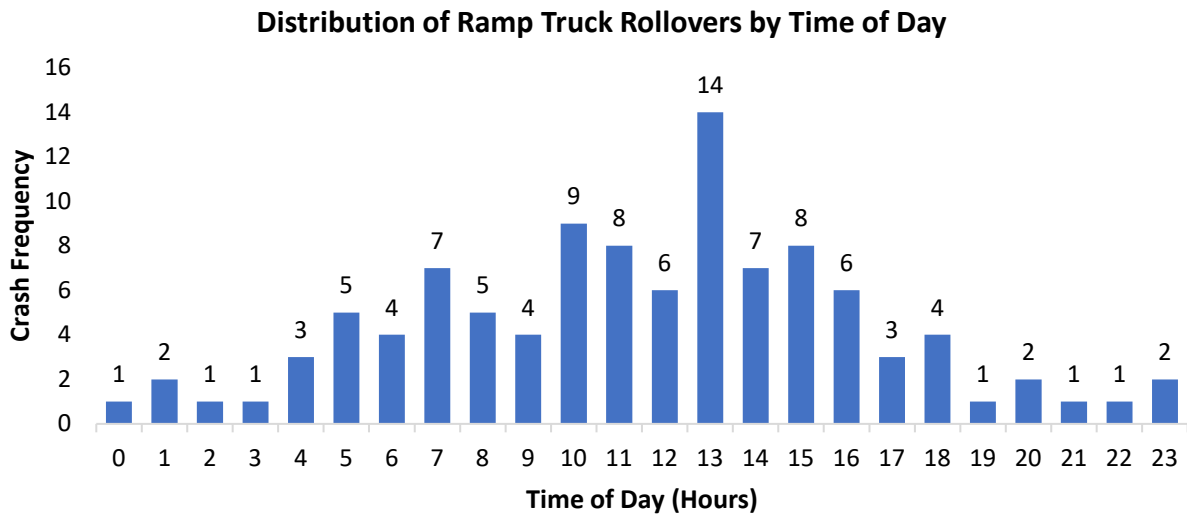


Figure 33. Distribution of ramp truck rollovers by time of day

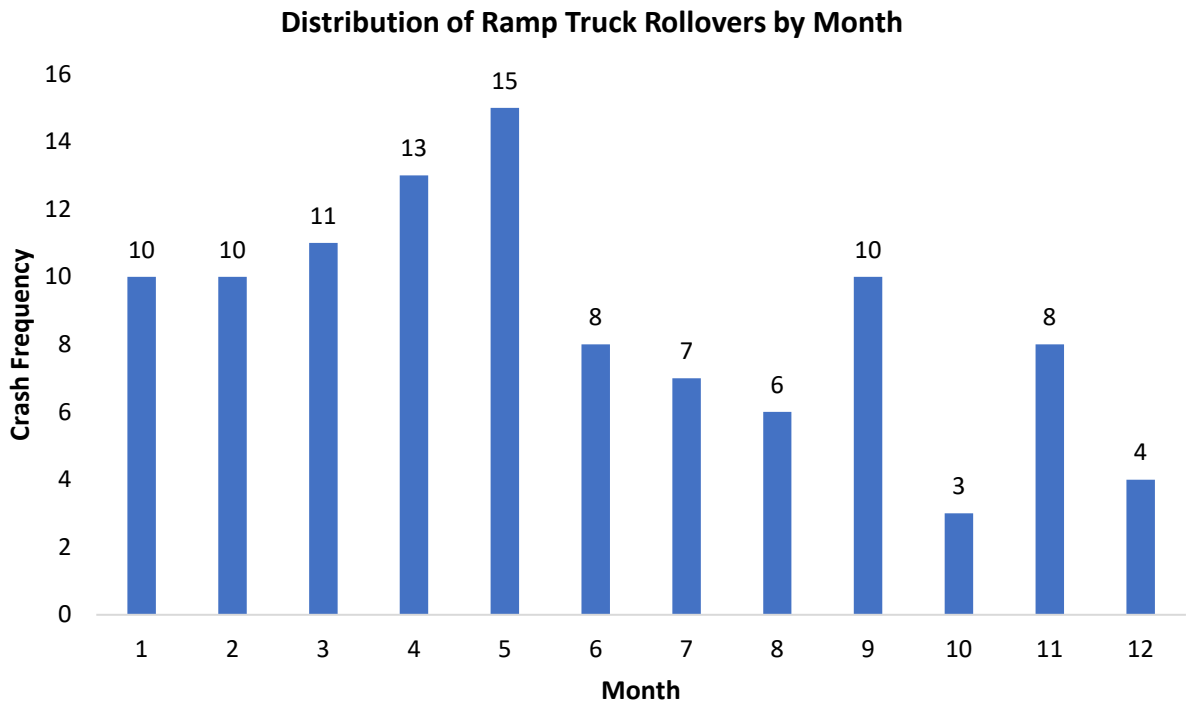


Figure 34. Distribution of ramp truck rollovers by month

Table 5. Rollover distribution based on hour and day

Hour	Sunday	Monday	Tuesday	Wednesday	Thursday	Friday	Saturday	Total
0	—	—	1	—	—	—	—	1
1	—	—	1	—	1	—	—	2
2	—	—	—	—	1	—	—	1
3	—	1	—	—	—	—	—	1
4	—	—	2	1	—	—	—	3
5	—	2	1	—	2	—	—	5
6	—	1	—	3	—	—	—	4
7	—	3	—	—	1	2	1	7
8	1	—	—	2	—	1	1	5
9	—	1	1	1	1	—	—	4
10	—	1	1	1	3	2	1	9
11	—	3	2	1	1	1	—	8
12	—	1	1	2	2	—	—	6
13	1	2	2	3	3	2	1	14
14	—	1	3	1	2	—	—	7
15	—	2	2	1	2	1	—	8
16	—	1	2	—	2	1	—	6
17	—	—	—	1	—	2	—	3
18	—	—	—	—	1	3	—	4
19	—	—	—	1	—	—	—	1
20	—	—	—	1	—	1	—	2
21	—	—	—	—	—	1	—	1
22	—	—	—	1	—	—	—	1
23	—	1	—	1	—	—	—	2
Total	2	20	19	21	22	17	4	105

Table 5 through 7 show the temporal distributions of ramp truck rollovers in terms of hour vs. day, day vs. month, and hour vs. month, respectively. Each table is color coded with red representing large values and green representing small values. Note that these tables only show when ramp truck rollovers are more likely to happen. To find out which time windows are more dangerous, we need to take truck traffic volumes into consideration. As shown in Figure 35 and Figure 36, the distributions of heavy truck traffic can vary significantly from one location to another.

Table 6. Rollover distribution based on day and month

Day	Month												Total
	1	2	3	4	5	6	7	8	9	10	11	12	
Sunday	—	1	—	—	1	—	—	—	—	—	—	—	2
Monday	1	1	1	3	3	1	2	—	5	1	1	1	20
Tuesday	1	1	3	2	3	2	2	3	—	—	1	1	19
Wednesday	5	2	3	—	2	3	1	1	2	1	1	—	21
Thursday	2	3	1	6	3	1	1	—	3	1	1	—	22
Friday	1	2	2	1	3	—	1	2	—	—	4	1	17
Saturday	—	—	1	1	—	1	—	—	—	—	—	1	4
Total	10	10	11	13	15	8	7	6	10	3	8	4	105

Table 7. Rollover distribution based on hour and month

Hour	Month												Total
	1	2	3	4	5	6	7	8	9	10	11	12	
0	—	—	1	—	—	—	—	—	—	—	—	—	1
1	—	—	1	1	—	—	—	—	—	—	—	—	2
2	—	—	—	—	1	—	—	—	—	—	—	—	1
3	—	1	—	—	—	—	—	—	—	—	—	—	1
4	—	—	—	—	1	—	1	1	—	—	—	—	3
5	—	1	—	2	—	—	1	—	1	—	—	—	5
6	2	—	—	—	—	1	—	1	—	—	—	—	4
7	1	—	1	1	1	—	—	1	1	1	—	—	7
8	—	1	—	—	—	—	—	—	1	1	1	1	5
9	—	1	—	2	—	—	—	—	—	1	—	—	4
10	—	1	—	1	1	1	—	1	1	—	3	—	9
11	—	1	—	2	1	—	—	1	1	—	2	—	8
12	1	—	1	—	—	1	—	—	2	—	—	1	6
13	2	—	2	2	1	1	3	—	1	—	1	1	14
14	—	1	—	—	4	1	—	—	1	—	—	—	7
15	2	1	2	—	1	—	1	—	—	—	1	—	8
16	—	1	1	1	1	—	1	—	—	—	—	1	6
17	—	—	—	—	2	—	1	—	—	—	—	—	3
18	—	1	—	1	1	1	—	—	—	—	—	—	4
19	1	—	—	—	—	—	—	—	—	—	—	—	1
20	1	—	—	—	—	1	—	—	—	—	—	—	2
21	—	—	1	—	—	—	—	—	—	—	—	—	1
22	—	—	—	—	—	1	—	—	—	—	—	—	1
23	—	—	1	—	—	—	—	—	1	—	—	—	2
Total	10	10	11	13	15	8	7	6	10	3	8	4	105

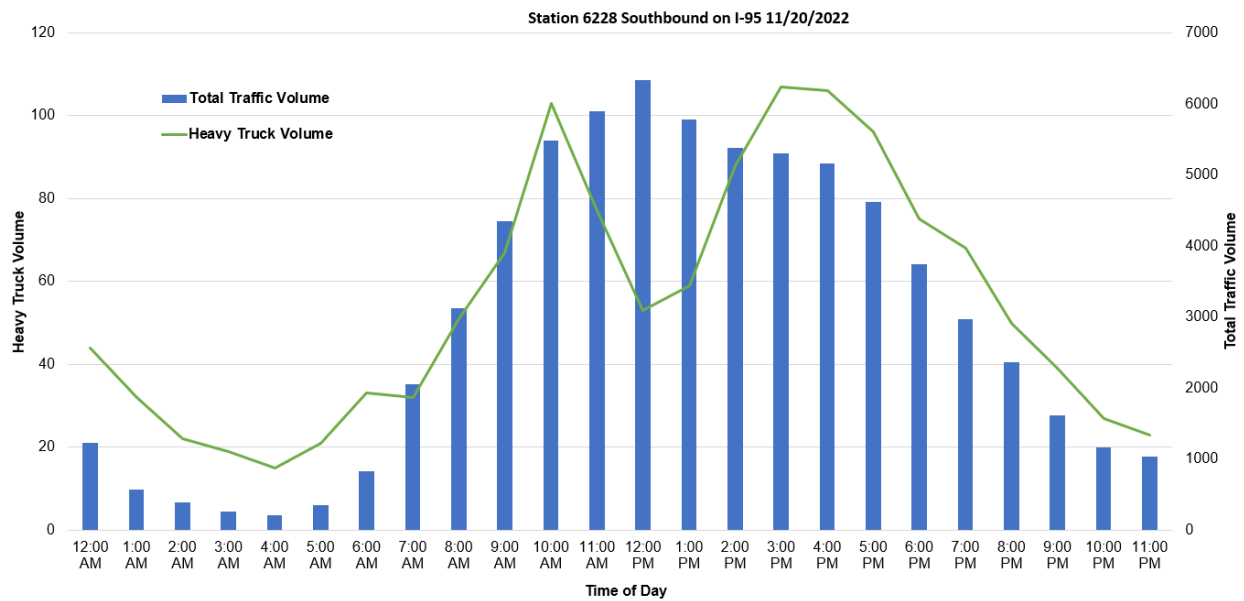


Figure 35. Traffic volumes at counting station 6228 on I-95 southbound

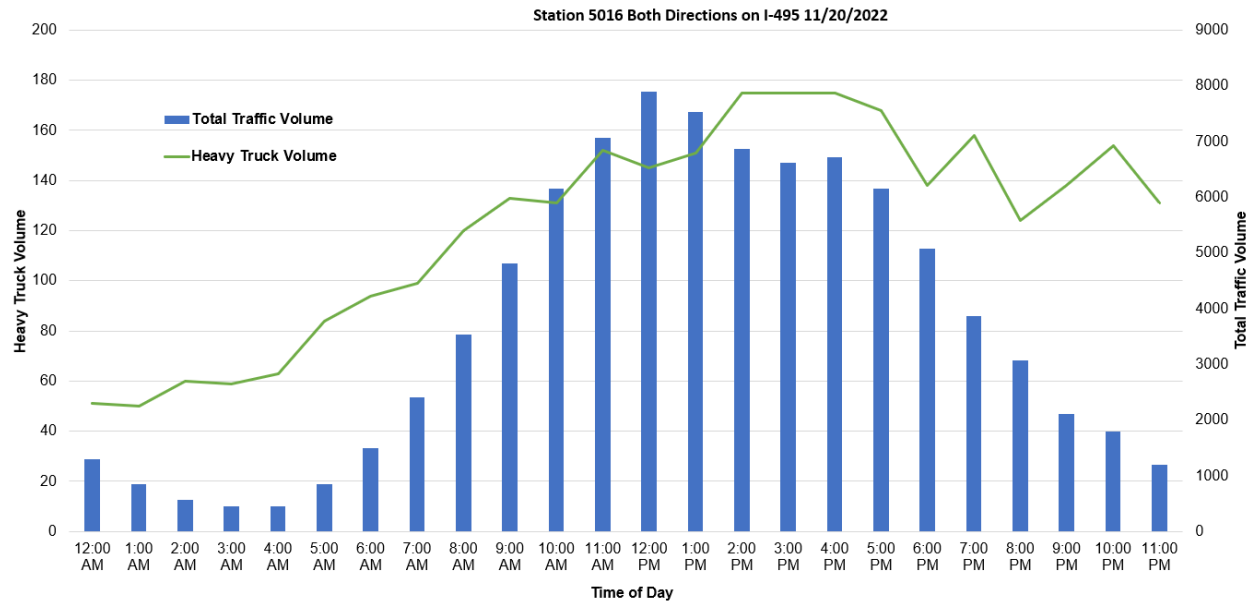


Figure 36. Traffic volumes at counting station 5016 on I-495 for both directions

4.3. Main Causes of Ramp Truck Rollovers

Figure 37 presents the main causes of ramp truck rollover crashes analyzed in this study. It is found that:

- Speeding was the leading cause of ramp truck rollovers. It contributed to 59 of the 105 rollovers (56.2%).
- Most of the truck rollovers were single-vehicle crashes (involving only a truck). There were only 4 rollovers that involved multiple vehicles. Of those 4 rollovers, two did not attribute fault to the truck driver.
- None of the 105 rollovers were related to drunk driving and only one was under the influence of marijuana.
- Only one crash occurred inside Route 128. This most likely was because there were more heavy trucks on highways outside Route 128, suggesting that risk exposure such as truck traffic volumes should be considered in determining the most dangerous ramps. Some ramps had more truck rollovers mainly because there were more truck traffic. However, such risk exposure data currently is not widely available.
- Although some of the rollovers were attributed to load shift, it is likely that speeding also played a role in the load shift. For slow-moving vehicles, it is less likely for load shift to happen.

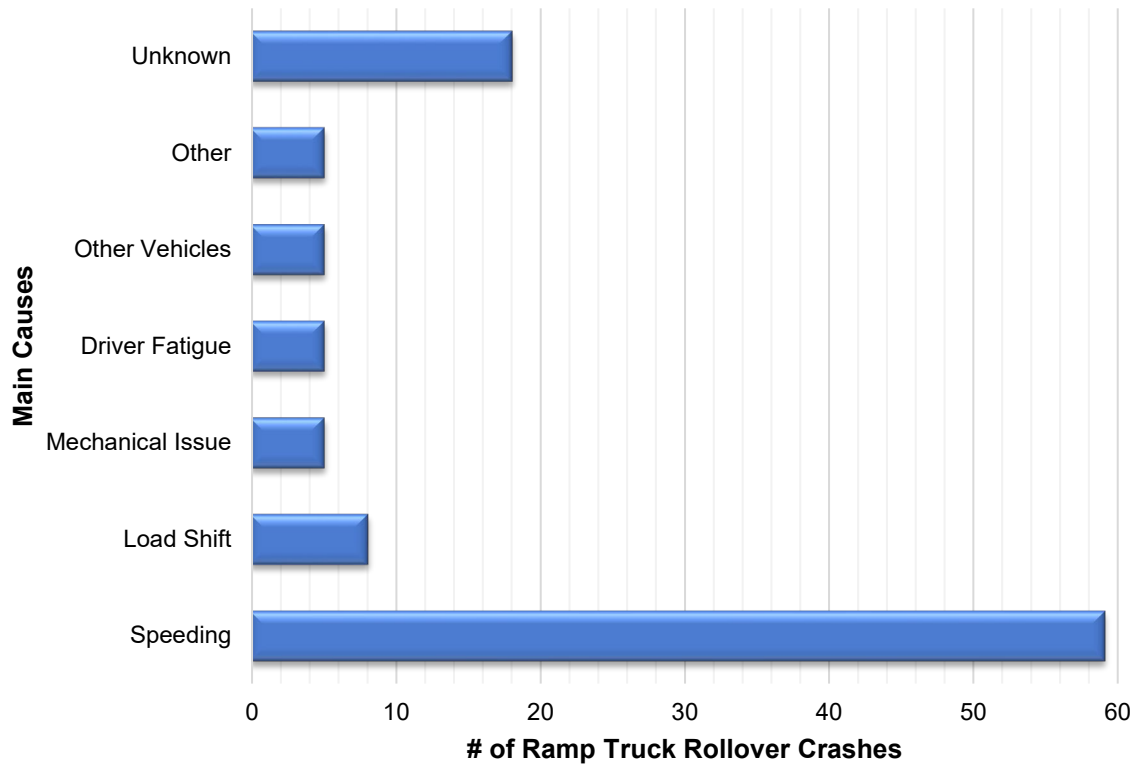


Figure 37. Main causes of heavy truck ramp rollover crashes

4.4. Discussion

Since speeding is the most important contributing factor to ramp truck rollovers, properly setting advisory speeds is critical. The ball bank indicator method is typically used by state DOTs to determine the advisory speeds for horizontal curves and ramps. This method requires multiple field test runs through a curve or ramp to obtain the advisory speed. These test runs are often conducted using passenger vehicles instead of heavy trucks. Although the obtained advisory speeds are safe for passenger vehicles, they may not be sufficiently safe for heavy trucks. Also, it may be necessary to provide different ramp advisory speeds for heavy trucks and passenger vehicles as in [18].

5.0 Vehicle Detection and Tracking from Drone Videos

5.1 Vehicle Detection from Aerial Images

Video-based traffic data analysis has received substantial attention in recent years primarily because of the developments in deep learning and computer vision. Such attention can also be attributed to the wide applications of UAV or drone technologies, which generate a huge demand for aerial traffic video data analytics that are difficult to do manually. Deep learning and computer vision can quickly turn traffic videos into useful information for decision making and play a critical role in video-based traffic data analysis.

Over the past several decades, substantial effort has been devoted to solving the general-purpose image-based object detection problem. Although significant progress has been made, there are still many issues to be resolved. Vehicle detection from aerial images is a more specific version of the general-purpose object detection problem and it comes with some unique challenges. One such challenge is that objects (i.e., vehicles) in drone videos can appear in any orientation. This makes the use of horizontal bounding boxes (HBB) not suitable because of the potentially large non-object space enclosed in the detected bounding boxes [56]. Furthermore, if the objects happen to be densely packed and arranged in a tilted fashion, applying non-maximum suppression will result in missed objects. These two issues are illustrated in Figure 38. Another hurdle that a traditional object detection algorithm such as Convolutional Neural Networks (CNN) might encounter is confusing background objects with vehicles. Since from a top-down view both buildings and other structures can appear to have a rectangular shape, similar to that of vehicles [57].

To overcome the disadvantages of an HBB, an oriented bounding box (OBB) is generally preferred for processing drone-captured traffic videos. OBBs can enclose vehicles with minimal inclusion of the background. This is especially helpful when trying to detect heavy trucks, buses, and other large vehicles that are relatively longer in dimension as shown in Figure 38.



Figure 38. Two instances where OBBs are better suited than HBBs

5.2 Related Work

5.2.1 Aerial Image Datasets

Developing deep learning models for processing aerial videos requires a large amount of annotated training data. Fortunately, several high-resolution aerial image datasets are available to facilitate rapid research and development in the domain of video-based traffic observation and analytics. These datasets have objects (e.g., vehicles) either segmented or annotated using OBBs. Among them, DOTA v1.5 [56] is a popular benchmark dataset with 2,806 images and 403,318 instances belonging to 16 different categories. This dataset has images ranging from 800×800 to $20,000 \times 20,000$ pixels and the instances occur in a wide range of orientations and scales. DIOR-R [58] is a similar aerial dataset with 23,463 images. It consists of 192,518 annotated (using OBB) instances belonging to 20 categories. HRSC2016 [59] is another popular dataset with OBB annotations and instance segmentation. The UCAS-AOD [60] dataset has images collected from Google Earth and has OBB annotations of cars and planes.

Semantic segmentation datasets [61,62,63,64] have also been instrumental in developing architectures and models specifically for aerial imagery. In certain situations, it can be advantageous to have segmentation annotations as opposed to simple OBB annotations, as segmentation annotations can capture the detailed boundaries of irregularly shaped objects. However, in the case of vehicle detection from drone-captured images, both segmentation and OBB yield comparable detection results, and the advantages of one over the other are apparent only in a few exceptional circumstances.

An issue with existing datasets for this research is that the data is mostly collected using satellites. Google Earth is one common source for such images. This type of data is helpful but not good enough for training deep-learning models to handle videos from a different source such as a drone. In our research, some drone videos were recorded using both top-down and slanted views. The images captured using a slanted view are quite different from those using the top-down view and Google Earth images. Hence, we decided to annotate some drone-captured videos to develop a new annotated image dataset specifically for this study.

5.2.2 Rotated Object Detection

Most advances in object detection using OBB are based on modifying models that detect HBB. One of the first approaches proposed for detecting rotated vehicles in aerial images was by modifying Faster R-CNN [65]. et al. [66] introduced a novel image cascade and feature pyramid network (FPN) and rotation region strategy, which significantly improved location accuracy. We used a modified FPN with a ResNet backbone in our detection model. RoI-transformer [67] is another approach where a Rotated Region of Interest (RoI) learner transforms horizontal RoI to rotated RoI. While we did not employ this transformer model, we did devise a data augmentation strategy that drew from the RoI-transformer approach.

Yi et al. [68] employed box boundary-aware vectors (BBAV) on the center keypoint of objects to determine the OBB. Lang et al. proposed DAFNe [69], which is a one-stage anchor-free model based on RetinaNet and can detect oriented objects. In [70] the concept of “centerness”

was further generalized to obtain “oriented centerness.” Although we did not directly utilize BBAV or the concept of oriented centerness, we incorporated a notion of focus through a customized RoI alignment technique.

5.3 Methodology

Our proposed approach is a pipeline consisting of three primary components: the vehicle detection module, the tracking unit, and the analytics unit. Figure 39 illustrates the fundamental steps involved in the entire process. The inputs to the system are drone videos. To effectively perform vehicle detection and tracking, the videos are first stabilized and then fed into the vehicle detection module.

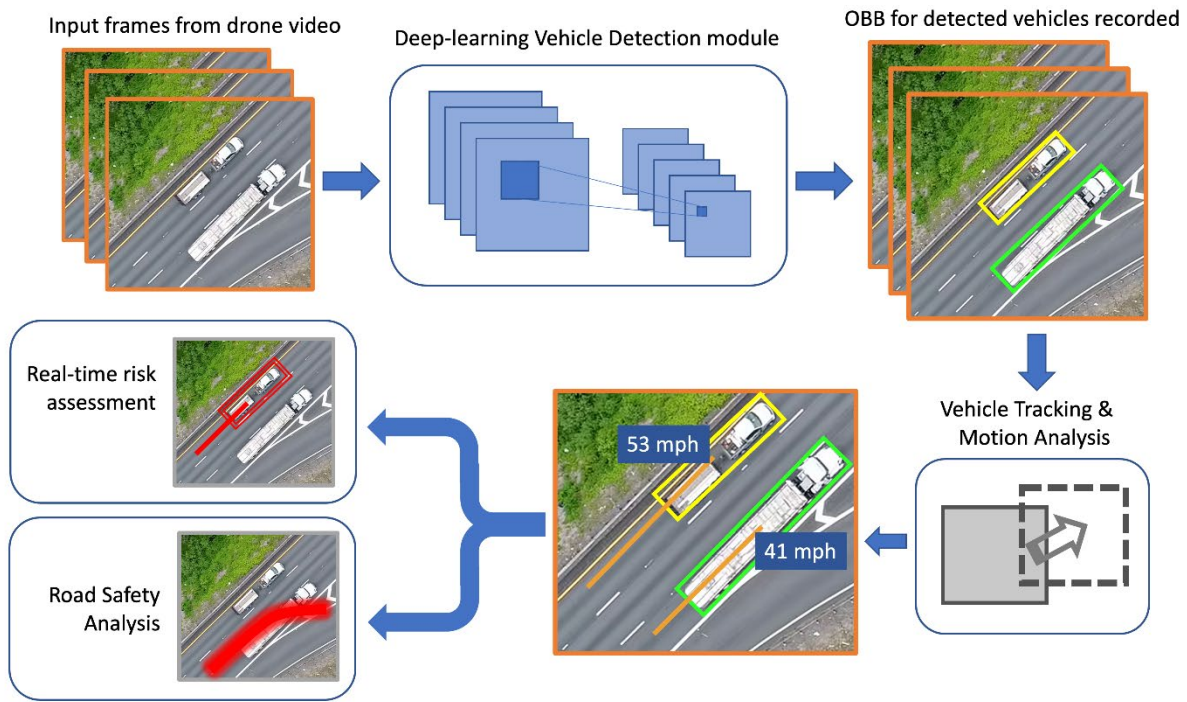


Figure 39. High-level representation of the proposed pipeline

After extensive experiments with various deep learning architectures and models, we decided to adopt a modified Rotated Mask-RCNN model for the detection module. Rotated Mask R-CNN is a revised form of Mask R-CNN [71] with the additional ability to detect objects using OBB. As shown in Figure 40, this model is a two-stage detector, where the first stage proposes regions of interest and in the second stage OBBs and segmentation masks are generated.

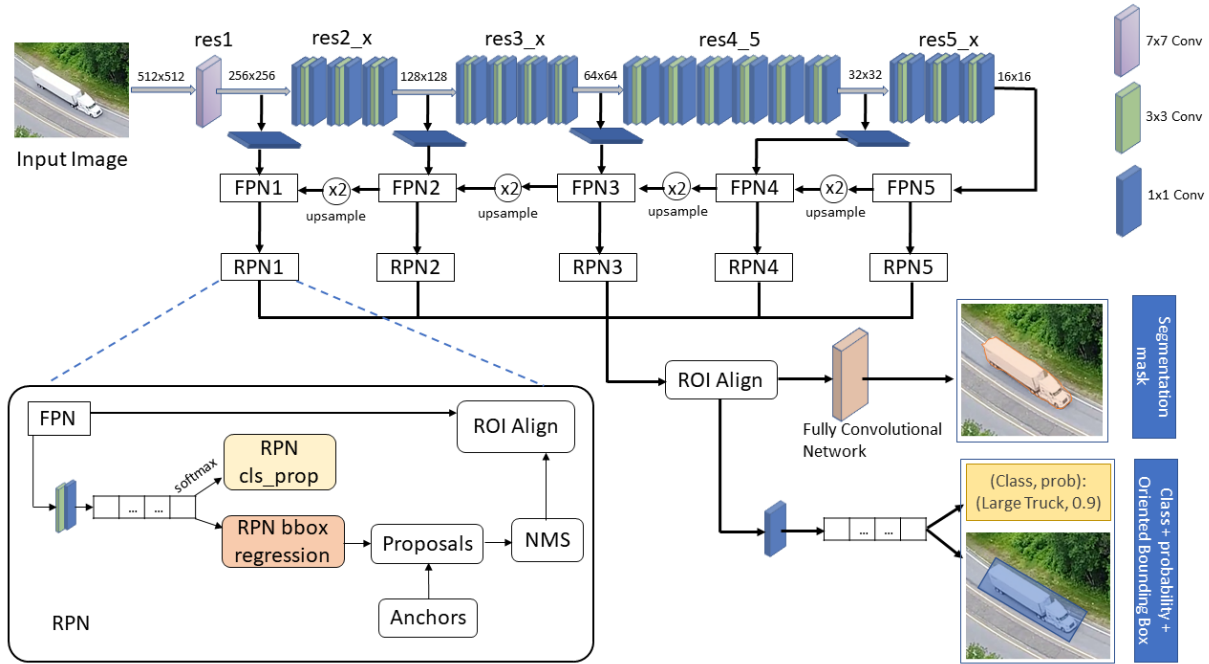
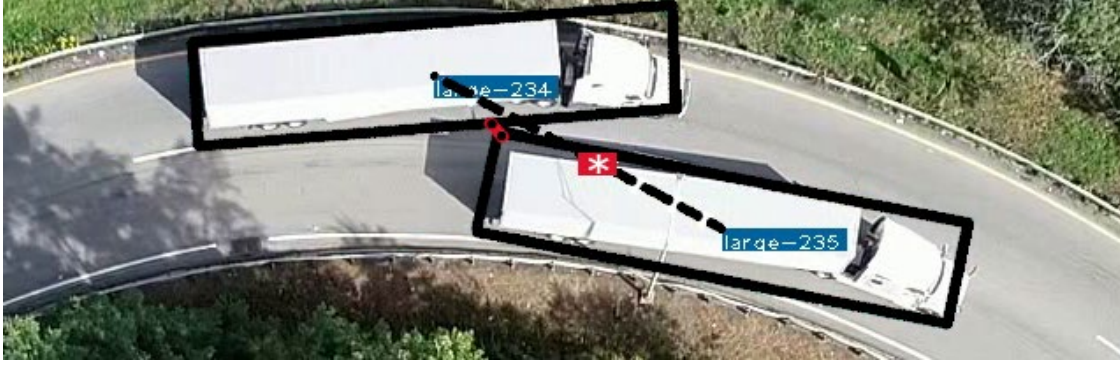


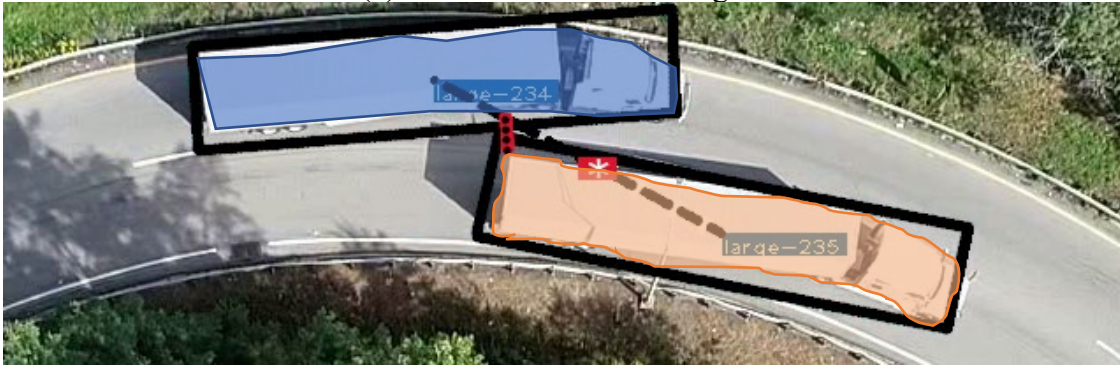
Figure 40. Overview of the Mask R-CNN model used for vehicle detection

For the backbone of the model, we chose ResNet-50 because of its relatively smaller size and similar performance compared to some of the larger models. This ensures that we have a fast and effective Mask R-CNN model. Additionally, we used FPN [72] to extract multiscale feature maps. FPN is a flexible framework that can be used with a variety of detection architectures, making it a versatile tool for object detection in different domains. Using FPN for the Region Proposal Network (RPN) further increases the model's efficacy in recalling objects. By combining features from multiple levels in the network, FPN can capture richer semantic information about the input image. This can improve the accuracy of object detection and reduce false positives. We made several additional modifications to the model, including adapting the pooling operation, using rotated non-maximum suppression (NMS), and changing the regression targets, to enable object detection with OBBs.

An advantage of using Mask R-CNN is that we can have the segmentation results. Although we use the OBB results for most of the subsequent analysis, the segmentation masks can be useful in situations where two large vehicles are traveling close to each other on a curve and there is considerable overlap between the corresponding OBBs. In this case, the segmentation results will allow us to calculate the distance more accurately between the two vehicles as shown in Figure 41. In Figure 41, the distances measured are represented by solid red lines marked by black dots.



(a) Distance measured using OBBs



(b) Distance measured using segmentation masks

Figure 41. Segmentation masks more accurately measure the distance between large vehicles

In addition to Mask R-CNN with a ResNet-50 backbone, we also implemented and tested single stage object detectors such as FCOS and Rotated-YOLO. Mask R-CNN models with ResNet-101, ResNet-152, and ResNet-164 were also tested. However, we found that bigger models did not perform any better than the ones with ResNet-50. To keep this report brief, the testing results considering other model structures are not included here.

5.4 Dataset

Our dataset includes over 3,200 high-quality images captured by drones at highway ramps. These images have been manually annotated and labelled. This section describes how we collected, prepared, and annotated these images. We would like to acknowledge the invaluable assistance provided by the MassDOT Aeronautics Division, which made this dataset possible.

The traffic videos were recorded at seven distinct sites and nine different locations within Massachusetts. One of the sites consisted of three different locations. For the recording process, a DJI drone equipped with a high-resolution 4K camera was used. The recordings were all done during the daytime, with weather conditions ranging from sunny to cloudy. Table 8 provides a summary of the video durations captured at each site, along with the corresponding numbers of annotated images/frames.

Table 8. Video datasets collected from 9 locations in Massachusetts

Location	Video duration (min)	No. of frames annotated	No. of frames selected for training and validation
Andover	15	1,674	430
Auburn	92	275	200
West Springfield North	116	184	184
West Springfield South	61	287	287
West Springfield South (Old toll)	63	194	194
Freetown North	124	169	169
Freetown South	124	36	36
New Bedford	147	200	200
Sturbridge	122	202	202
Total	874	3,221	1902

The research team thoroughly examined the recorded videos and extracted frames for annotation. The resulting images were then divided into training, validation, and testing sets, with the corresponding numbers summarized in Table 9. Additionally, Table 9 provides a summary of the numbers of vehicles of different types that appear in the training, validation, and testing datasets.

During the initial model development phase, we only had data from the Andover and Auburn sites. We annotated 1,674 images from Andover and 275 images from Auburn. Later, as more data was collected from other locations, we adjusted the numbers of images from Andover and Auburn in the training and testing sets accordingly. Ensuring a balanced distribution of images from all locations helps to improve the performance of deep learning models and reduce the risk of model overfitting.

Table 9. Vehicle types over training, validation, and testing sets after data augmentation

Data Type	Training	Validation	Testing	Total
Number of images	2,594	631	100	3,325
Number of small vehicles	18,502	4,968	522	23,992
Number of medium vehicles	1,831	417	41	2,289
Number of large vehicles (18 wheelers)	3,018	763	166	3,947

We also considered data augmentation to increase the size of our dataset and improve model performance. Random rotation, image blurring, and vertical and horizontal flipping of images are common image data augmentation techniques. For high-resolution images, another effective technique is image patching. This essentially divides the original high-resolution images into smaller patches. We applied image patching, random vertical flip, and random rotation in the range $\pm 45^\circ$ to increase the dataset size by 75% from 1,902 (Table 8) images to 3,325 (Table 9) images. Table 9 shows how the classes are distributed in the final dataset.

5.5 Evaluation

We experimented with several models to detect vehicles using OBB. All models were trained once without data augmentation and once by augmenting the data with patches. Patches are sections of the original high-resolution images that are added to the existing training and testing sets.

Table 10 presents the mean Average Precision (mAP) results of all the models tested. R-50 and R-101 represent ResNet-50 and ResNet-101 models, respectively. These two models are pretrained on the ImageNet dataset. FPN stands for Feature Pyramid Network. The Oriented Mask-RCNN model was finally chosen because of its good performance on our dataset and small size. This model outperforms other much larger models, such as the Oriented RCNN ResNet-101 model, on the augmented MassDOT aerial dataset. The chosen Oriented Mask-RCNN with ResNet-50 backbone has a total of 43.75 million parameters, which is considerably smaller than other models.

Table 10. Performance of models trained and evaluated with OBB ground truth

Model	MassDOT Aerial Dataset (Developed in this study)	Augmented MassDOT Aerial Dataset	DOTA
Faster RCNN OBB R-50-FPN	68.3	75.5	64.6
Faster RCNN OBB R-101-FPN	73.4	79.5	68.2
Oriented RCNN R-50-FPN	81.5	82.5	75.9
Oriented RCNN R-101-FPN	83.0	85.7	76.3
RetinaNet OBB R-101-FPN	82.6	84.2	70.6
Oriented FCOS R-50-FPN	78.0	80.8	72.8
Oriented Mask-RCNN R-50	81.7	86.4	76.1

The training of the Oriented Mask-RCNN model considered three types of losses: classification loss, mask loss, and OBB loss. Figure 42 shows how the different losses change over the training period. Figure 43 shows the improvement in classification accuracy as the training progresses.

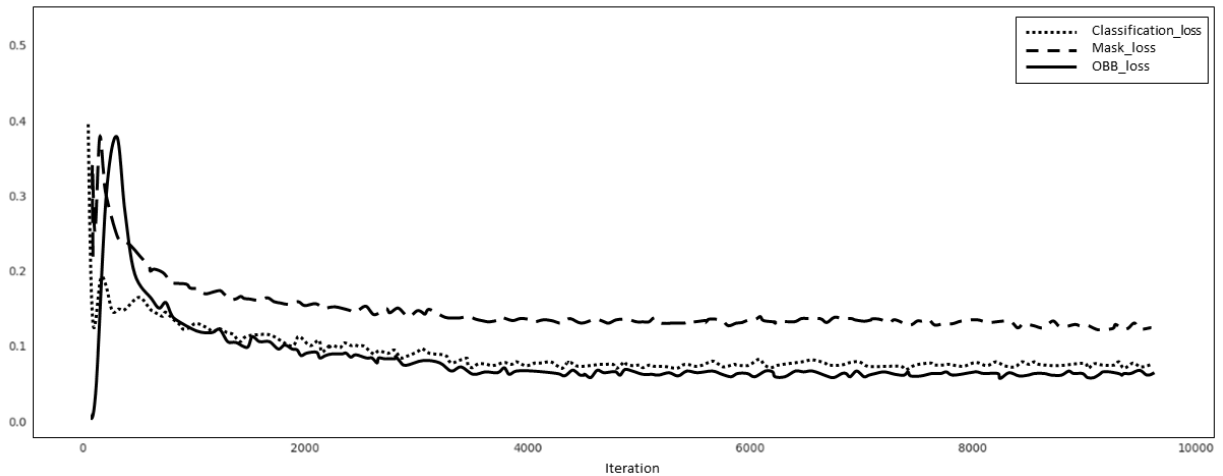


Figure 42. Changes of loss function values over the training epochs

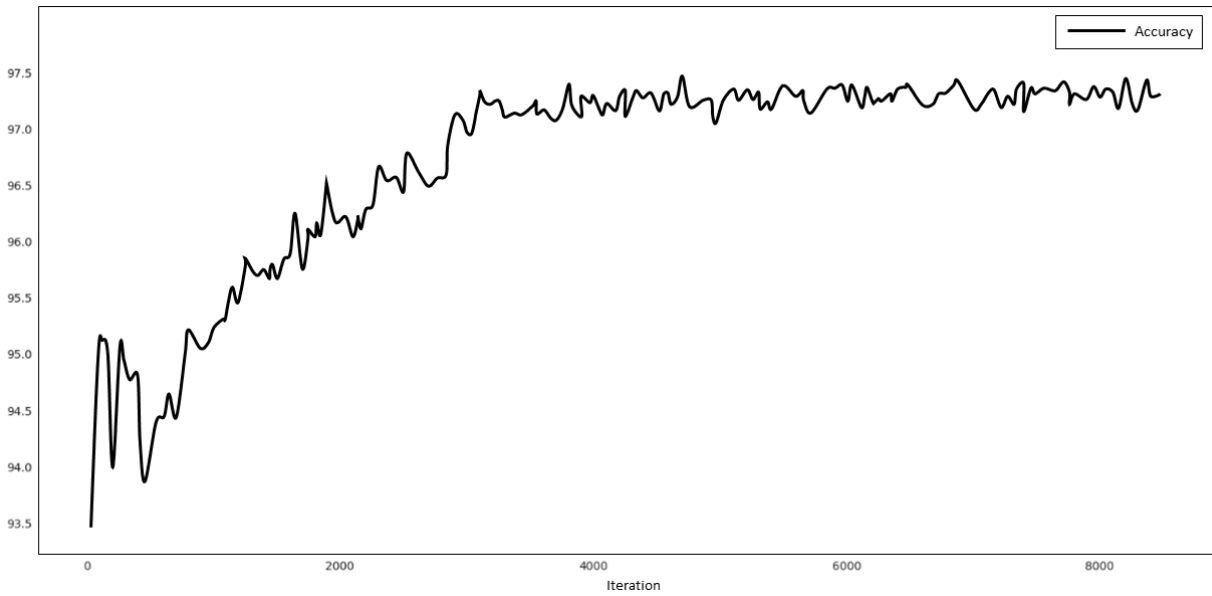


Figure 43. Overall classification accuracy improvements over time

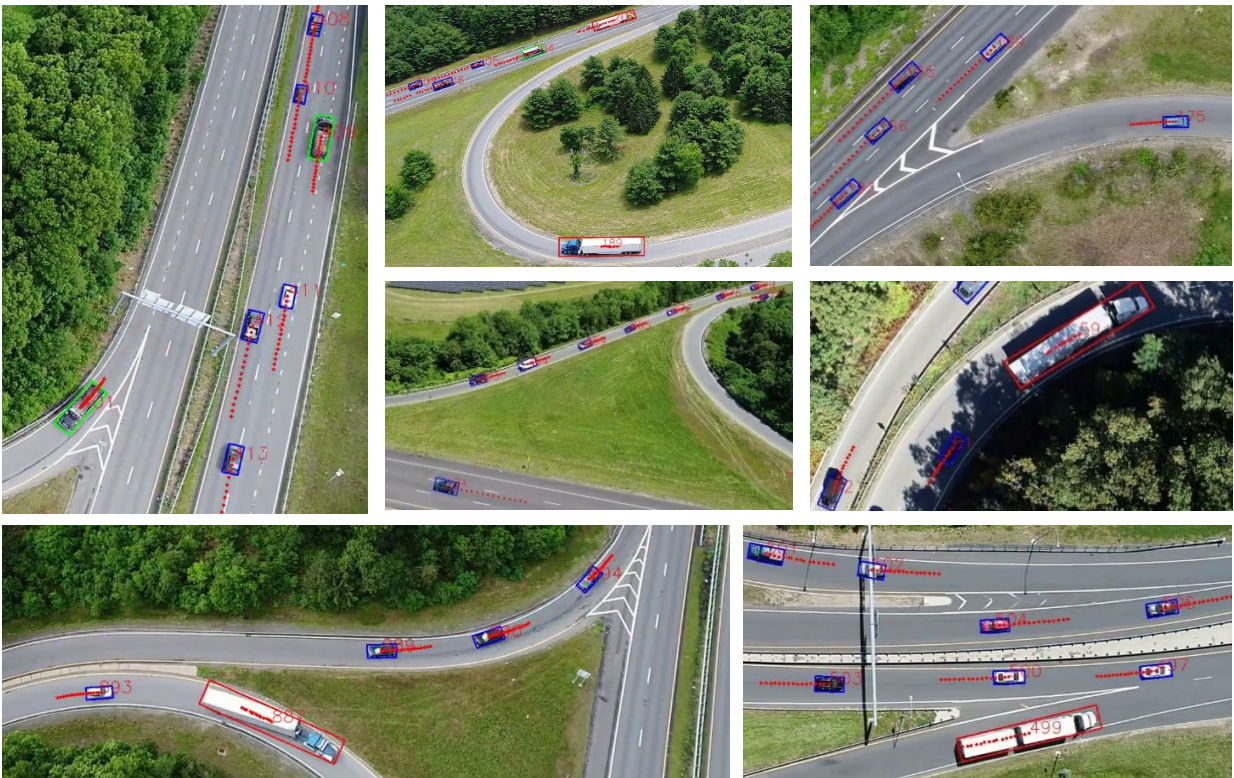


Figure 44. Detection samples of the MassDOT aerial dataset using Oriented Mask-RCNN

A few sample detection results are shown in Figure 44, suggesting that the developed object detection algorithm works very well. The vehicle detection results obtained from the algorithm

are utilized in the downstream pipeline to derive the trajectories of each vehicle. It is crucial to have accurate detection results, as poor detection performance can negatively impact the tracking accuracy. The good performance of the detection algorithm is also supported by the corresponding vehicle tracking results. We tested our tracking algorithm on a set of 10 videos. The duration of these videos ranged between 30 seconds to 45 seconds, and in total they had over 120 individual vehicles. The tracking algorithm did not lose track of any of the vehicles during the test.

SORT and Deep-SORT are two popular tracking algorithms. However, they work only on HBB, whereas our tracking method works with OBB. In comparison to the SORT algorithm, our tracking algorithm achieves a much faster performance while simultaneously reducing the computation time by 30%. The improved speed and reduced computation requirements make our tracking algorithm a more feasible and effective option for real-time tracking applications.

This page left blank intentionally.

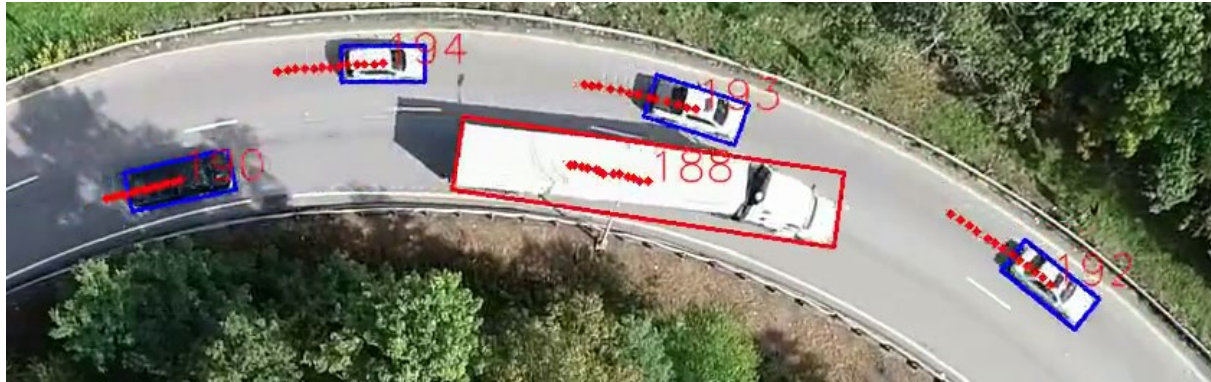
6.0 Vehicle Trajectory Processing and Analysis

6.1 Vehicle Tracking and Trajectory Smoothing

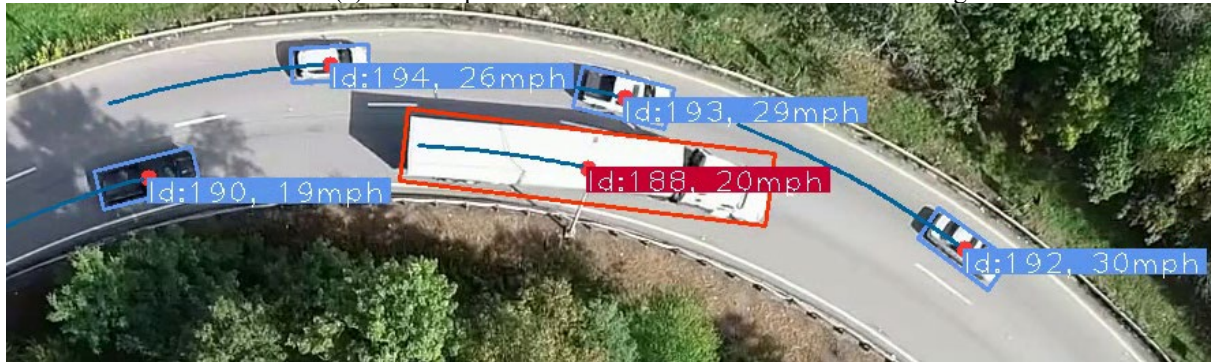
To track the detected vehicles, we developed a simple, yet very effective algorithm suited especially for OBBs. The algorithm includes a smoothing component that removes unwanted noise in the generated vehicle trajectories. Using this algorithm, the speeds and trajectories of all vehicles are generated. Additional algorithms have also been developed to analyze the trajectories and automatically identify high-risk events such as harsh decelerations and unsafe lane changes. Visualization of tracking results and speed estimation after smoothing is applied to the trajectories.

Figure 45 shows an example of how the results appear after applying the basic tracking and the post-processing smoothing algorithms. In Visualization of tracking results and speed estimation after smoothing is applied to the trajectories.

Figure 45, small vehicles are marked by blue bounding boxes and large trucks are marked by red ones.



(a) The output of the detection module with basic tracking.



(b) Visualization of tracking results and speed estimation after smoothing is applied to the trajectories.

Figure 45. Sample outputs of the vehicle detection and tracking modules

Our algorithms can effectively and accurately detect and track vehicles in most cases. However, partial occlusion due to trees, traffic signs, and highway gantries sometimes can negatively affect

the algorithm performance. Figure 46 shows some examples of how partial occlusion can result in inaccurate detection of vehicle dimension and trajectory.

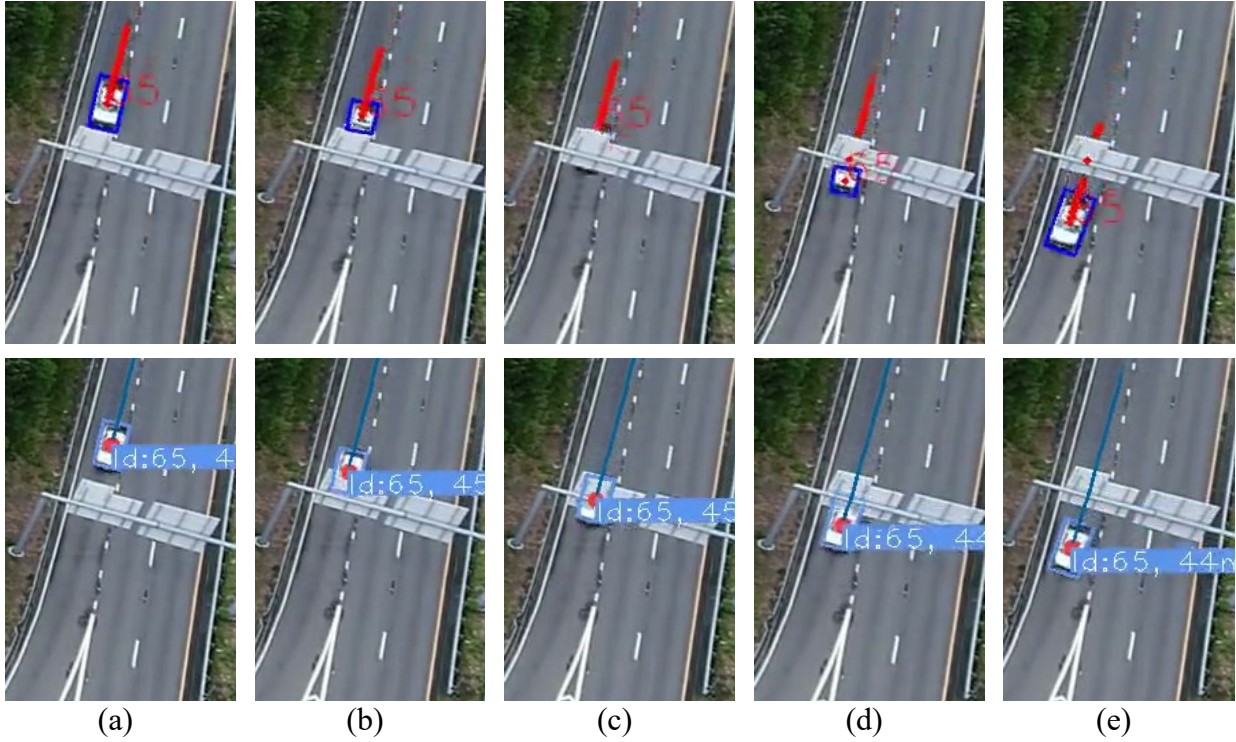


Figure 46. A small car is occluded by an overhead traffic sign at Freetown South

In addition to occlusion, detection noises might be introduced that affect the accuracy of the generated vehicle trajectory, since the detected OBBs do not always match vehicles precisely. To remove such noises and smooth out the trajectory points, we implement the Savitzky–Golay filter, a type of digital filter used to smooth out number series. The Savitzky–Golay smoothing is done by a process called convolution, which takes successive subsets of data points and fits them to a low degree polynomial. Figure 46 is an example of how this filter can be used to fill gaps in trajectories due to occlusion. In the top row, the tracking of the vehicle is done successfully, but the detection itself is inaccurate. The bottom row is the result after the Savitzky–Golay filter is applied.

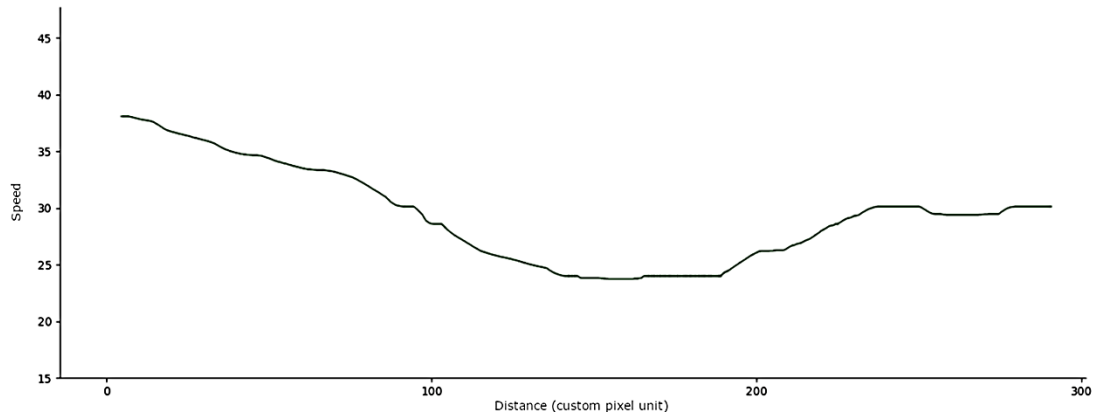
6.2 Speed Estimation

Once the OBBs and vehicle trajectories are obtained, the next step is to calculate the vehicle speeds. To achieve this, a sliding-window method is utilized, which eliminates any remaining noise that may be present in the tracking results. This process results in a smooth sequence of values, enabling accurate and reliable calculation of the vehicle speeds. Figure 47 illustrates how speeds are calculated and visualized for a vehicle of interest at the Freetown South site. This analysis can be done for any vehicles in the collected videos (e.g., for a particular travel

direction, a type of vehicle, or a specific region in the video). For the example shown in Figure 47, only vehicles taking the exit ramp are analyzed, not mainline through vehicles.



(a) The trajectory of a heavy truck. The blue lines indicate the paths along which we measure the speed.



(b) Speed profile of the truck in (a).

Figure 47. Visualization of the changing speed of a truck

To calculate speeds, it is important to accurately derive the equivalent distance of each pixel in the video. It is intuitive that pixels further away from the drone/camera should be longer than pixels right underneath the drone. To derive the corresponding distances of each pixel, one can reference the lengths of pavement markings or the lengths of vehicles. For example, the length of a typical semitrailer is 53 feet. By recording how the dimension of a semitrailer changes (measured in terms of the number of pixels) as it travels along the road, we can easily derive the equivalent distances of pixels along the path of the semitrailer. Such distances allow us to turn pixels/second into ft/second and accurately calculate vehicle speeds.

The speeds of different vehicles of the same type at the same location are averaged and these average speeds along the entire ramp are then plotted. These plots are provided in Appendix A and are used in Chapter 7 for developing safety countermeasures.

6.3 Validating the Estimated Speed Results

To evaluate the accuracy of the estimated vehicle speeds, we calculated the average speeds of individual vehicles over a selected ramp segment and compared them with the speeds estimated based on the computer vision algorithms. The average segment speeds were calculated following the steps below:

- Select two key points (e.g., light poles, beginning and ending points of a guardrail) from the video for each site.
- Record the times (t_1 and t_2) a vehicle passes the two key points based on timestamps in the drone video.
- Measure the distance (L) between the two key points using the MassDOT road network geodatabase. The average segment speed is simply $L/(t_2 - t_1)$.

The preceding average segment speeds are compared to the instantaneous speeds of individual vehicles (estimated by the computer vision algorithms) sampled at equal time intervals. If the average segment speeds are close to the average instantaneous speeds (e.g., values are only off by a small margin), the accuracy of the estimated speeds is considered acceptable, otherwise we repeat the process in Section 6.2 to further improve the speed estimation accuracy. Table 11 lists the locations and the segment distances considered to calculate the average segment speeds. Figure 48 shows the selected segments at two sites: West Springfield (North drone) and Sturbridge.

Table 11. Locations and the travel distance for average speed calculation

Location	Distance in meters
Freetown (North drone)	172
Freetown (South drone)	170
Sturbridge	270
West Springfield (North drone)	170
West Springfield (South drone)	150
West Springfield (South old toll)	93.5
Auburn	133



Figure 48. Sturbridge (top) and West Springfield (bottom) locations

6.4 Detecting High-Risk Events

Algorithm 1. Speeding detection

Input: Vehicle tracks T , threshold Θ , window α , drone video V

Output: Dictionary result: $\{\text{vehID}: [\text{frameNo}, \dots]\}$

result := $\{\}$

foreach t in T do:

 result[t.vehID] = $[\]$

for $i := \alpha$ to $V.\text{totalFrames}$:

 foreach t in T do:

 # *getSpeed()* returns the speed of a vehicle

 if $\text{getSpeed}(t.\text{vehID}, \text{from} := i - \alpha, \text{to} := i) > \Theta$:

 result[t.vehID].append(i)

return result

The speed estimation and trajectory results are further used to automatically identify high-risk events, such as speeding, sudden decelerations, stalled vehicles, risky lane changes, and last-minute lane changes. Six algorithms have been proposed in this study to detect the above risky events. These algorithms are developed in a generic way such that they can be reused at all

locations without modifications. In all the algorithms, T refers to the collection of trajectories for all vehicles of interest. Threshold Θ and window α are the speed threshold and sliding window width, respectively. The first algorithm provided above is for detecting speeding vehicles.

Algorithm 2 is for detecting vehicles that follow other vehicles too closely. The `getDistFromVeh()` function returns the minimum distance between two vehicles (i.e., Oriented Bounding Boxes); however, if the distance between two oriented bounding boxes is smaller than 10 pixels, this function then returns the minimum distance between the segmentation masks of the two vehicles for reasons illustrated in Figure 41.

Algorithm 2. Traveling too close to other vehicles

Input: Vehicle tracks T , dist threshold Θ , drone video V
Output: Dictionary result: $\{\text{vehID:}[(fNo, \text{vehID}), \dots]\}$
 $\text{result} := \{\}$
foreach t in T do:
 $\text{result}[t.\text{vehID}] = []$
for $i := 1$ to $V.\text{totalFrames}$:
 foreach t in T do:
 # *getDistFromVeh()* returns a list of tuples,
 # returns a list: $[(vehID, dist), \dots]$
 $\text{distance_list} = \text{getDistFromVeh}(i, t.\text{VehID}, T)$
 if $\text{len}(\text{distance_list}) \neq 0$:
 foreach d in distance_list do:
 if $d[1] > \Theta$:
 $\text{result}[t.\text{vehID}].\text{append}(i, d[0])$
return result

We have also developed and implemented an algorithm (Algorithm 3) to detect vehicles that are about to run off the highway. This was done using a segmentation mask of the road. Under normal conditions, taking a union of the road mask and a vehicle OBB will result in the same area as that of the road mask. However, if a vehicle is too close to the pavement edge, taking a union of the two would result in an increased area. Since we did not have actual run-off-road incidents to test this algorithm, it was tested using some generated synthetic data.

Algorithm 3. Vehicles moving out of the road

Input: Vehicle tracks T , road segmentation mask σ , drone video V
Output: Dictionary result: $\{\text{vehID:}[\text{frameNo}, \dots]\}$
 $\text{result} := \{\}$
foreach t in T do:
 $\text{result}[t.\text{vehID}] = []$
for $i := 1$ to $V.\text{totalFrames}$:
 foreach t in T do:
 if $\text{getAreaOfUnion}(t.\text{vehID}, \sigma) \neq \text{Area}(\sigma)$:
 $\text{result}[t.\text{vehID}].\text{append}(i)$
return result

Algorithm 4 is to detect stalled vehicles. We define stalled vehicles as cars and trucks that are completely stationary within a short time window. This time window is defined in terms of the number of video frames.

Algorithm 4. Stalled vehicle detection

Input: Vehicle tracks T , window α , drone video V

Output: Dictionary result: {vehID: [frameNo,...]}

result := {}

foreach t in T do:

 result[t.vehID] = []

for $i := \alpha$ to V .totalFrames:

 foreach t in T do:

 # *getSpeed(vID, x, y)* returns the avg. speed of a

 # vehicle vID between frame no. x and y

 if $\text{getSpeed}(t.\text{vehID}, \text{from} := i - \alpha, \text{to} := i) = 0$:

 result[t.vehID].append(i)

return result

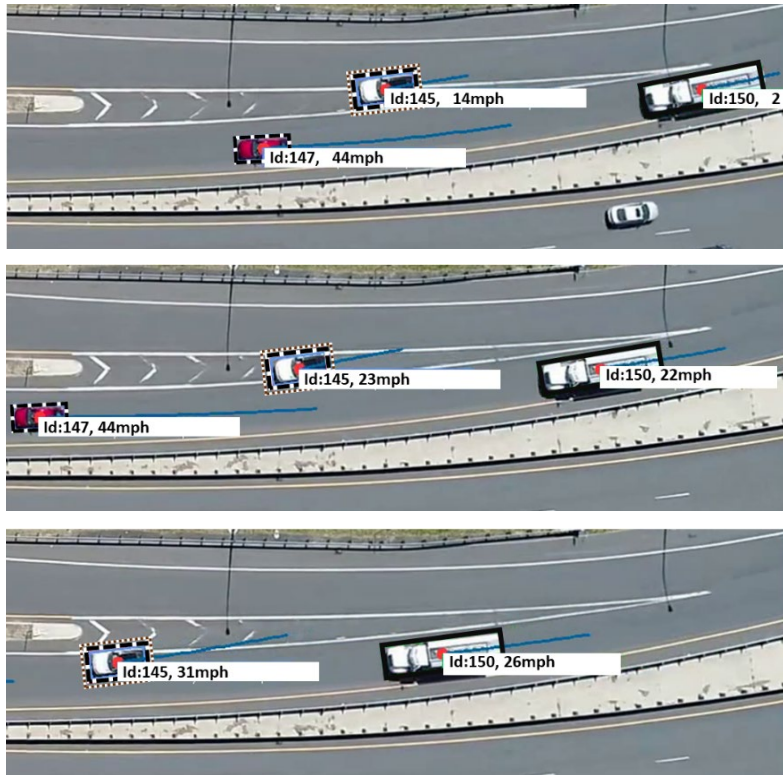


Figure 49. A medium-sized vehicle is seen to slow down so that a vehicle in front of it can safely merge onto the freeway

A simple modification of Algorithm 4 enables it to detect both stalled and slow-moving vehicles (Algorithm 5). Using Algorithm 5 together with road segmentation allows us to detect vehicles that slow down or stop in areas of interest. With this method, we were able to detect quite a few

slow-moving vehicles in the gore area at the West Springfield (South drone) site. These vehicles were singled out if they spent more than 1.5 seconds either on the exit lane or in the gore area before being able to merge into the through lane. A detected example is shown in Figure 49, where vehicle #145 first slowed down, waited in the gore area, and accelerated to merge. A medium-sized truck (vehicle #150, indicated by a solid black OBB) had to slow down so that vehicle #145 could safely merge. During the 1-hour data collection period, we observed multiple scenarios like this, which indicates that this weaving area (Figure 50) is not providing sufficient length for vehicles to safely weave and merge. In Figure 50, the red dot corresponds to the gore area in Figure 49.

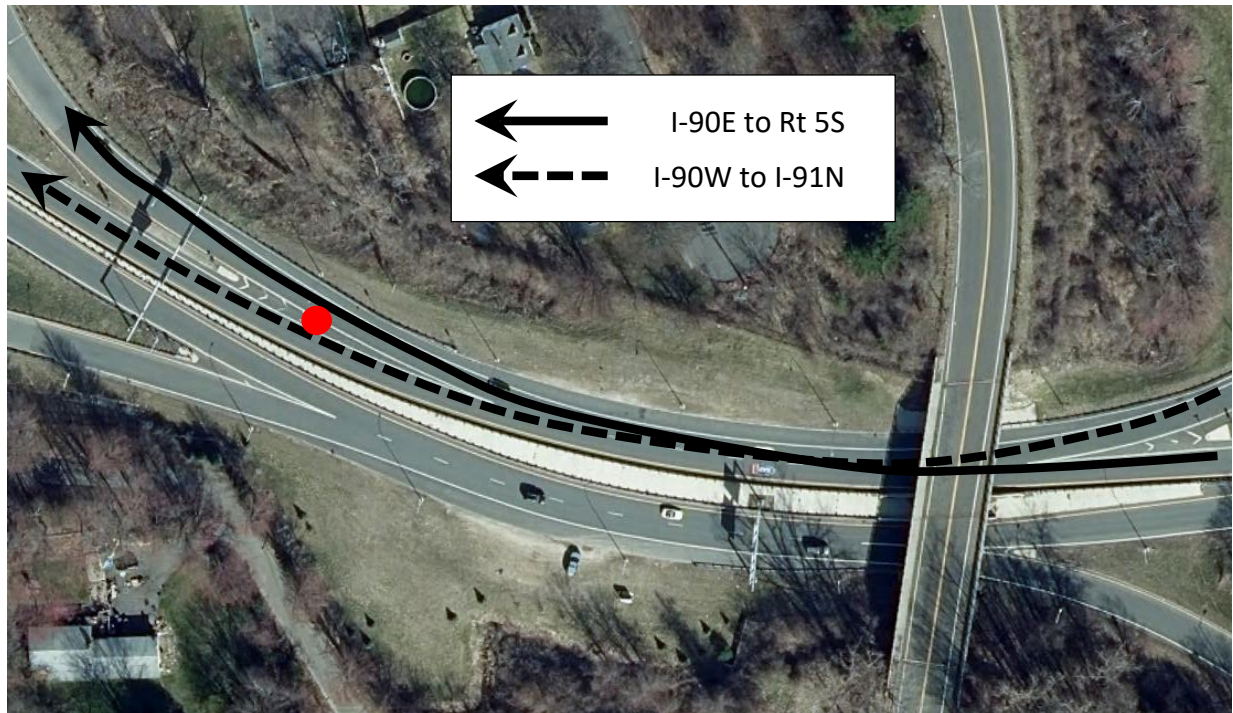


Figure 50. Weaving area at the West Springfield site (South drone)

Sudden lane changes and last-minute decisions to take the exit are very dangerous. Figure 51 shows two such instances recorded at the Freetown South and West Springfield (South drone) locations. Late and sudden lane changes are defined as incidents that occur within 120 feet of the gore area. Algorithm 6 was applied to the West Springfield (South drone) and the Freetown South locations.

Algorithm 5. Stalled/Slow vehicle on exit pavement marking

Input: Vehicle tracks T , threshold Θ , window α , road segmentation mask σ , drone video V
Output: Dictionary result: $\{\text{vehID}: [\text{frameNo}, \dots]\}$
result := {}
foreach t in T do:
 result[t.vehID] = []
for $i := \alpha$ to $V.\text{totalFrames}$:
 foreach t in T do:
 if $\text{getSpeed}(t.\text{vehID}, \text{from} := i - \alpha, \text{to} := i) < \Theta$ and
 $\text{getAreaOfUnion}(t.\text{vehID}, \sigma) \neq \text{Area}(\sigma)$:
 result[t.vehID].append(i)
return result

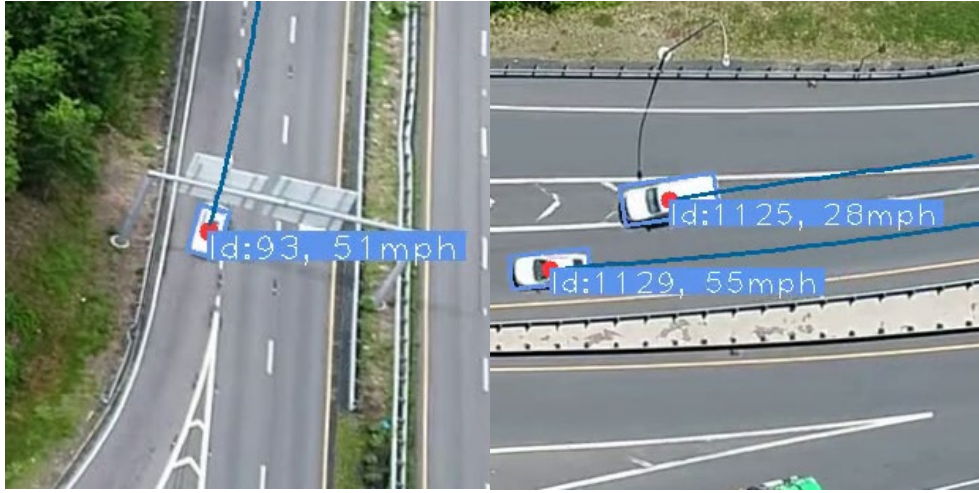


Figure 51. Unsafe lane changes: (left) Freetown South, (right) West Springfield South

Algorithm 6. Late lane changes

Input: Vehicle tracks T , threshold Θ , lane segmentations: $(\sigma_0, \sigma_1, \dots, \sigma_n)$, window α , drone video V
Output: Dictionary result: $\{(\text{vehID}: \text{frameNo}), \dots\}$
result := {}
for $i := 1$ to $V.\text{totalFrames}$:
 foreach t in T do:
 if $\text{getLane}(t.\text{vehID}, \sigma) \neq \text{getLaneHistory}(t.\text{vehID}, \alpha)$
 and
 $\text{vehicleLocation}(t.\text{vehID}) < \Theta$:
 result[t.vehID] := i
return result

The parameters used in these six algorithms are fine-tuned to better suit the characteristics of the sites studied in this research. Such parameters can be easily modified so that these algorithms can

be applied to other sites in the future. We also manually reviewed all videos to identify risky events. The manually identified risky events were compared to those detected by the proposed algorithms and they overall matched well.

6.5 Visualizing Risky Events using t-SNE

t-Distributed Stochastic Neighbor Embedding (t-SNE) is an unsupervised machine learning algorithm widely used for exploratory data analysis and visualizing high-dimensional data. It is also adopted in this study for modeling and visualizing high-dimensional vehicle speed profiles in a 2D space. One objective of adopting this machine learning algorithm is to see whether it can automatically filter out unsafe driving behavior or trajectories. Figure 52 through Figure 60 show the t-SNE visualizations of vehicles' speed profiles from different locations. These figures suggest that small and large vehicles clearly exhibit different speed profiles. Most large trucks are grouped together at the bottom, while small and medium vehicles are not clearly separated based on their speed profiles.

While t-SNE plots can reveal underlying patterns or structures in data, it can be difficult to interpret the plots accurately. The clustering of data points in t-SNE plots may not always correspond to meaningful groupings or categories in the data. In Figure 52, most of the rapid decelerations are on the left of the graph. In Figure 53, which shows t-SNE for West Springfield South, incidents of late lane changes and stalling over the pavement markings (Figure 80c later in this report) are on the right.

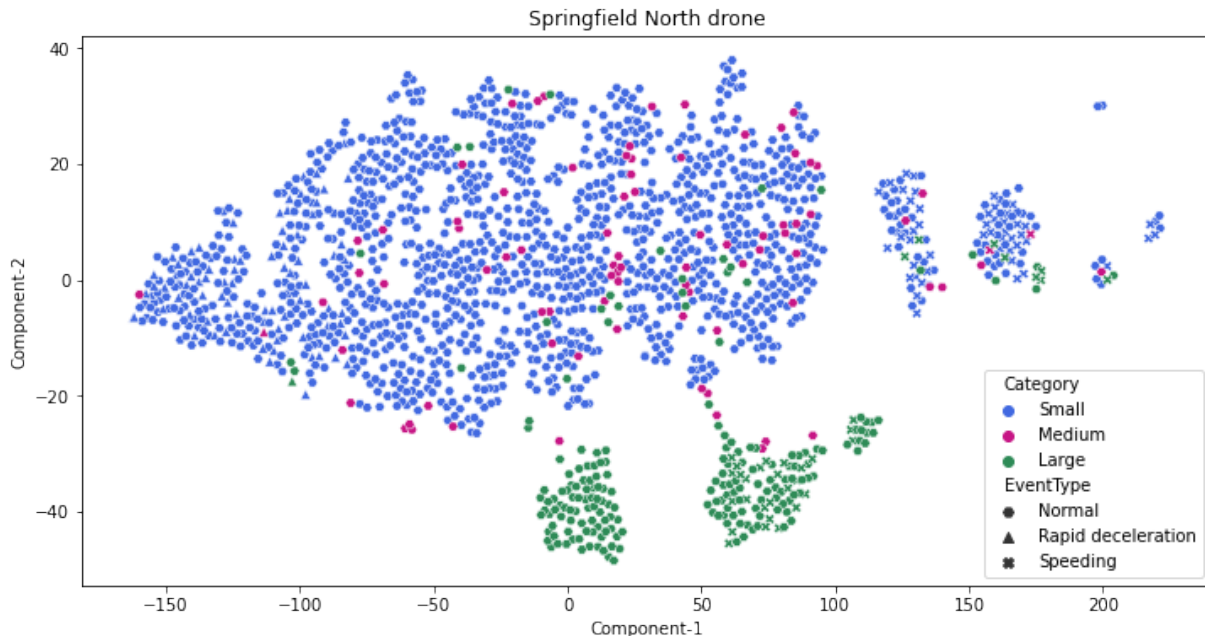


Figure 52. t-SNE for West Springfield North

In Figure 54, most of the late lane changes appear to be on the upper left quadrant of the visualization. This location of the Freetown North drone (Figure 55) does not have many

vehicles taking the exit. Those taking the exit late appear to be concentrated in the bottom of the plot. In Figure 56, a few incidents of rapid deceleration are concentrated in the upper left of the plot. However, the incidents of taking the exit late are scattered across the plot without a clear pattern. In Figure 57, vehicles following closely are concentrated toward the right.

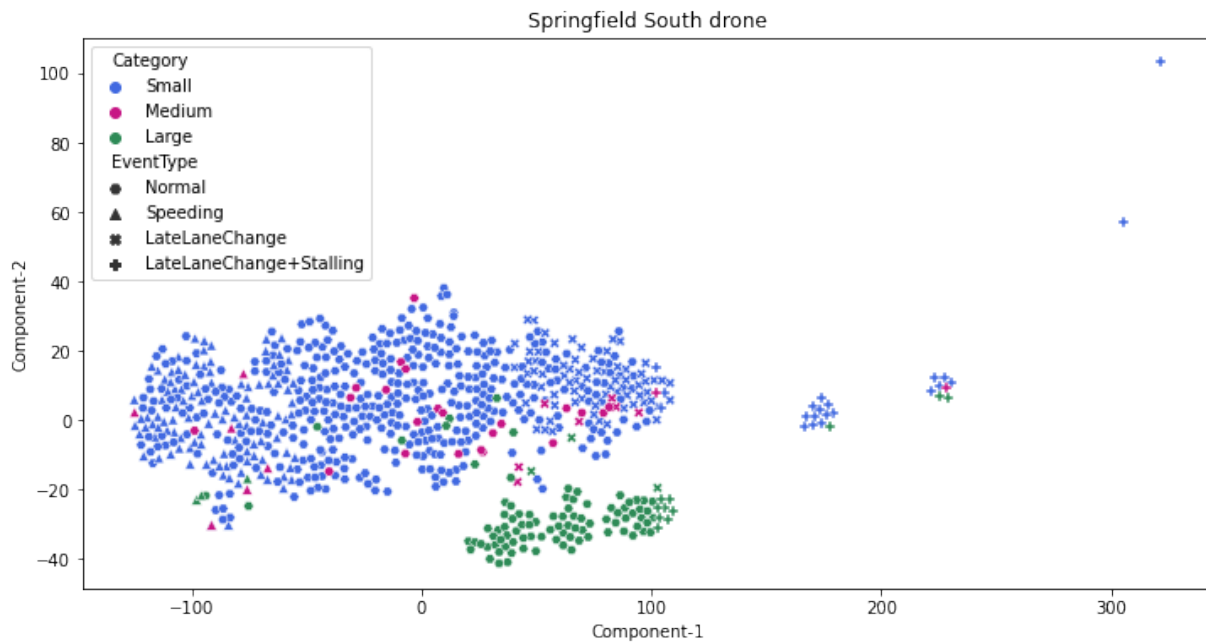


Figure 53. t-SNE for West Springfield South

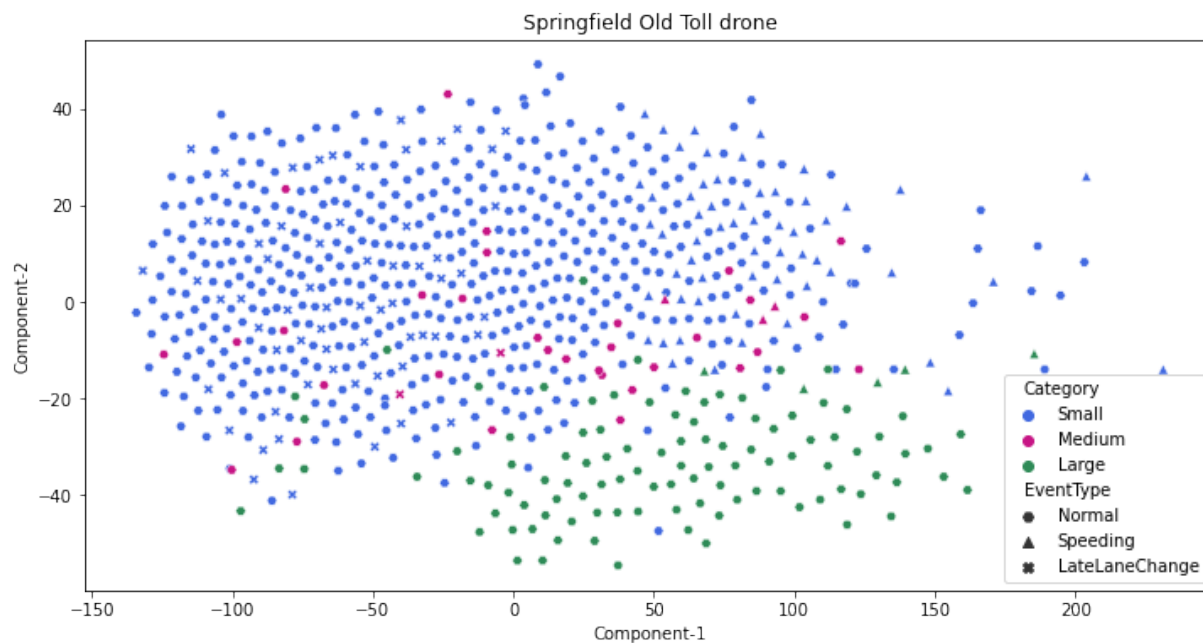


Figure 54. t-SNE for West Springfield, old toll gate

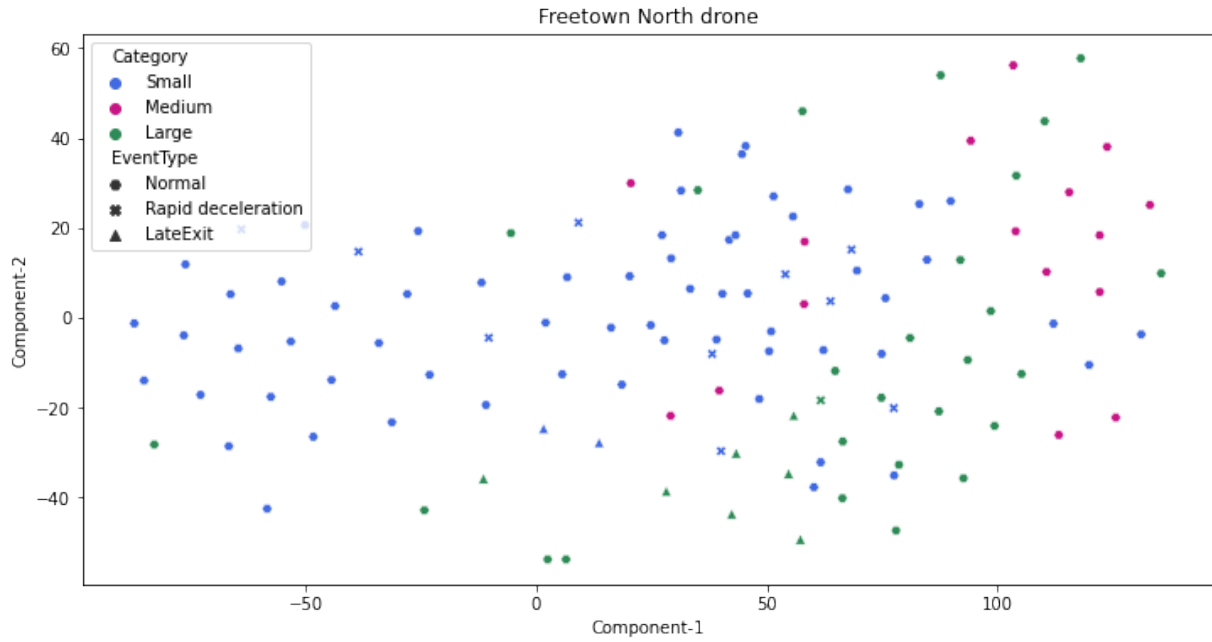


Figure 55. t-SNE for Freetown North drone

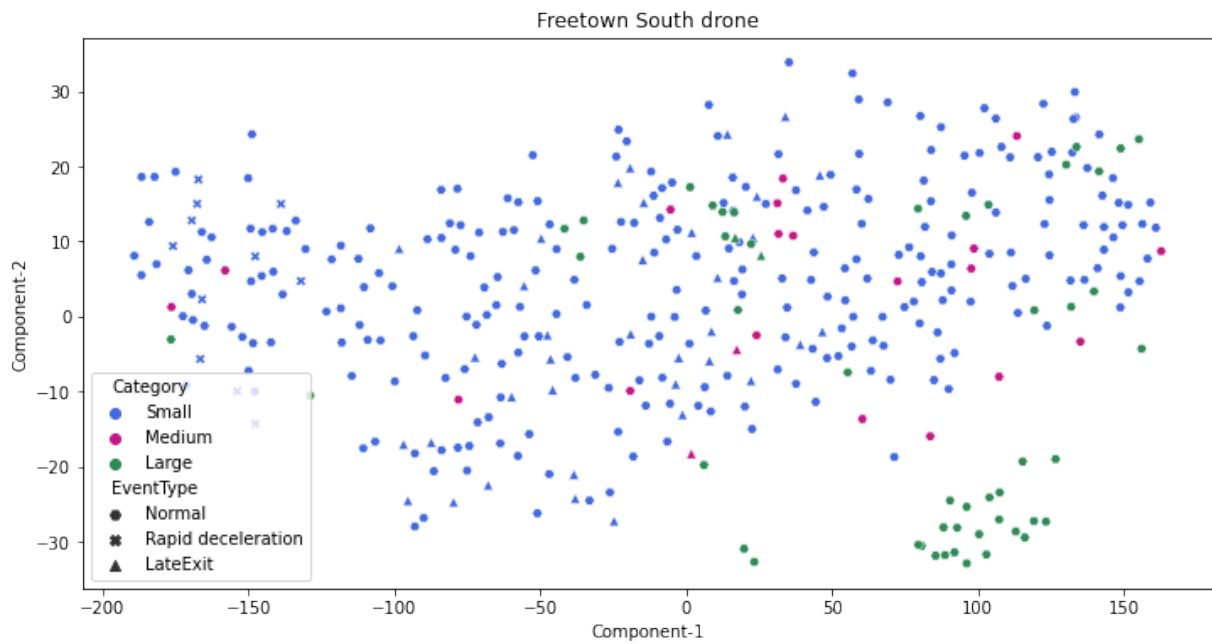


Figure 56. t-SNE for Freetown South drone

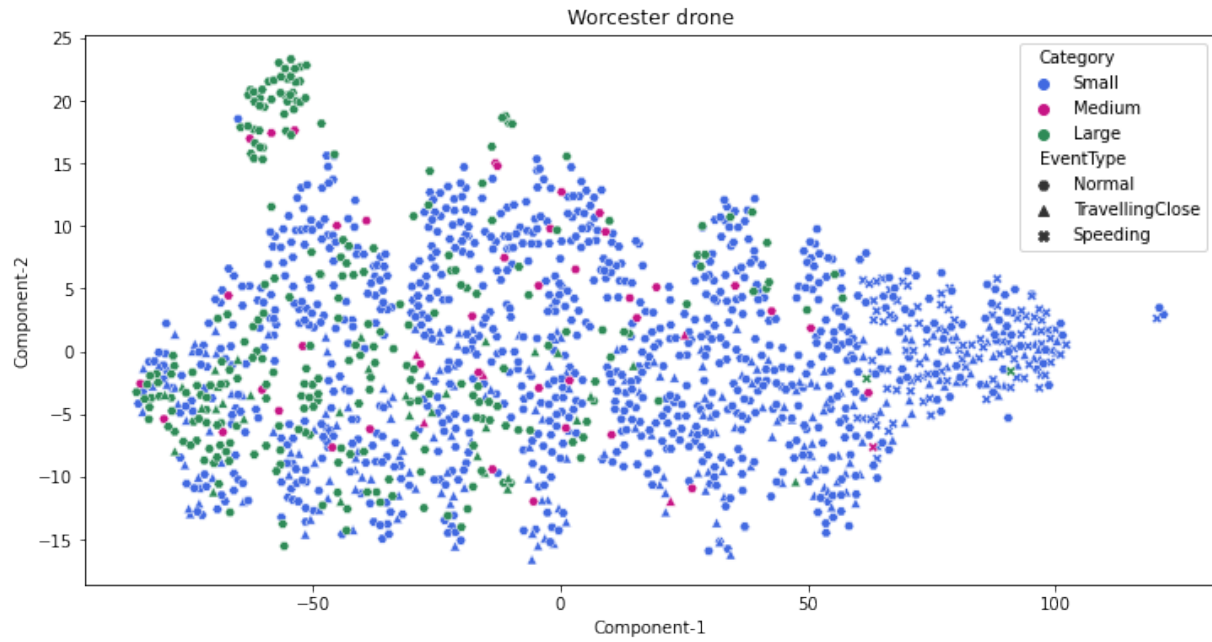


Figure 57. t-SNE for Auburn (or Worcester)

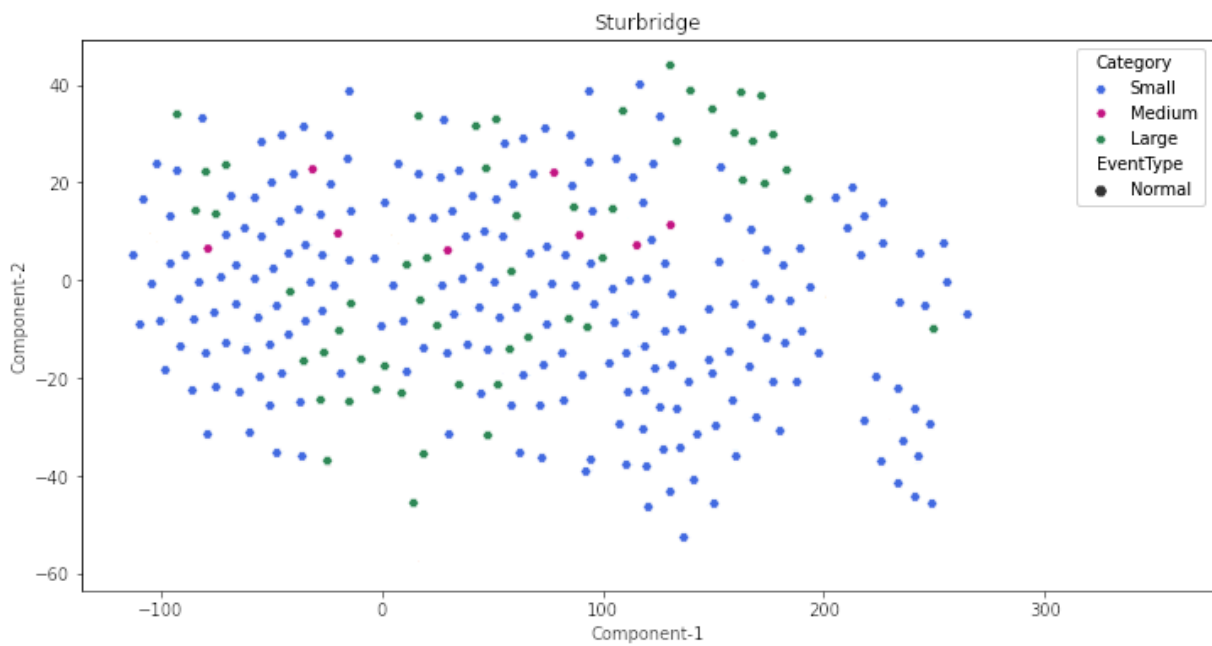


Figure 58. t-SNE for Sturbridge

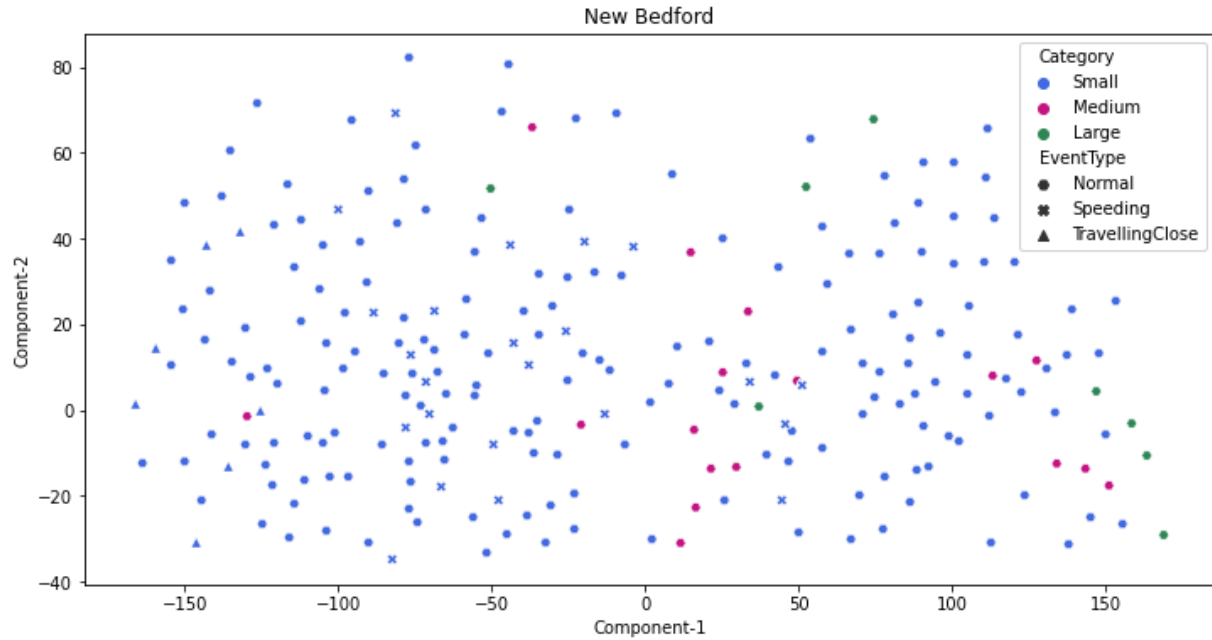


Figure 59. t-SNE for New Bedford

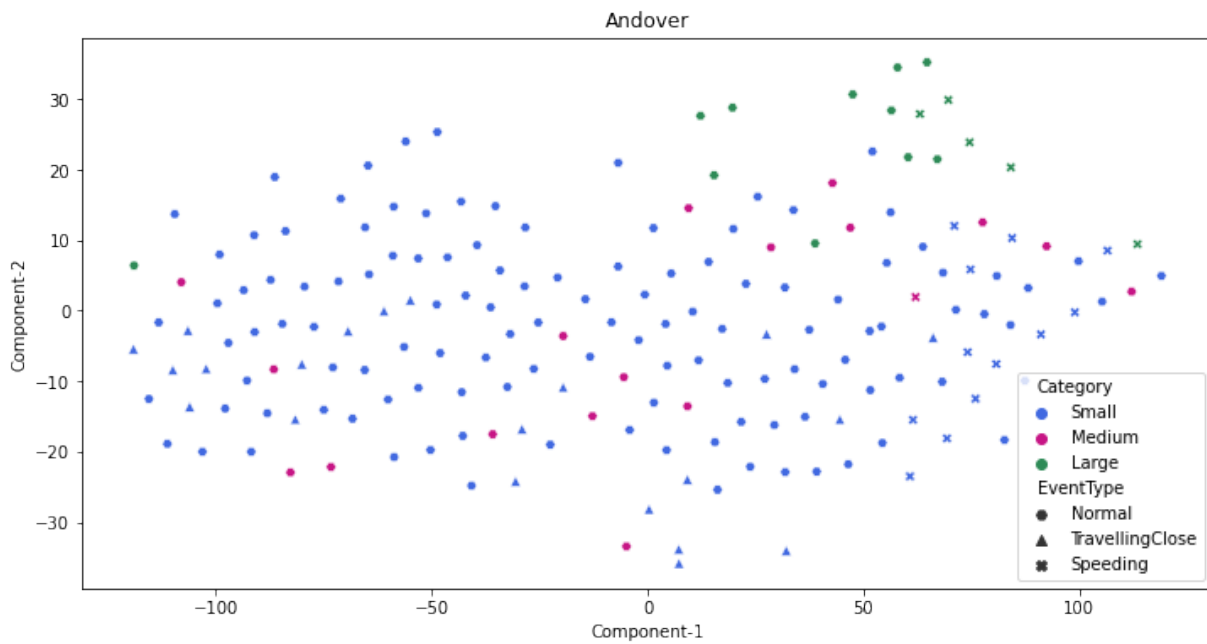


Figure 60. t-SNE for Andover

6.6 Vehicle Speed Profile Clustering Analysis

With the processed speed data in hand, we can further analyze and understand driving patterns at each ramp. For instance, we have calculated the average speeds at different cross sections of a

ramp. Another application is to perform a clustering analysis on the trajectory data. Cluster Analysis or clustering categorizes data points (vehicle trajectories in this study) into different clusters/groups so that similar data points are assigned to the same group.

Commonly used clustering algorithms are not directly applicable to time series or trajectory data. Several modifications to the basic clustering algorithms have been proposed to adapt them for trajectory and time series data clustering [73,74,75]. For the modified clustering algorithms, the distance measure is a critical component of the clustering process [58].

In our study, we did not simply use the original speed profiles of individual vehicles as the input for clustering analysis. Instead, we calculated the differences between the observed speeds and the mean speeds of all vehicles in that category at different cross sections. The speed differences for each vehicle were used as the input for clustering analysis. Figure 61 shows the speed profile clustering result for the West Springfield-South location using the modified DBSCAN algorithm [74] which groups the speed profiles based on how similar or dissimilar they are. Figure 62 is the speed profile clustering results for the West Springfield-Old toll gate location.

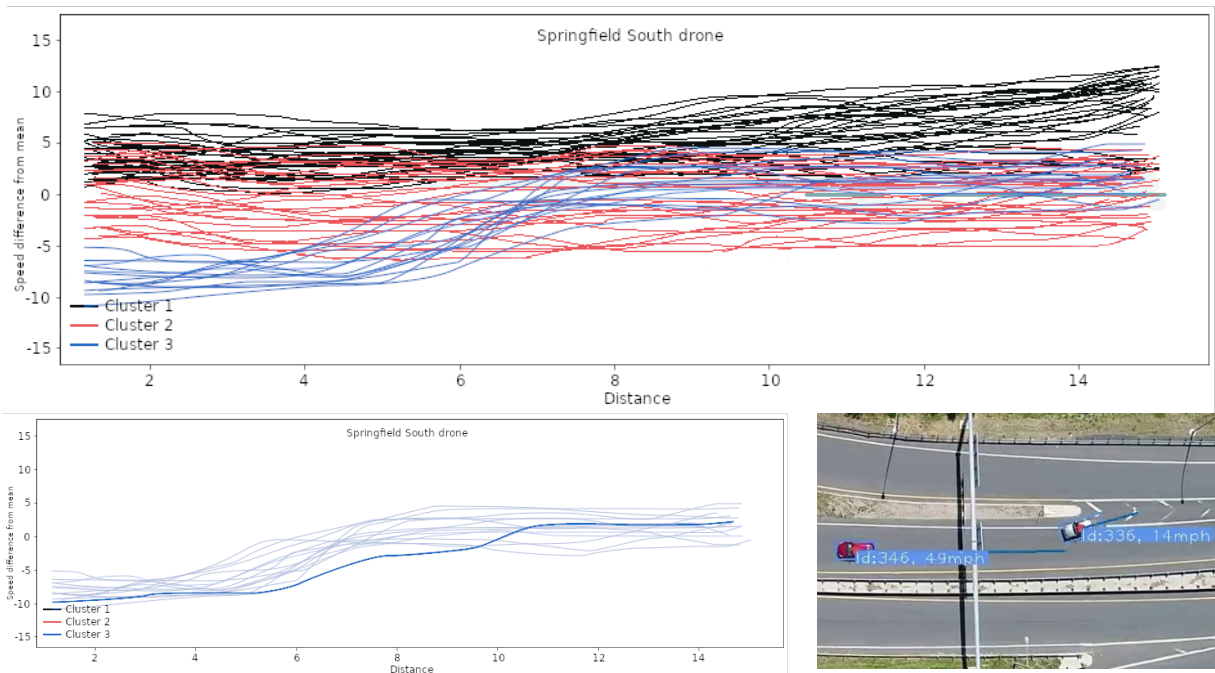


Figure 61. Speed profile clustering for West Springfield South

In Figure 61, the lower chart highlights one specific vehicle from the West Springfield-South location. This vehicle's speed profile belongs to category 3. We further examined the speed profiles in category 3 and found that they are mostly for vehicles that start slowly and sometimes even come to a full stop. These vehicles often face challenges to safely merge into the through lane. The results suggest that clustering analysis can potentially be used to automatically identify abnormal or risky driving behavior as well.

Distances (i.e., horizontal axis) in all figures in this section are relative as we used a custom pixel unit to allow alignment and aggregation of vehicles from different locations. Additional clustering analysis results are presented in Figure 62 through Figure 69. For the remaining sites, the clustering analysis sometimes did not yield meaningful results because the speed profiles were too similar. Specifically, for West Springfield-North, Auburn (also called Worcester in this report), Andover and Sturbridge, the clustering algorithm yielded only one trajectory cluster. Further research and experimentation with other clustering algorithms is needed. Another possible reason is that the sample sizes are too small.

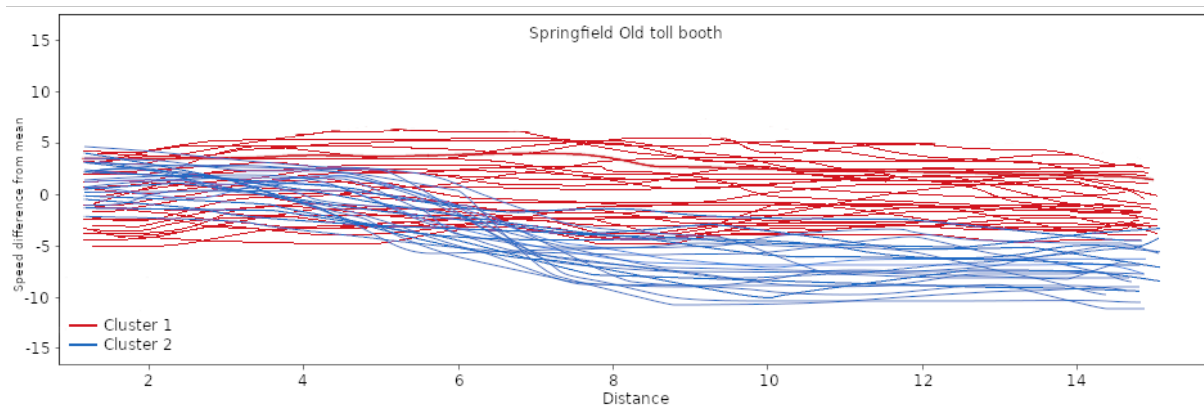


Figure 62. Clustering result of West Springfield-Old toll gate

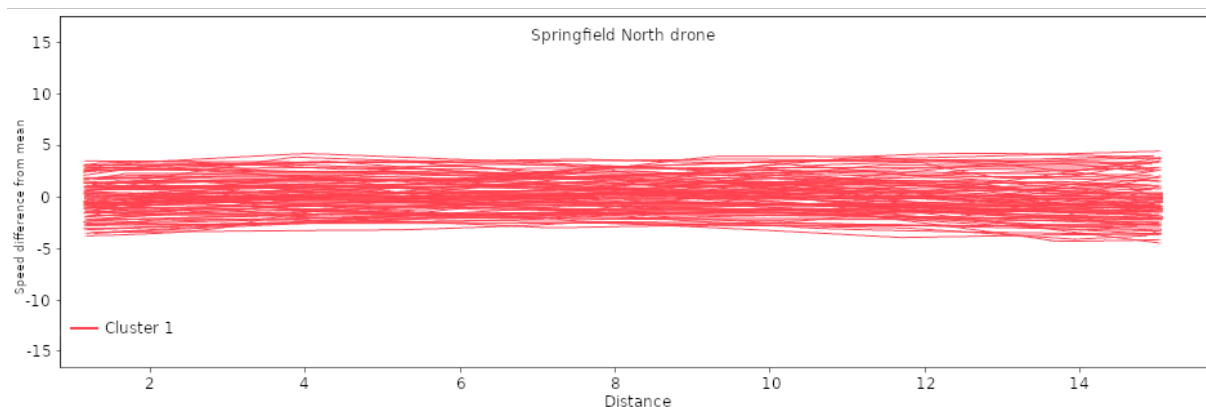


Figure 63. Clustering result of West Springfield-North

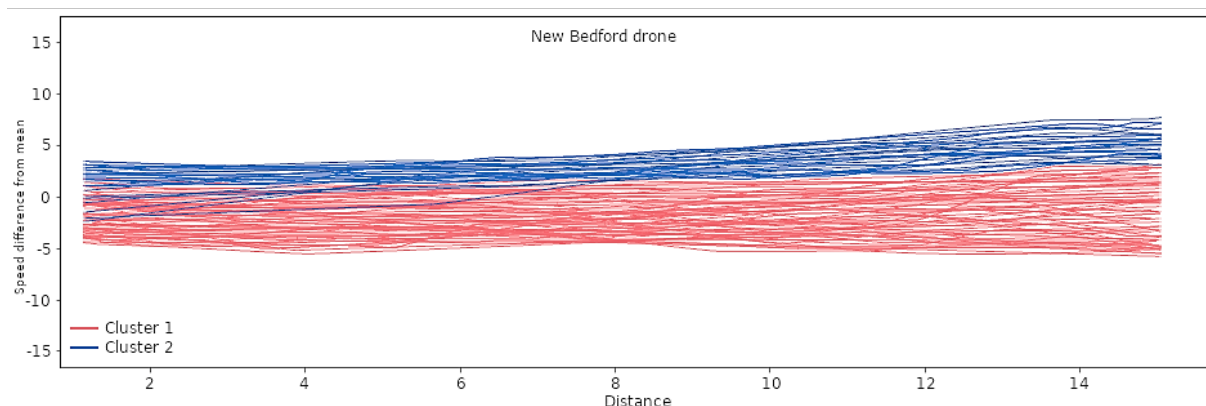


Figure 64. Clustering result of New Bedford

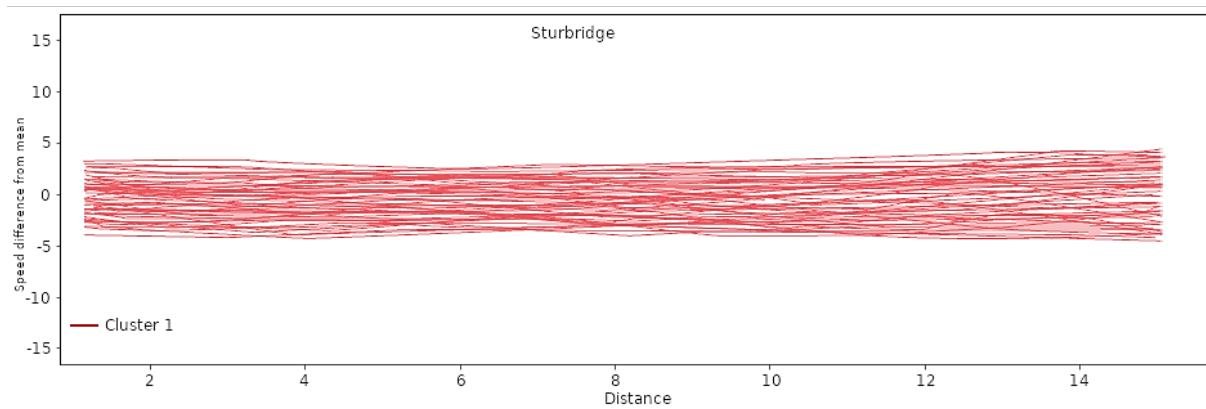


Figure 65. Clustering result of Sturbridge

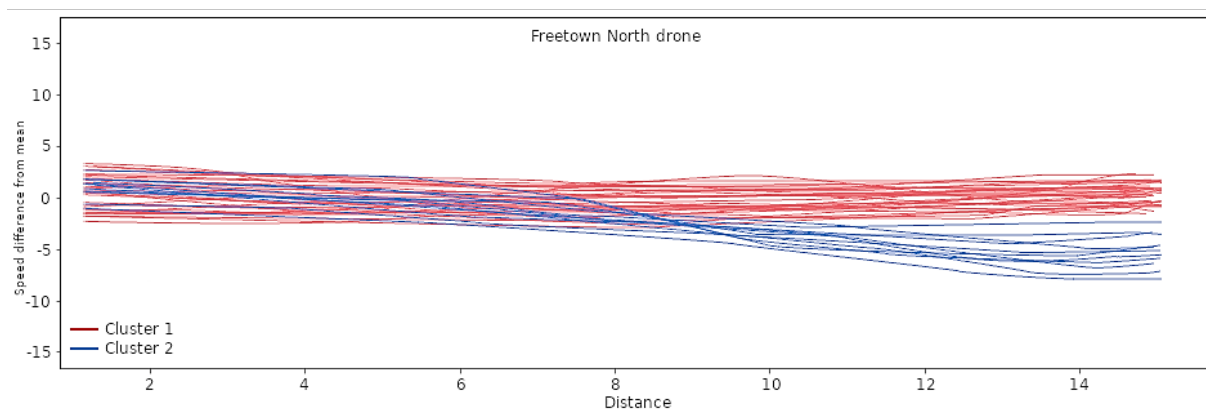


Figure 66. Clustering result of Freetown North

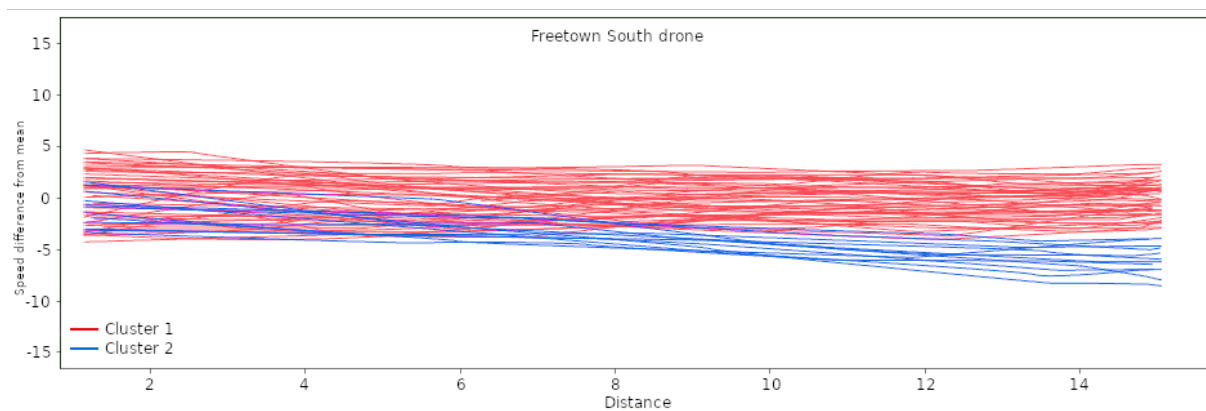


Figure 67. Clustering result of Freetown South

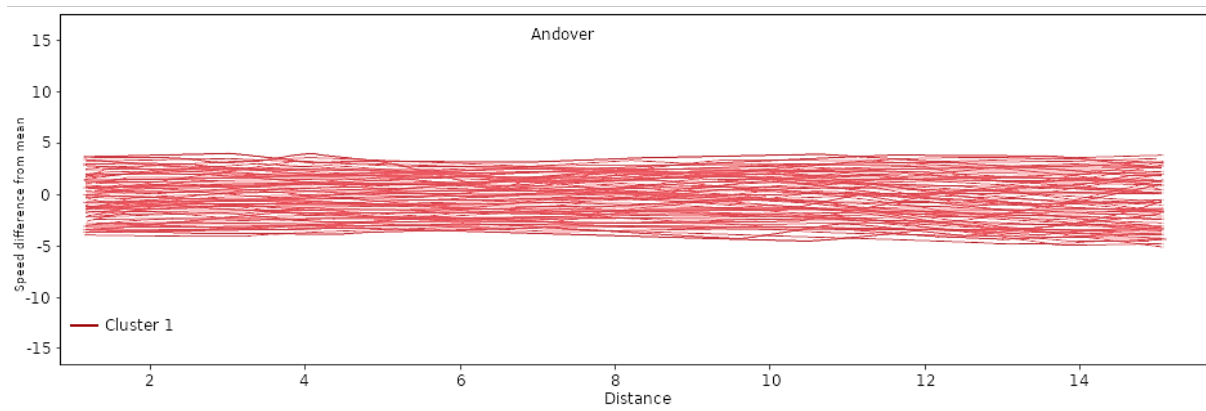


Figure 68. Clustering result of Andover

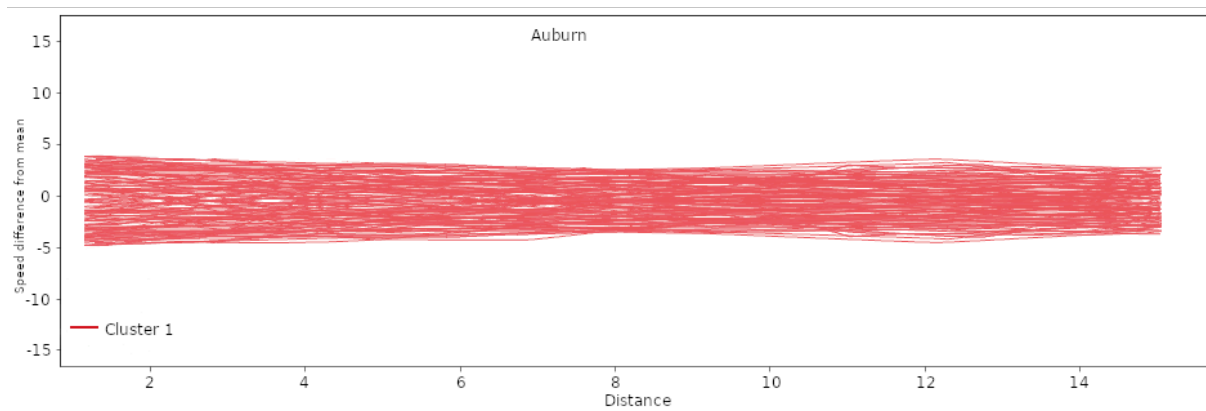


Figure 69. Clustering result of Auburn

7.0 Detailed Site Analysis and Recommendations

This chapter provides a detailed analysis of each site and specific recommendations for improving ramp safety. The analysis and recommendations are mainly based on the following factors: locations and types of traffic signs, slope, curve radius, crash history, and observed vehicle trajectories. The slopes and radii of the selected ramps are provided in Figure 83 through Figure 89 at the end of this chapter. The traffic volume information at these sites is provided in Table 12.

Table 12. Observed traffic volumes at the selected ramps

Location	Truck rollovers (1/2015–2/2022)	Observed Volume				Hourly Volume			
		Small	Medium	Large	Total	Small	Medium	Large	Total
Andover	0	58	2	6	66	232	8	24	264
Auburn (Worcester)	4	1,228	48	310	1,586	801	31	202	1,034
West Springfield North	4	1,371	84	240	1,695	709	43	124	877
West Springfield South	0	673	37	118	828	662	36	116	814
West Springfield Old toll gate	0	1,093	55	141	1,289	1,041	52	134	1,228
Freetown North	2	69	17	34	120	33	8	16	58
Freetown South	1	337	11	37	385	163	5	18	186
New Bedford	2	993	71	28	1,092	405	29	11	446
Sturbridge	3	65	8	82	155	32	4	40	76

7.1 Andover Site

This ramp is in Andover, MA connecting I-495N to I93N. There are two 25 mph advisory speed signs located close to each other at the beginning of the ramp as shown in Figure 70. This ramp has a roughly -1.5% slope, which was derived using the LiDAR data obtained from the United States Geological Survey (USGS) website. The elevation profile of this ramp is shown in Figure 83.

Andover was the first site that we collected data from. It was selected mainly because there was a parking lot there owned by MassDOT that made it an ideal location for testing the drone. From January 2015 to February 2022, there were no heavy truck rollovers at this site. Since it was the first site, we spent a lot of time testing the drone and experimenting with different altitudes and angles. Therefore, we only obtained about 15 minutes of useful videos from this site. During this short period, we observed two types of risky events listed in Table 13: (1) approaching too fast or

following too closely, and (2) last-minute lane change. Some examples of such risky events are provided in Figure 71.

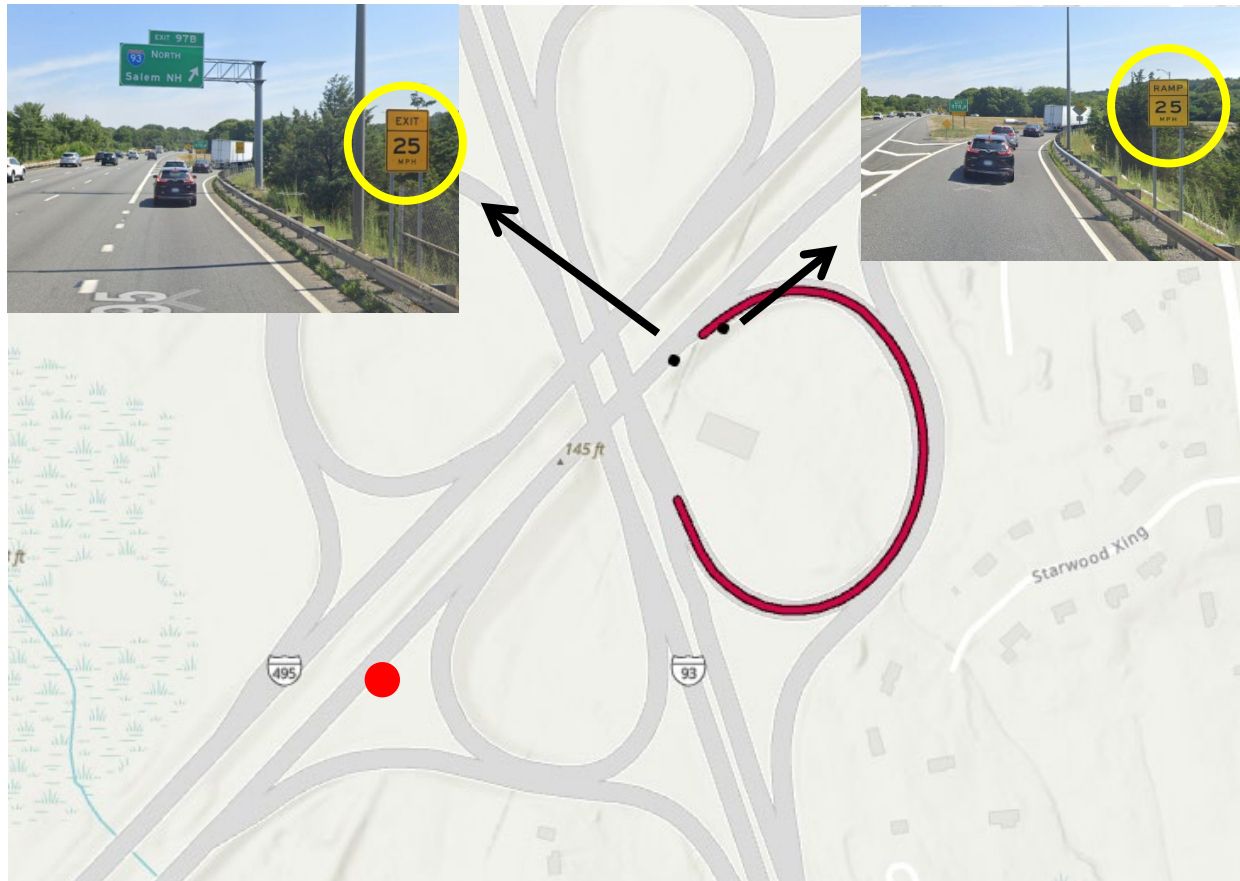


Figure 70. Advisory speed sign locations: Andover

Source: I-495N Exit #97B, Andover, MA; digital image, July 2022, “Street View,” Google Maps (<http://www.googlemaps.com>: accessed 1 January 2023).

Table 13. Risky events observed at the Andover site

Type of risky events	Number of observations
Approaching too fast/following too closely	29
Last-minute lane change	1

There are no obvious roadway geometry issues at this site. Given that there were 29 instances (within 15 minutes) of vehicles either approaching the ramp too fast or following other vehicles too closely, it might be necessary to introduce measures that can reduce speed variations among vehicles. A possible solution is to add one advisory speed sign at an upstream location (e.g., the red dot in Figure 70), so that drivers can have longer time to adjust their speeds. Another solution could be upgrading the existing W13-3 signs in Figure 70 to W13-7 signs, which may increase driver compliance with the advisory speed. The single case of last-minute lane change (Figure

71c) could be due to driver distraction, which probably can be better addressed through other strategies such as safety campaigns.

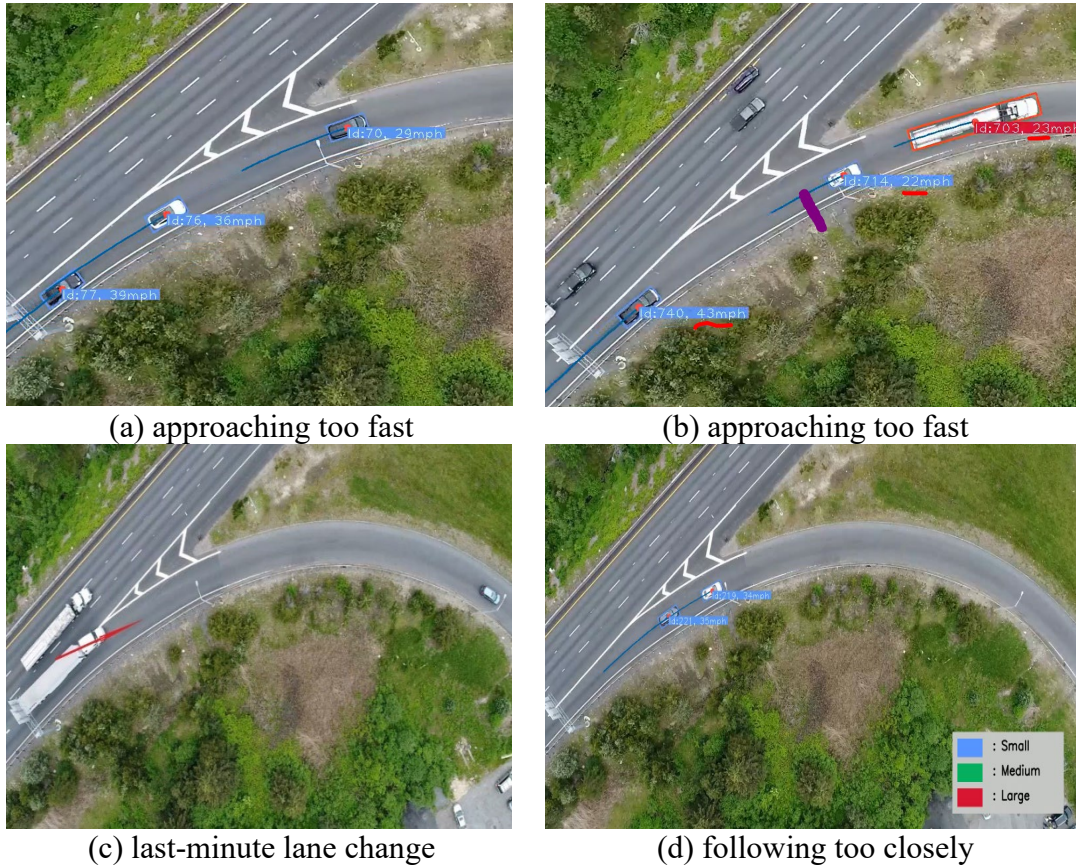


Figure 71. Risky events at the Andover site

7.2 Auburn/Worcester Site

The Auburn ramp connects I-290S to I-90W and has two lanes. It has three 25 mph advisory speed signs and four truck rollovers as shown in Figure 72. The ramp starts with a -2.5% slope followed by a roughly $+1\%$ upgrade as shown in Figure 84.

Based on the speed profiles and drone videos, we observed the following three types of risky events shown in Table 14 at the Auburn site. Some sample risky events are presented in Figure 73.

Figure 73(a) shows a truck traveling too fast and between two lanes. When traveling on a ramp at a high speed, it is more difficult to adjust lateral position than on a straight segment or at a low speed. Figure 73(b) shows that a fast-moving vehicle (#331 at 34 mph) approaches a slower vehicle (#328 at 30 mph) and later follows it closely. Figure 73(c) shows a slow vehicle (#136 at 27 mph) changes from the left lane into the right lane and blocks a fast-moving vehicle (#140 at 40 mph) in the right lane.



Figure 72. Advisory Speed sign locations: Auburn/Worcester

Source: I-290S to I-90W ramp, Auburn, MA; digital image, August 2022, “Street View,” Google Maps (<http://www.googlemaps.com>: accessed 1 January 2023).

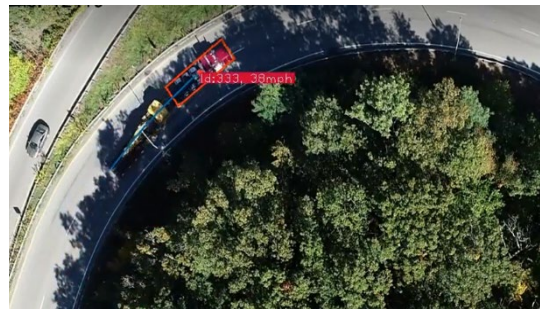
Table 14. Risky events observed at the Auburn/Worcester site

Type of risky events	Number of observations
Approaching too fast	15
Unsafe lane changes	34
Traveling between lanes	15

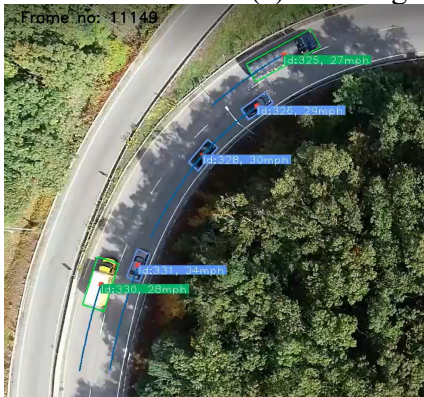
Our recommendations for this site are:

1. For such a sharp curve on a downgrade (Figure 84), lane changes should be prohibited on this ramp. A solid double white line in conjunction with an R4-9 “Stay in Lane” sign probably should be used instead of the current dashed line.
2. We observed heavy trucks in both lanes (sometime between lanes). Trucks probably should be restricted to the left lane only by using advance signage. If a truck rollover happens (usually overturn to the left side on this ramp), it would be less likely to block the right lane and cause damage to the vehicle traveling on its left). The potential downside of this strategy is that the rollover may block the opposite direction.

3. Separating trucks and smaller-sized vehicles could contribute to more uniform speeds (smaller speed variances) in each lane. A dual-advisory speed sign can then be used to give heavy trucks and smaller-sized vehicles different advisory speeds as shown in Figure 2 and reference [18].
4. This site already has three rollover warning signs. However, approaching the ramp too fast is still a major problem. The crash history shows that the recent four truck rollovers (crash numbers #4510434, #4542938, #4670358, and #4882571) on this ramp were all caused by speeding. Many studies [7,8,9,10,12,14] have suggested that adding continuously flashing beacons or speed triggered beacons to rollover warning signs can help to reduce vehicle speeds and improve safety. MassDOT may want to convert one of the three warning signs into a dynamic warning sign. The beacons should be activated when a speeding vehicle is detected. Another option is that the beacons are activated when a speeding truck is detected.



(a) traveling between lanes and approaching too fast



(b) following too closely



(c) unsafe lane change

Figure 73. Risky events at the Auburn/Worcester site

7.3 Freetown North and South

The Freetown North ramp connects Route 24S to Route 79W, while the Freetown South ramp connects Route 24N to Route 79E. Both ramps are very similar in terms of geometry. The North ramp has an advisory speed of 25 mph, and the South ramp has 30 mph. The locations of the advisory speed signs are illustrated in Figure 74. As shown in Figure 85, the North ramp is on a -1.8% downgrade and the South ramp is also on a downgrade but with a smaller slope of

–0.8%. Both Freetown ramps have much lower large truck volumes than the Auburn and West Springfield sites as shown in Table 12.

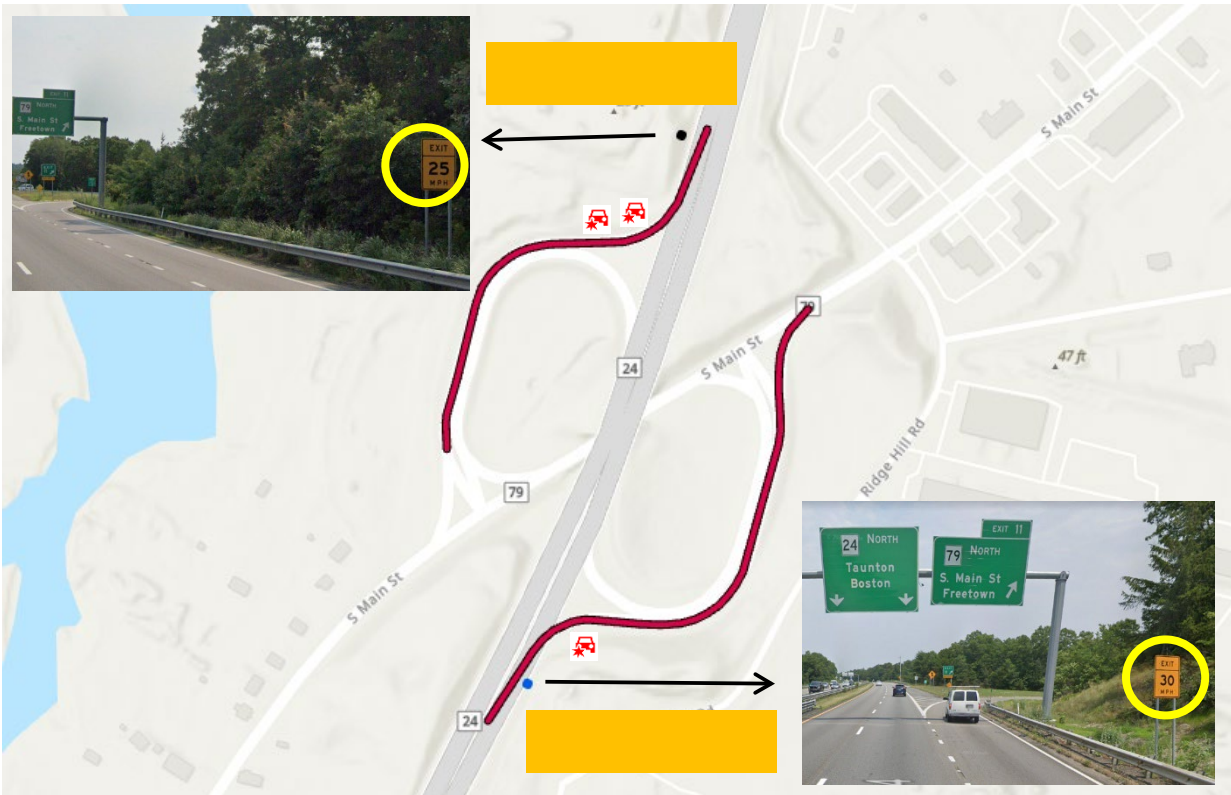


Figure 74. Advisory speed sign locations: Freetown North and South

Source: MA Route 24N Exit #11 and MA Route 24S Exit #11, Freetown, MA; digital image, July 2021, “Street View,” Google Maps (<http://www.googlemaps.com>: accessed 1 January 2023).

7.3.1 Freetown North

The two most significant risky events at this site are approaching too fast and unsafe lane changes as listed in Table 15. A few examples are provided in Figure 75. Most of the unsafe lane changes are related to exiting vehicles.

The trajectory data suggests that most unsafe lane changes were due to exiting traffic. Although existing signs all conform to the MUTCD, it may be helpful to move the exit speed advisory sign (Figure 74) further upstream so that drivers can be better prepared. As shown in Figure 74, the current W13-2 sign is about 200 ft ahead of the beginning of the exit ramp, which gives drivers limited time to adjust their speeds. At the Andover site, we observed only 1 last-minute lane change in about 15 minutes. At Freetown North, we observed 17 of them in about 124 minutes. The Andover ramp connects two major interstate highways (I-495N to I-93N). Drivers are unlikely to miss the exit ramp. While for the Freetown North ramp, it connects Route 24 to a principal arterial (Route 79). Unless a driver uses GPS or is familiar with this area (and pay close attention to exit signs), this exit ramp is more likely to be missed than the Andover ramp.

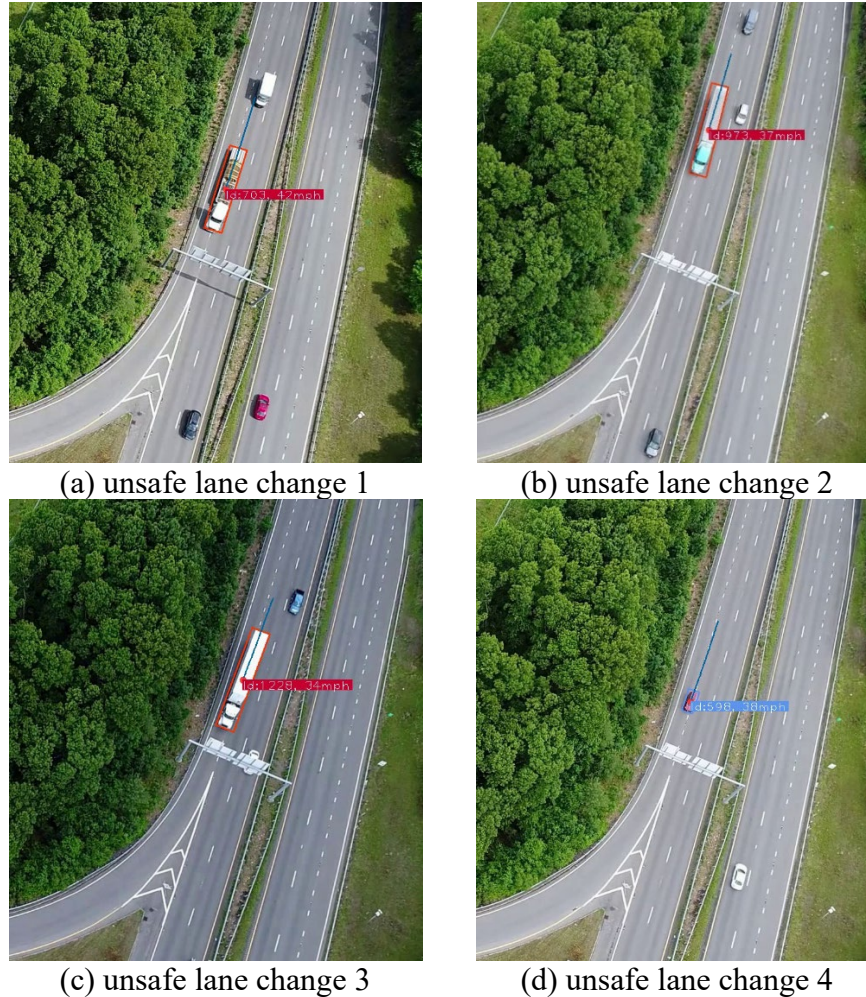


Figure 75. Sample risky events at the Freetown North ramp

Table 15. Risky events observed at the Freetown North site

Type of risky events	Number of observations
Approaching too fast	3
Unsafe lane changes	17

Between January 2015 and February 2022, there were two truck rollovers at this ramp. Both occurred near the very beginning of the ramp. One was due to speeding (crash number #4191801) and the other one (crash number #4367096) was caused by fatigued driving (and potentially speeding). The deceleration lane taper starts about 790 ft upstream of the exit ramp (670 ft for the Freetown South ramp). It is difficult to precisely measure and separate the taper and deceleration lane itself from Google Satellite Image. A rough estimate of the Freetown North ramp deceleration lane length using Google Satellite Image is about 500 ft, which appears to be adequate based on the findings in [76]. Therefore, the main challenge is how to prompt drivers to change into the deceleration lane and slow down. As shown in Figure 93 in Appendix A, the average truck speed entering the Freetown North ramp is close to 30 mph, although the advisory

speed is 25 mph. For speed reduction purposes, various pavement markings discussed in Section 2.3 may be considered for the deceleration lane.

7.3.2 Freetown South

As shown in Table 15, unsafe lane change and approaching too fast are still the two dominant risk events for the Freetown South ramp. Two examples are provided in Figure 76. Figure 76(a) shows a fast-approaching vehicle (vehicle #75 at 53 mph) changing lane at the last minute. Figure 76(b) shows a vehicle (#279) traveling at 52 mph when approaching the beginning of the exit ramp. Note that the advisory speed for this exit ramp is only 30 mph.

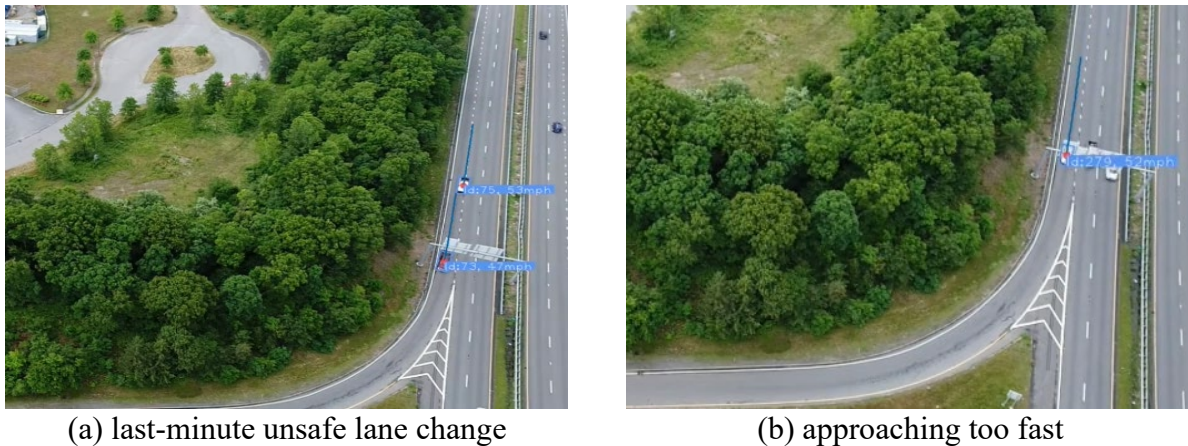


Figure 76. Sample risky events at the Freetown South ramp

Table 16. Risky events observed at the Freetown South site

Type of risky events	Number of observations
Approaching too fast	18
Unsafe lane changes	18

As shown in Figure 89, the initial segments of the Freetown North and South ramps have significantly smaller radii than other exit ramps. This was one of the main reasons that we selected these two exit ramps for collecting drone data. Given the sharp curves, it may be helpful to add a static or dynamic truck rollover warning sign at both Freetown North and South ramps. This is particularly important for Freetown South, since its deceleration lane length (not including taper) is about 450 ft measured based on Google Satellite Image, which is less than the recommended safe value in [76].

The advisory speed for Freetown South is 5 mph higher than that for Freetown North. However, the South ramp has a slightly sharper curve (radius = 170 ft) compared to the North ramp (radius = 186 ft). It is recommended that the advisory speed for the South ramp be reduced to 25 mph. Comparing Figure 93 and Figure 94 in Appendix A suggests that the average large truck speed when entering the Freetown South ramp is greater than 30 mph, while the corresponding speed for Freetown North is slightly below 30 mph. This difference might be attributed to the fact that

the South ramp advisory speed is 5 mph higher than the North ramp speed. In addition, the South ramp has a shorter deceleration lane than the North ramp.

Another suggestion for both Freetown North and South ramps is to add a W13-2 and a W13-3 sign. As shown in Figure 77 and Figure 78, when the difference between the mainline speed limit and the ramp advisory speed is greater than 25 mph, these two signs are needed. The speed limit for Route 24 is 65 mph and the current advisory speeds are 25 mph and 30 mph, respectively. Therefore, W13-2 and W13-3 would be helpful in this case. In particular, adding the W13-2 sign may prompt drivers to change into the deceleration lane earlier.

Figure 2C-3. Example of Advisory Speed Signing for an Exit Ramp

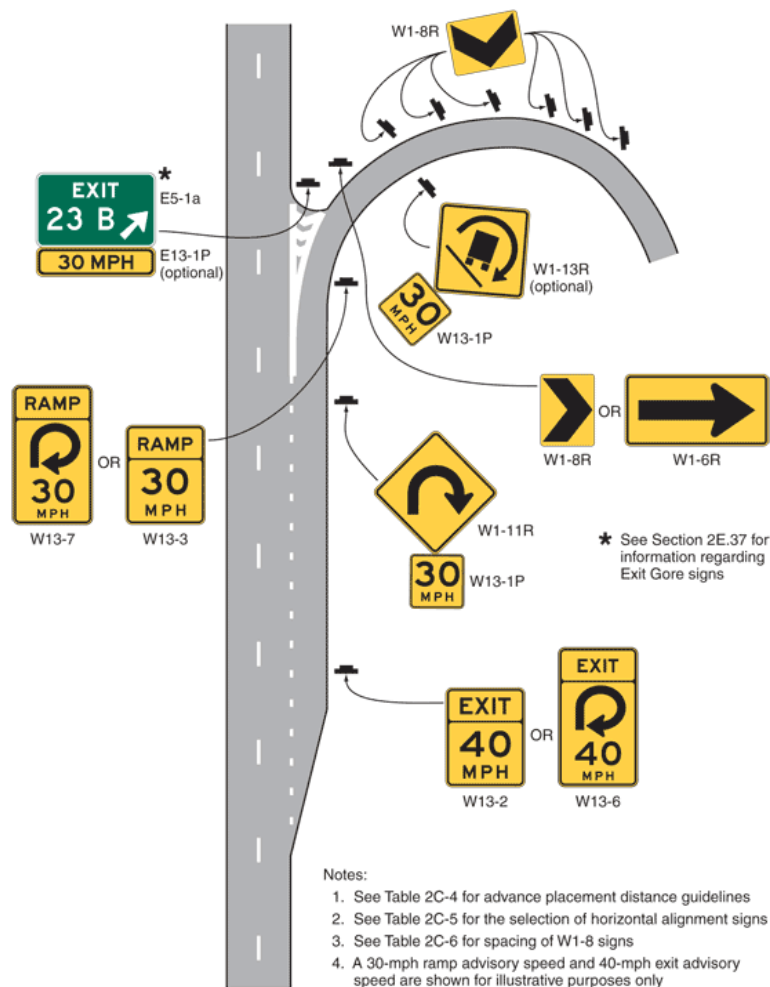


Figure 77. Example of Advisory Speed Signing for an Exit Ramp

Source: MUTCD, Figure 2C-3 [77].

Table 2C-5. Horizontal Alignment Sign Selection

Type of Horizontal Alignment Sign	Difference Between Speed Limit and Advisory Speed				
	5 mph	10 mph	15 mph	20 mph	25 mph or more
Turn (W1-1), Curve (W1-2), Reverse Turn (W1-3), Reverse Curve (W1-4), Winding Road (W1-5), and Combination Horizontal Alignment/Intersection (W1-10) (see Section 2C.07 to determine which sign to use)	Recommended	Required	Required	Required	Required
Advisory Speed Plaque (W13-1P)	Recommended	Required	Required	Required	Required
Chevrons (W1-8) and/or One Direction Large Arrow (W1-6)	Optional	Recommended	Required	Required	Required
Exit Speed (W13-2) and Ramp Speed (W13-3) on exit ramp	Optional	Optional	Recommended	Required	Required

Note: Required means that the sign and/or plaque shall be used, recommended means that the sign and/or plaque should be used, and optional means that the sign and/or plaque may be used. See [Section 2C.06](#) for roadways with less than 1,000 AADT.

Figure 78. Horizontal Alignment Sign Selection

Source: MUTCD, Table 2C-5 [77].

7.4 West Springfield

The West Springfield site has three segments: North, South, and South (Old toll gate). They correspond to Segments 1, 2, and 3, respectively in Figure 22. Our focus is on West Springfield-North and West Springfield-South. These two segments start at the green line in Figure 79 and continue north toward I-91. The elevation profiles for these two segments are shown in Figure 86, suggesting that they start with a -3% downgrade and are followed by a $+4\%$ upgrade. The lowest point is underneath the bridge (red dot in Figure 79). Figure 79 shows the locations of five advisory speed signs. Two of them are on the ramp of interest and the other three are on adjacent ramps.

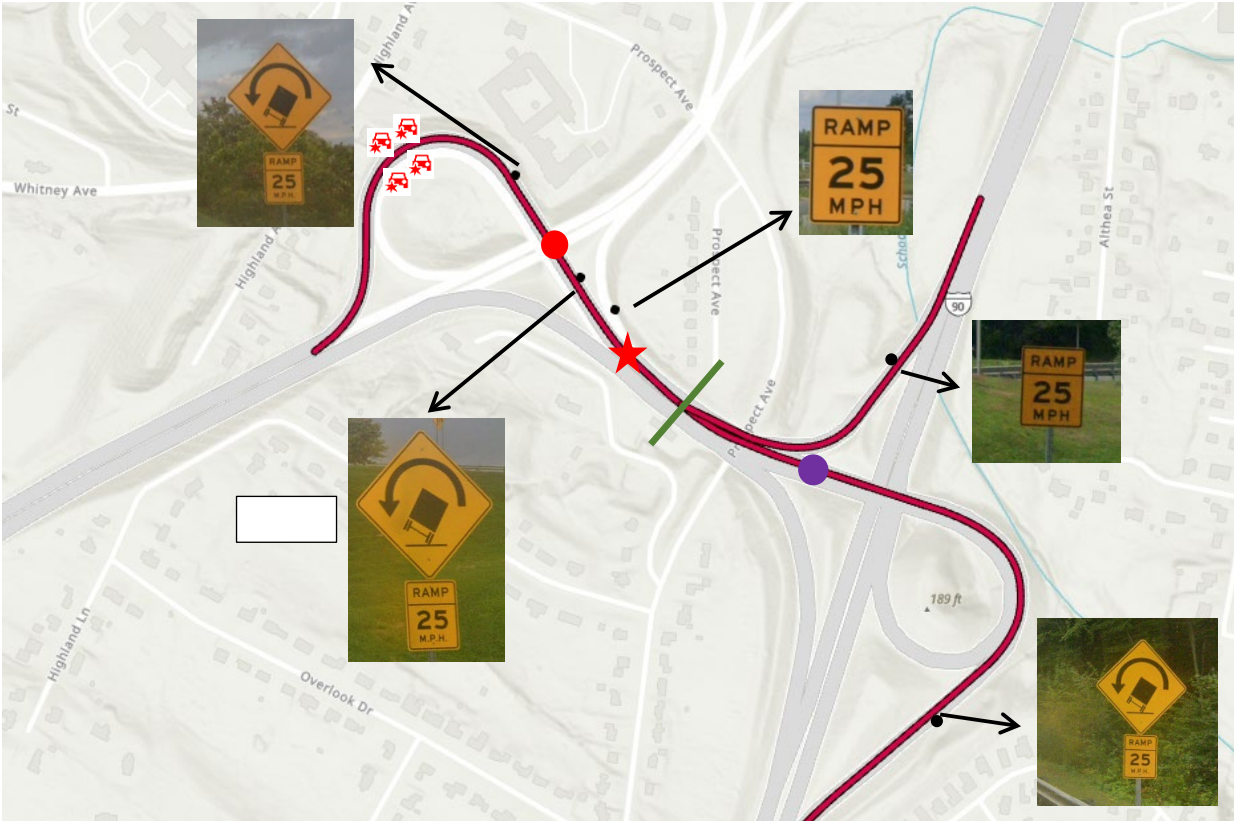
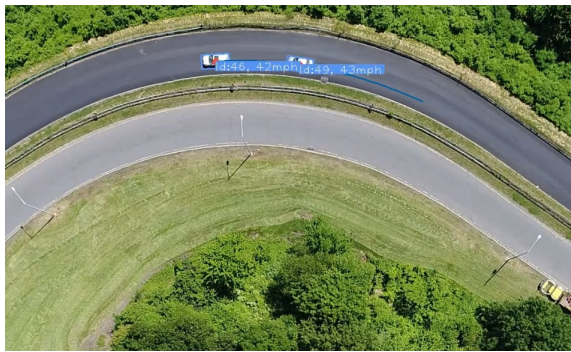


Figure 79. Advisory Speed sign location: West Springfield

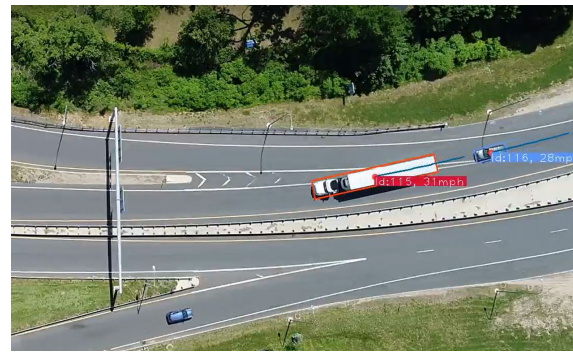
Source: I-90W to I-91 Ramp and I-90E to I-91 Ramp, West Springfield, MA; digital image, August and September 2022, “Street View,” Google Maps (<http://www.googlemaps.com>: accessed 1 January 2023).

The average speed profiles results in Figure 90 through Figure 92 suggest that the average large truck speeds for the first two West Springfield segments (Old toll gate and South) have never been below 30 mph. The average truck speed goes slightly below 30 mph when they are halfway through the red segment in Figure 90 (i.e., West Springfield-North). Note that the advisory speed here is 25 mph. Another important observation is that the average truck speed goes up in Figure 91, reaching approximately 34 mph. This is most likely due to the -3% downgrade that overlaps with the segment in Figure 91.

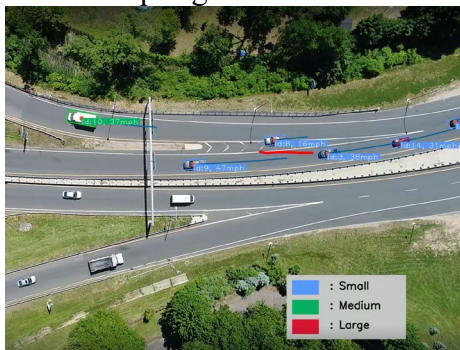
The main problems at West Springfield-North and South are approaching too fast and following too closely, last-minute lane changes, and waiting in traffic for a lane change. The frequencies of these risky events are listed in Table 17. Waiting in traffic for lane change (Figure 80c) is related to last-minute lane change (Figure 80b and Figure 80d) but is more dangerous. In Figure 80c, vehicle #8 slows down to 8 mph and waits for a safe gap to merge, while vehicles before and after it in the through lane are traveling at approximately 40 mph.



(a) Approaching too fast and closely: West Springfield North



(b) Last-Minute Lane change: West Springfield South



(c) Waiting for lane change: West Springfield South



(d) Last-minute lane change: West Springfield South

Figure 80. Risky events at the West Springfield North and South sites

Table 17. Risky events observed at West Springfield North and South

Type of risky events	Number of observations
Approaching too fast	62
Last-minute lane change	164
Waiting in traffic for lane change	62

Given the high approaching speeds and the large number of last-minute lane changes at this site, the following recommendations are provided:

1. The existing 25 mph advisory speed seems to be reasonable. However, apparently speed compliance among truck drivers is a major issue. There was a toll plaza right before this ramp, which was removed in 2016. The crash history at this location shows that there were no truck rollovers on this ramp between 1/1/2008 and 12/31/2014 and 4 rollovers (crash numbers #4333162, #4840839, #4844305, and #4917505 all due to speeding) after the removal of the toll plaza in 2016. Therefore, it is important to take measures to reduce truck speeds. MassDOT may consider dynamic warning signs and pavement markings at this site.

2. The existing static signs can be replaced by dynamic speed feedback signs to increase driver speed compliance, particularly the first static sign (Sign A in Figure 79) before the bridge. This first static sign is on the -3% downgrade. The data in Figure 91 clearly shows that the average truck speed increases in this downgrade segment.
3. The merging vehicles in the right lane (Figure 80c) may give vehicles in the left lane the impression that they are on the freeway mainline. However, the left-lane vehicles will soon enter a sharp curve which is typically not seen on a freeway mainline. A W1-11L sign before the bridge (red dot in Figure 79) may give drivers a better idea of what is ahead of them and prompt them to slow down.
4. An additional 25 mph advisory sign may be added near the purple dot in Figure 79, letting drivers know that the ramp has not ended yet and to not speed up too soon. Another benefit of doing this is that it may make it easier for vehicles in the right lane (from I-90W exit ramp) to merge into the left through lane (Figure 80c). We observed 164 last-minute lane changes and 62 waiting in traffic for lane changes near the red star in Figure 79 in just 1 hour. Having similar speeds in both the left lane and the entrance ramp (i.e., the I-90W exit ramp) may make lane changes /weaving maneuvers easier.

7.5 New Bedford

The New Bedford ramp connects Route 140S to I-195W. It has two 30 mph advisory speed signs as shown in Figure 81. Figure 87 shows that this ramp consists of a short (about 500 ft) downgrade of -2.4% and a $+1.7\%$ upgrade of 1,200 ft. Two truck rollovers (crash numbers #4269428 and #4313118) occurred toward the end of the ramp during the study period, and both were due to speeding. This ramp has a much lower large truck volume than the Auburn and West Springfield sites as shown in Table 12. Its large truck volume is similar to those of the two Freetown sites and the Sturbridge site.

Unlike previous ramps, we did not observe any risky events here. The New Bedford ramp has two major curves separated by a relatively straight and long segment. The crash history suggests that speeding at the second curve is the main problem. The elevation profile of this ramp (Figure 87) suggests that the first ramp is on a downgrade and the second curve is on an upgrade. The upgrade for the second curve theoretically should help to slow vehicles down and improve safety. We suspect that the smaller radius of the second curve is the main reason for its worse safety record than the first curve. Figure 89(e) shows that the first curve has a radius of 501 ft and the second curve has a radius of 257 ft (almost half of the first curve). However, the advisory speeds for both curves are 30 mph.

We acknowledge that advisory speeds need to be determined by considering other factors such as superelevation and pavement conditions in addition to horizontal curves. However, the accuracy of airborne LiDAR data is not sufficient for us to accurately determine the superelevation and pavement conditions. Thus, our recommendation to reduce the second advisory speed to 25 mph is based on the horizontal curve, elevation profile, and crash history data. The same advisory speed for the two curves could be justified by their different superelevations.



Figure 81. Advisory speed sign location: New Bedford

Source: MA Route 140S to I-195W Ramp, New Bedford, MA; digital image, July 2021, “Street View,” Google Maps (<http://www.googlemaps.com>: accessed 1 January 2023).

The ball bank indicator method has been widely used by state DOTs to determine the optimal speeds for horizontal curves. A limitation of this method is that the data collection is often done using passenger cars, not heavy trucks. The drone video data collected in this study is only 147 minutes long and cannot reflect all driving conditions (e.g., heavy traffic, nighttime, snow, rain) at this site. To fully understand the truck rollover risks at this site, MassDOT may want to conduct a long-term data collection effort using roadside radar sensors. Some new radar sensors can detect and track individual vehicles and generate trajectories similar to what the drone+computer vision solution can do. The drone solution in this research can be quickly set up and is ideal for short-term data collection. Although the roadside radar method requires more effort to set up, it can well complement the drone solution and generate trajectory data for several weeks or months.

7.6 Sturbridge

The Sturbridge ramp connects Route 15 to I-84S. Based on the 2008 Google Street View and 2020 Bing Maps Streetside data, this ramp does not have any advisory speed signage. The adjacent exit ramp from I-84S to Route 15 does have a 30-mph advisory speed sign as shown in Figure 82. The elevation profile in Figure 88 suggests that this Sturbridge ramp consists of a 650-ft +2.8% upgrade, an 800-ft -1.8% downgrade, and a 400-ft +2% upgrade. The large truck

volume at this Sturbridge site during the data collection period is much lower than those of the Auburn and West Springfield sites as shown in Table 12. However, this site had 3 truck rollovers during the 1/2015-2/2022 period compared to 4 for both West Springfield and Auburn.

Figure 89(f) shows that this ramp consists of four curves, and one of them has a very small radius of 188 ft. This is approximately where three truck rollovers (crash numbers #4192226, #4357792, and #4391299) occurred between January 2015 and February 2022. Two of them were due to speeding. According to the truck driver, the third rollover was caused by “radio microphone fell and got wedged in between steering wheel and dashboard.” As a comparison, the radii for the entrance curves of the two Freetown ramps are 186 ft and 170 ft, and their corresponding advisory speeds are 25 mph and 30 mph, respectively.

No risky events have been identified from the 122-minute drone videos taken at this site. Due to a truck stop near this site, the Sturbridge ramp is expected to have a high truck traffic volume. One thing worth noting is that all three rollovers occurred toward the end of the downgrade segment (around 1,200 ft in Figure 88) and in the center of the sharpest curve with a radius of 188 ft (Figure 89f). In other words, these rollovers occurred where a downgrade meets a sharp curve. In addition, there is no advisory speed sign and there is a relatively straight segment before the sharp curve. The straight segment may prompt vehicles to accelerate.

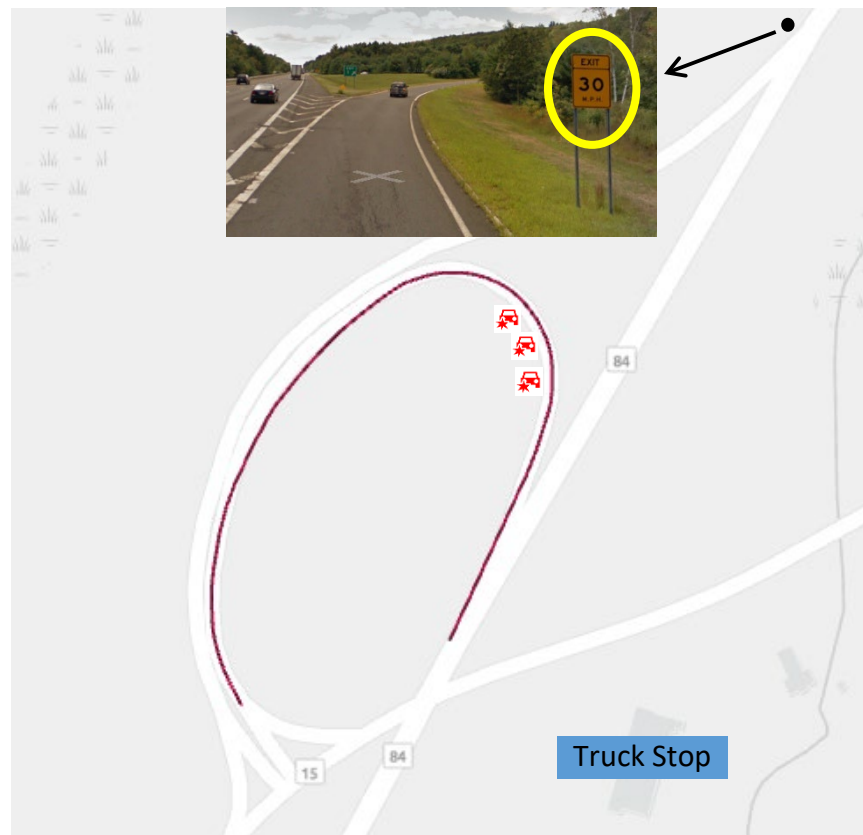


Figure 82. Advisory speed sign location: Sturbridge

For this Sturbridge site, our recommendations are:

1. An advisory speed sign is needed given the sharp curve and downgrade. MassDOT may also consider dynamic warning or dynamic speed feedback signs specifically for heavy trucks.
2. A W1-11R sign and a W1-13R sign to warn drivers of the upcoming sharp curve. Since this ramp is near a truck stop and serves a busy interstate (I-84). A lot of long-haul truck trips are anticipated, and truck drivers may not be familiar with this route/ramp.
3. Although many pavement markings have been proposed to reduce vehicle speed, the New York state example in Figure 14 and reference [28] suggests that roadside signs might be a better option for states in the Northeast region. At the New York state site, pavement markings were installed and tested around 2004. However, this site has been using an overhead dynamic warning sign since 2007 until now (Figure 14). Due to snow plowing and deicing activities, pavement markings may require frequent maintenance, making them a less desirable solution for Massachusetts.
4. Conduct a before-and-after study to evaluate the chosen strategy's effectiveness. This study can be conducted at any of the sites investigated in this research.

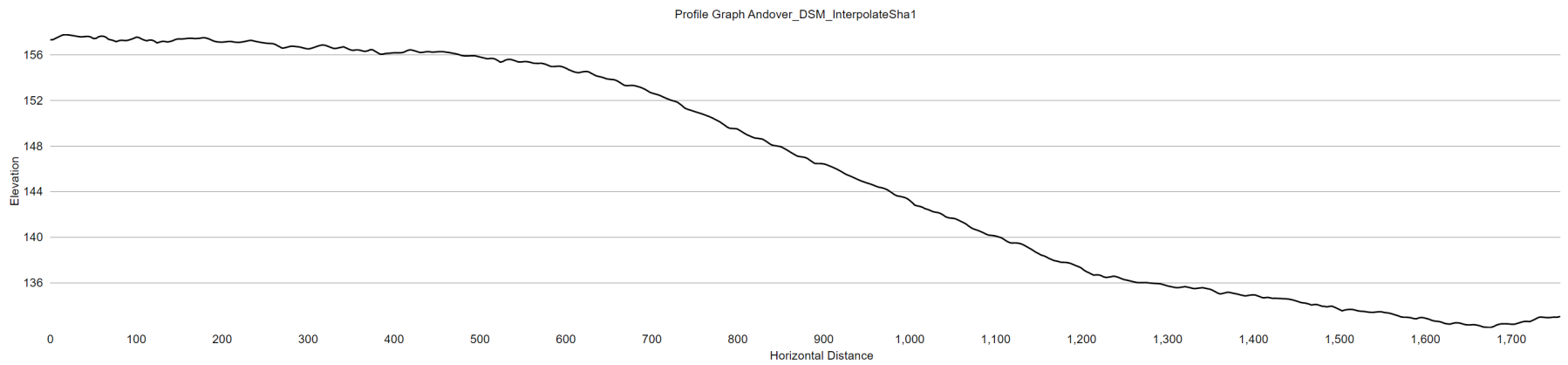


Figure 83. Ramp elevation profile for Andover

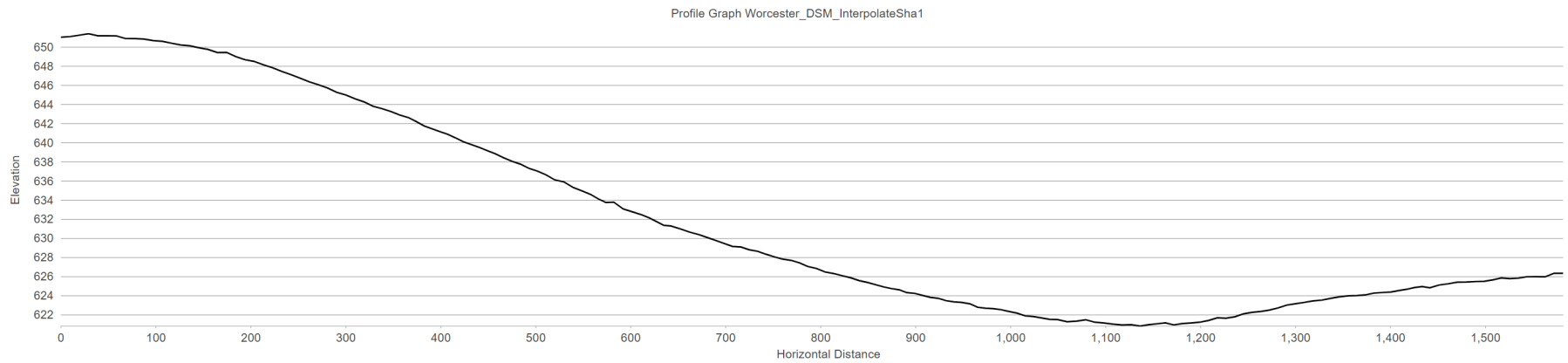


Figure 84. Ramp elevation profile the Auburn/Worcester

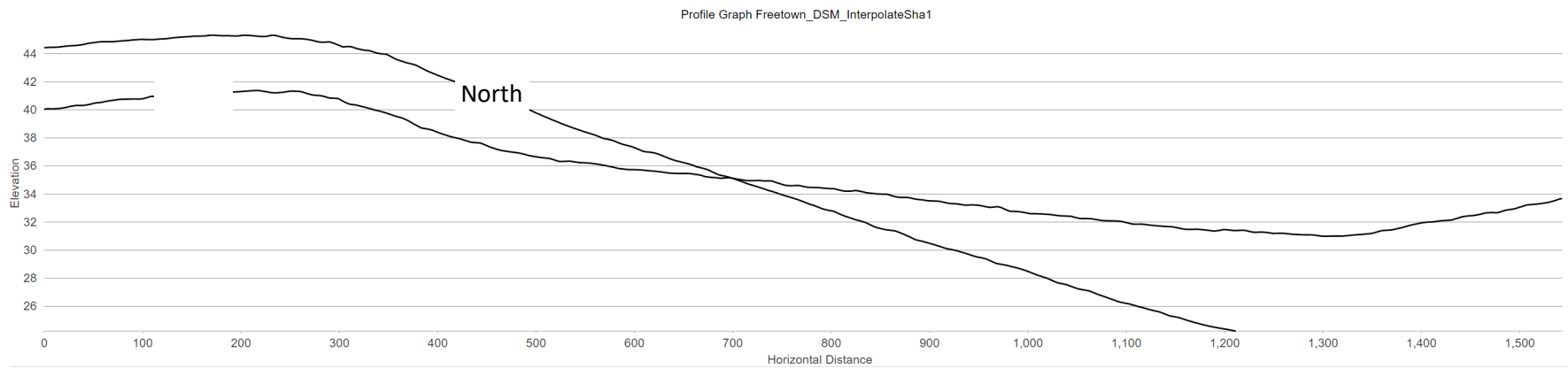


Figure 85. Ramp elevation profile for Freetown North and South

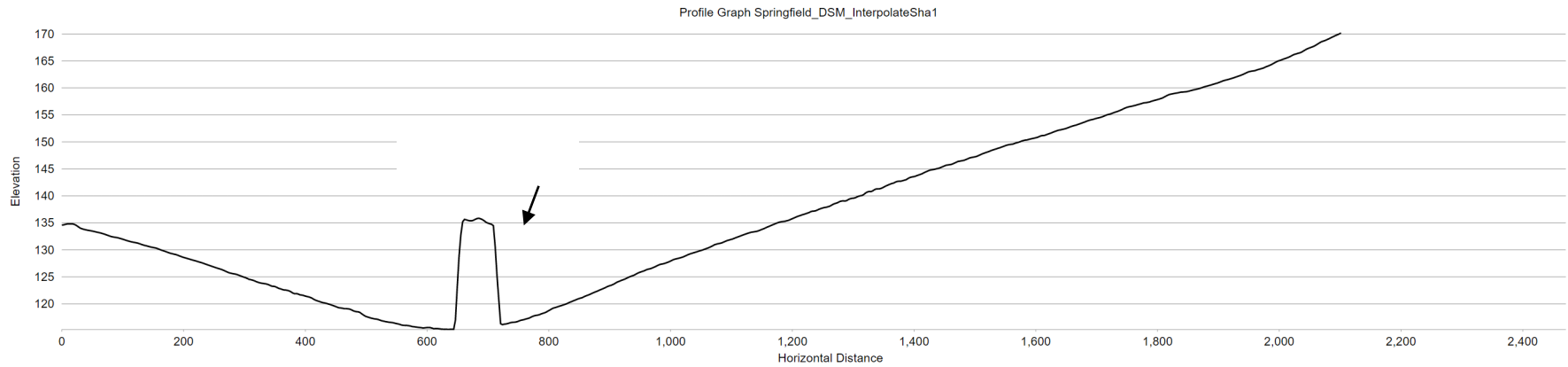


Figure 86. Ramp elevation profile for West Springfield-North

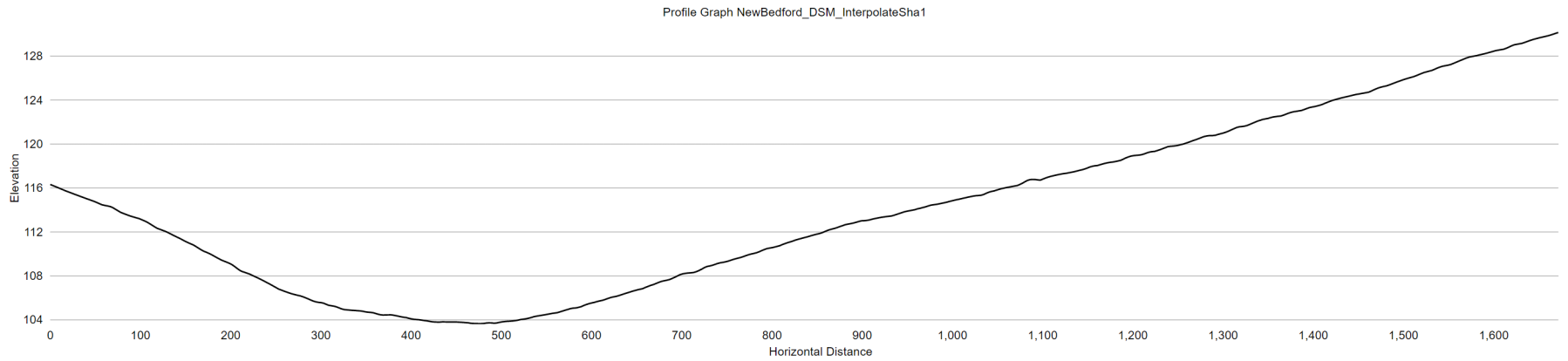


Figure 87. Ramp elevation profile for New Bedford

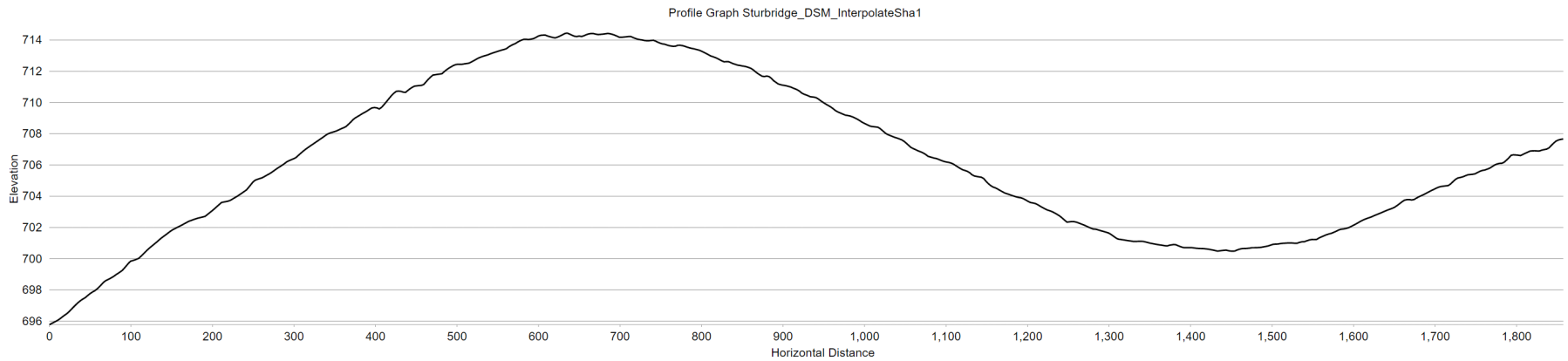
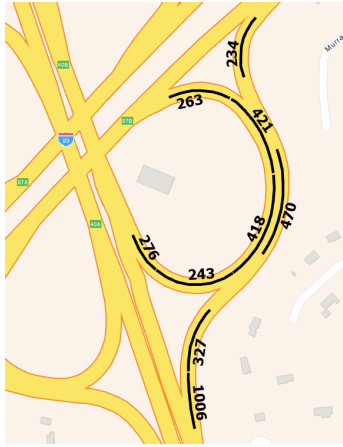
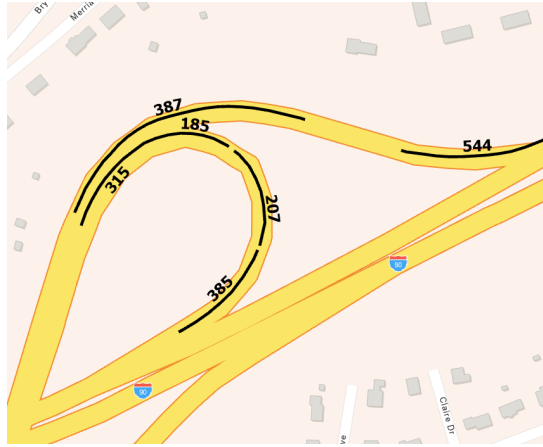


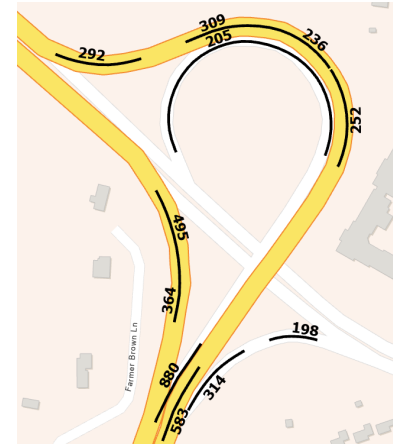
Figure 88. Ramp elevation profile for Sturbridge



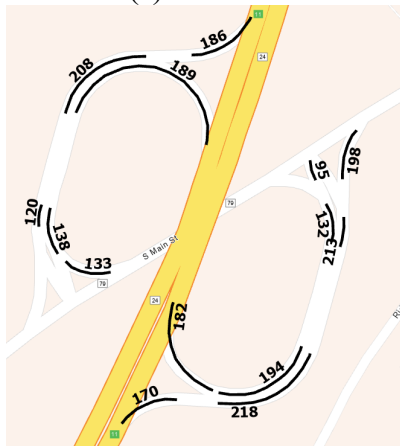
(a) Andover



(b) Auburn/Worcester



(c) West Springfield



(d) Freetown North and South



(e) New Bedford



(f) Sturbridge

Figure 89. Radii for the selected ramps

8.0 Conclusions and Discussion

This research focuses on understanding the root causes of highway ramp truck rollover crashes by considering a wide range of factors, including vehicle trajectories, ramp slopes and radii, locations and types of traffic signs, and crash history. Drones are utilized to collect highway traffic data from seven high-risk ramps. A suite of algorithms has been developed to detect and track vehicles, estimate vehicle speeds, generate vehicle trajectories, and extract risky events. On the other hand, a thorough review of literature and best practices on reducing highway ramp truck rollovers has been conducted and highway ramp truck rollover crash data in Massachusetts has been carefully reviewed. The extracted vehicle trajectory data is linked to truck rollover history, traffic signage, advisory speeds, roadway geometry, etc. in order to identify correlations and cost-effective countermeasures.

Through this study, a relatively lightweight yet highly accurate Oriented Mask-RCNN model is developed for vehicle detection, and the Savitzky–Golay filter is adopted for vehicle tracking. Additional algorithms are also developed to analyze the extracted vehicle trajectories to

- Calculate average speed profiles by vehicle classification.
- Identify high-risk events (and use them as surrogate safety measures) such as unsafe and last-minute lane changes, approaching too fast, and following other vehicles too closely.
- Cluster trajectories into different groups to automatically identify abnormal trajectories.
- Visualize high-dimensional vehicle speed profiles on a 2-dimensional plane.

The average speed profiles and clustering analysis provide valuable information helping us understand driver behavior along a ramp. In some cases, the clustering analysis results show clear differences among the trajectories of different groups/clusters. The detected high-risk events are important for identifying potential connections among traffic signage, roadway geometry, and safety hazards. Also, the t-SNE method shows potential to automatically identify abnormal trajectories.

The review results of literature and best practices suggest that various dynamic warning signs and pavement markings are the two most popular strategies for reducing vehicle speeds and improving horizontal curve (including ramp) safety. However, there has been a lack of thorough investigation of the effectiveness of such strategies (particularly pavement markings) using field data. Many of the evaluation studies were based on driving simulation and the conclusions were sometimes inconsistent.

The narratives of all ramp truck rollover crashes between January 2015 and February 2022 in Massachusetts have been reviewed. It is found that over 95% of ramp truck rollovers are single-vehicle crashes. Speeding is the predominant reason for such crashes and accounts for about 56% of all rollovers. Based on the locations of these rollover crashes, seven high-risk ramps are selected and further investigated. Traffic videos at these ramps are captured using drones, and vehicle trajectories are generated using the developed deep learning models. The locations and types of traffic signs, slopes, and curve radii of these ramps are also obtained and carefully

investigated together with the above trajectory results. Based on the analysis, some practical and specific safety improvement recommendations are provided for each site to MassDOT.

This study finds drones to be a very useful and handy tool for short-term traffic data collection. They can cover a larger area than roadside cameras due to their height and can be deployed quickly. However, drone deployment is limited by weather conditions and battery life. For long-term data collection to cover various weather and lighting conditions, emerging high-definition radar sensors might be a better choice.

Some of the selected ramps are at a high risk of having truck rollover crashes. One example is the West Springfield site, which has had 4 truck rollovers since the removal of a nearby toll plaza in 2016. The collected data seems to suggest that speeding and insufficient weaving area length are generating safety hazards at this site. MassDOT may install dynamic warning signs and take other measures at these high-risk sites. It is recommended that MassDOT conduct before-and-after studies to quantify the benefits of such safety measures.

Overall, the developed deep-learning-based vehicle detection and tracking algorithms work well, despite challenges such as drone rotation and vibration. Some high-risk events have been successfully detected based on the generated vehicle trajectories and verified manually. The proposed trajectory analysis methods such as clustering and t-SNE diagrams can potentially be applied to trajectories generated by other sensors such as high-definition radar.

The proposed trajectory-based safety analysis approach provides important inputs for understanding driver behavior at/near highway ramps, and it can be used as an effective tool for road safety audits. This approach can be extended to cover other transportation facilities such as intersections, horizontal curves, and midblock pedestrian crossings and use data generated by radar or LiDAR sensors. Installing radar or LiDAR sensors will take more effort than using drones. However, radar and LiDAR can generate more data than drones over a longer period (e.g., several weeks/months), making them more suitable for before-and-after studies. Experience learned through this project suggests that trajectory-based safety analysis will play an increasingly important role in future traffic safety data analytics.

It would be very helpful to develop a generic set of guidelines for improving highway ramp safety. For example, if a ramp falls under category A, safety strategies 1, 2, and 3 should be implemented. However, doing so is very challenging, as ramp safety is affected by many factors such as curvature, slope, placements of traffic signs, number of lanes, and traffic compositions. A large amount of data from different ramps will be needed to draw such generic conclusions or guidelines.

9.0 References

- 1 National Highway Traffic Safety Administration (NHTSA). Overview of Motor Vehicle Crashes in 2020. Available online at <https://crashstats.nhtsa.dot.gov/Api/Public/ViewPublication/813266>, accessed on December 28, 2022.
- 2 Federal Motor Carrier Safety Administration (FMCSA). Large Truck and Bus Crash Facts 2020. Available online at <https://www.fmcsa.dot.gov/safety/data-and-statistics/large-truck-and-bus-crash-facts-2020>, accessed on December 28, 2022.
- 3 Massachusetts Department of Transportation (MassDOT). 2018 Massachusetts Strategic Highway Safety Plan. Available online at <https://www.mass.gov/doc/massachusetts-shsp-2018/download>, accessed on December 28, 2022.
- 4 Green, S. D. (2002). Prevent Heavy Truck Rollover. Traffic Safety (Chicago), 2(4).
- 5 McGee, H. W., & Strickland, R. R. (1994). An Automatic Warning System to Prevent Truck Rollover on Curved Ramps. Public Roads, 57(4).
- 6 Fontaine, M. D. (2003). Engineering and technology measures to improve large truck safety: state of the practice in Virginia (No. VTRC 03-TAR13). Virginia Transportation Research Council.
- 7 Freedman, M., Olson, P. L., & Zador, P. L. (1992). Speed actuated rollover advisory signs for trucks on highway exit ramps.
- 8 Bergan, A. T., Bushman, R. J., & Taylor, B. (1998, January). Intelligent truck rollover advisory systems. In Intelligent transportation systems (Vol. 3207, pp. 140-147). SPIE.
- 9 Strickland, R. R., & McGee, H. W. (1998). Evaluation results of three prototype automatic truck rollover warning systems. Transportation research record, 1628(1), 41-49.
- 10 McGee, H., & Strickland, R. (1998). Evaluation of Prototype Automatic Truck Rollover Warning Systems (No. FHWA-RD-97-124; 3A1c0312). United States. Federal Highway Administration.
- 11 Baker, D., Bushman, R., & Berthelot, C. (2001). Effectiveness of truck rollover warning systems. Transportation research record, 1779(1), 134-140.
- 12 Bola, R. S. (1999). Evaluation of a Truck-Activated Rollover Warning System (No. FHWA/CA/TE-99/11,).
- 13 Knoblauch, R. L., & Nitzburg, M. (1993). Ramp Signing for Trucks.
- 14 Middleton, D. (1994). A STUDY OF SELECTED WARNING DEVICES FOR REDUCING TRUCK SPEEDS. INTERIM REPORT (No. FHWA/TX-95/1232-28).
- 15 Stevens, S., & Richards, S. H. (1997). Condition responsive truck rollover warning systems: alternative system designs (No. CONF-971094-1). Oak Ridge National Lab.(ORNL), Oak Ridge, TN (United States).

- 16 Yao, C. C., Hsu, J. Y., Liao, Y. S., & Li, M. H. (2014). Implementation of Real-Time Vehicle Rollover Prevention System (No. 2014-01-0149). SAE Technical Paper.
- 17 Stevens, S. S., Chin, S. M., Hake, K. A., Hwang, H. L., Rollow, J. P., & Truett, L. F. (2001). Truck roll stability data collection and analysis. ORNL/TM-2001/116). Oak Ridge, Tennessee, USA: Center for Transportation Analysis, Oak Ridge National Laboratory.
- 18 Voigt, A. P., Stevens Jr, C. R., & Borchardt, D. W. (2008). Dual-advisory speed signing on freeway-to-freeway connectors in Texas. *Transportation Research Record*, 2056(1), 87-94.
- 19 Gates, T. J., Mahmud, M. S., Savolainen, P. T., Zhao, D., Zockaie, A., & Ghamami, M. (2022). Evaluation of Dynamic Speed Feedback Signs on Freeway Interchange Ramps (No. SPR-1704). Michigan. Dept. of Transportation. Research Administration.
- 20 Mohamed Abdel-Aty PHD, P. E. (2012). Dynamic Speed Monitoring on Sharp Curves Utilizing a Wireless Solar-Powered Dynamic Speed Monitoring System. Institute of Transportation Engineers. *ITE Journal*, 82(7), 24.
- 21 Hallmark, S. L., Qiu, Y., Hawkins, N., & Smadi, O. (2015). Crash modification factors for dynamic speed feedback signs on rural curves. *Journal of Transportation Technologies*, 5(01), 9.
- 22 Monsere, C. M., Nolan, C., Bertini, R. L., Anderson, E. L., & El-Seoud, T. A. (2005). Measuring the impacts of speed reduction technologies: Evaluation of dynamic advanced curve warning system. *Transportation research record*, 1918(1), 98-107.
- 23 Retting, R. A., McGee, H. W., & Farmer, C. M. (2000). Influence of experimental pavement markings on urban freeway exit-ramp traffic speeds. *Transportation research record*, 1705(1), 116-121.
- 24 Wood, J., & Donnell, E. T. (2020). Empirical Bayes before-after evaluation of horizontal curve warning pavement markings on two-lane rural highways in Pennsylvania. *Accident Analysis & Prevention*, 146, 105734.
- 25 Hunter, M., Boonsiripant, S., Guin, A., Rodgers, M. O., & Jared, D. (2010). Evaluation of effectiveness of converging chevron pavement markings in reducing speed on freeway ramps. *Transportation research record*, 2149(1), 50-58.
- 26 Drakopoulos, A., & Vergou, G. (2001). An Evaluation of the Converging Chevron Pavement Marking Pattern Installation on Interstate 94 at the Mitchell Interchange South-to-West Ramp in Milwaukee County, Wisconsin. Marquette University.
- 27 Ding, N., & Jiao, N. (2021). Long-term effectiveness of reverse linear perspective markings on crash mitigation in car-following: evidence from naturalistic observations. *Accident Analysis & Prevention*, 159, 106273.
- 28 Katz, B. J. (2004). Pavement markings for speed reduction. Science Applications International Corporation.
- 29 Hussain, Q., Alhajyaseen, W. K., Reinolsmann, N., Brijs, K., Pirdavani, A., Wets, G., & Brijs, T. (2021). Optical pavement treatments and their impact on speed and lateral position at transition zones: A driving simulator study. *Accident Analysis & Prevention*, 150, 105916.

- 30 Zhao, X., Ding, H., Lin, Z., Ma, J., & Rong, J. (2018). Effects of longitudinal speed reduction markings on left-turn direct connectors. *Accident Analysis & Prevention*, 115, 41-52.
- 31 Guo, Y., Liu, P., Liang, Q., & Wang, W. (2016). Effects of parallelogram-shaped pavement markings on vehicle speed and safety of pedestrian crosswalks on urban roads in China. *Accident Analysis & Prevention*, 95, 438-447.
- 32 Ariën, C., Brijs, K., Vanroelen, G., Ceulemans, W., Jongen, E. M., Daniels, S.,... & Wets, G. (2017). The effect of pavement markings on driving behaviour in curves: a simulator study. *Ergonomics*, 60(5), 701-713.
- 33 Ding, H., Zhao, X., Rong, J., & Ma, J. (2013). Experimental research on the effectiveness of speed reduction markings based on driving simulation: A case study. *Accident Analysis & Prevention*, 60, 211-218.
- 34 Godley, S. T., Triggs, T. J., & Fildes, B. N. (2000). Speed reduction mechanisms of transverse lines. *Transportation human factors*, 2(4), 297-312.
- 35 Maroney, S., & Dewar, R. (1987). Alternatives to enforcement in modifying the speeding behavior of drivers. *Transportation Research Record*, 1111, 121-126.
- 36 Matírnez, A., Mántaras, D. A., & Luque, P. (2013). Reducing posted speed and perceptual countermeasures to improve safety in road stretches with a high concentration of accidents. *Safety science*, 60, 160-168.
- 37 Hussain, Q., Pirdavani, A., Ariën, C., Brijs, T., & Alhajyaseen, W. (2018). The impact of perceptual countermeasures on driving behavior in rural-urban transition road segments: a driving simulator study. *Advances in transportation studies*, 46.
- 38 Arnold, E. D., & Lantz, K. E. (2007). Evaluation of best practices in traffic operations and safety: phase I: flashing LED stop sign and optical speed bars (No. FHWA/VTRC 07-R34). Virginia Transportation Research Council.
- 39 Galante, F., Mauriello, F., Montella, A., Perneti, M., Aria, M., & D'Ambrosio, A. (2010). Traffic calming along rural highways crossing small urban communities: Driving simulator experiment. *Accident Analysis & Prevention*, 42(6), 1585-1594.
- 40 Gates, T. J., Qin, X., & Noyce, D. A. (2008). Effectiveness of experimental transverse-bar pavement marking as speed-reduction treatment on freeway curves. *Transportation Research Record*, 2056(1), 95-103.
- 41 Godley, S. T., Triggs, T. J., & Fildes, B. N. (2004). Perceptual lane width, wide perceptual road centre markings and driving speeds. *Ergonomics*, 47(3), 237-256.
- 42 Rossi, R., Gastaldi, M., Gecchele, G., Biondi, F., & Mulatti, C. (2014). Traffic-calming measures affecting perceived speed in approaching bends: On-field validated virtual environment. *Transportation Research Record*, 2434(1), 35-43.
- 43 Awan, H. H., Pirdavani, A., Houben, A., Westhof, S., Adnan, M., & Brijs, T. (2019). Impact of perceptual countermeasures on driving behavior at curves using driving simulator. *Traffic injury prevention*, 20(1), 93-99.

- 44 Firestine, M., McGee, H., & Toeg, P. (1989). IMPROVING TRUCK SAFETY AT INTERCHANGES. SUMMARY REPORT (No. FHWA-IP-89-024).
- 45 Ervin, R. D., Barnes, M., MacAdam, C., Scott, R., & Freitas, M. (1985). Impact of Specific Geometric Features on Truck Operations and Safety at Interchanges. Vol. I-Technical Report (No. FHWA/RD-86/057). United States. Federal Highway Administration.
- 46 McKnight, A. J., & Bahouth, G. T. (2009). Analysis of large truck rollover crashes. *Traffic injury prevention*, 10(5), 421-426.
- 47 Wang, J., & Council, F. M. (1999). Estimating truck-rollover crashes on ramps by using a multistate database. *Transportation research record*, 1686(1), 29-35.
- 48 Isaacs, B., Saito, M., & McKnight, C. E. (1998). Notice ratings as a management tool to reduce truck rollovers on ramps. *Journal of infrastructure systems*, 4(4), 156-163.
- 49 Tarko, A., Hall, T., Romero, M., & Jiménez, C. G. L. (2016). Evaluating the rollover propensity of trucks—A roundabout example. *Accident Analysis & Prevention*, 91, 127-134.
- 50 Perera, H. S., Ross Jr, H. E., & Humes, G. T. (1990). Methodology for estimating safe operating speeds for heavy trucks and combination vehicles on interchange ramps. *Transportation Research Record*, (1280).
- 51 Bligh, R. P., Sheikh, N. M., Abu-Odeh, A. Y., & Kiani, M. (2021). Review and Assessment of Current Modeling Techniques in Support of Next-Generation Rollover Research—Phase I (No. FHWA-HRT-21-045). United States. Federal Highway Administration. Office of Safety Research and Development.
- 52 Chou, C. C., Wagner, C. D., Yang, K. H., King, A. I., Hu, J., Hope, K., & Arepally, S. (2008). A review of math-based CAE tools for rollover simulations. *International journal of vehicle safety*, 3(3), 236-275.
- 53 Charlton, S. G. (2007). The role of attention in horizontal curves: A comparison of advance warning, delineation, and road marking treatments. *Accident Analysis & Prevention*, 39(5), 873-885.
- 54 Godley, S., Fildes, B., Triggs, T., & Brown, L. (1999). Perceptual countermeasures: experimental research (No. CR 182).
- 55 Hall, J. (1987). Effects of chevrons, post-mounted delineators, and raised pavement markers on driver behavior at roadway curves.
- 56 DOTA: A large-scale dataset for object detection in aerial images,” in *Proc. CVPR*, 2018.
- 57 Li, K., & Wang, B. (2021). DAR-Net: Dense Attentional Residual Network for Vehicle Detection in Aerial Images. *Computational Intelligence and Neuroscience*, 2021.
- 58 Su, H., Liu, S., Zheng, B., Zhou, X., & Zheng, K. (2019). A survey of trajectory distance measures and performance evaluation. *The VLDB Journal*, 29, 3-32.
- 59 Liu, Z., Yuan, L., Weng, L., & Yang, Y. (2017). A High Resolution Optical Satellite Image Dataset for Ship Recognition and Some New Baselines. *ICPRAM*.

- 60 Zhu, H., Chen, X., Dai, W., Fu, K., Ye, Q., & Jiao, J. (2015). Orientation robust object detection in aerial images using deep convolutional neural network. 2015 IEEE International Conference on Image Processing (ICIP), 3735-3739.
- 61 Javiera Castillo Navarro, Bertrand Le Saux, Alexandre Boulch, Nicolas Audebert, Sébastien Lefèvre. (2020). MiniFrance. IEEE Dataport. <https://dx.doi.org/10.21227/b9pt-8x03>.
- 62 Rahnmounfar, T. Chowdhury, A. Sarkar, D. Varshney, M. Yari and R. R. Murphy, "FloodNet: A High Resolution Aerial Imagery Dataset for Post Flood Scene Understanding," in IEEE Access, vol. 9, pp. 89644-89654, 2021.
- 63 Chiu, M.T., Xu, X., Wei, Y., Huang, Z., Schwing, A.G., Brunner, R., Khachatrian, H., Karapetyan, H., Dozier, I., Rose, G., Wilson, D., Tudor, A., Hovakimyan, N., Huang, T.S., & Shi, H. (2020). Agriculture-Vision: A Large Aerial Image Database for Agricultural Pattern Analysis. 2020 IEEE/CVF Conference on Computer Vision and Pattern Recognition (CVPR), 2825-2835.
- 64 Azimi, S.M., Henry, C., Sommer, L.W., Schumann, A., & Vig, E. (2019). SkyScapes - Fine-Grained Semantic Understanding of Aerial Scenes. 2019 IEEE/CVF International Conference on Computer Vision (ICCV), 7392-7402.
- 65 Tang, T., Zhou, S., Deng, Z., Zou, H., & Lei, L. (2017). Vehicle Detection in Aerial Images Based on Region Convolutional Neural Networks and Hard Negative Example Mining. Sensors (Basel, Switzerland), 17.
- 66 Azimi, S.M., Vig, E., Bahmanyar, R., Körner, M., & Reinartz, P. (2018). Towards Multi-class Object Detection in Unconstrained Remote Sensing Imagery. ACCV.
- 67 Ding, J., Xue, N., Long, Y., Xia, G., & Lu, Q. (2018). Learning RoI Transformer for Detecting Oriented Objects in Aerial Images. ArXiv, abs/1812.00155.
- 68 Yi, J., Wu, P., Liu, B., Huang, Q., Qu, H., & Metaxas, D.N. (2021). Oriented Object Detection in Aerial Images with Box Boundary-Aware Vectors. 2021 IEEE Winter Conference on Applications of Computer Vision (WACV), 2149-2158.
- 69 Lang, S., Ventola, F.G., & Kersting, K. (2021). DAFNe: A One-Stage Anchor-Free Deep Model for Oriented Object Detection. ArXiv, abs/2109.06148.
- 70 Tian, Z.; Shen, C.; Chen, H.; and He, T. 2019. FCOS: Fully Convolutional One-Stage Object Detection. In International Conference on Computer Vision (ICCV).
- 71 He, K., Gkioxari, G., Dollár, P., & Girshick, R.B. (2020). Mask R-CNN. IEEE Transactions on Pattern Analysis and Machine Intelligence, 42, 386-397.
- 72 T.-Y. Lin, P. Dollar, R. Girshick, K. He, B. Hariharan and S. Belongie, "Feature pyramid networks for object detection", Proc. IEEE Conf. Comput. Vis. Pattern Recognit. (CVPR), pp. 2117-2125, Jul. 2017.
- 73 Palma, A.T., Bogorny, V., Kuijpers, B., & Alvares, L.O. (2008). A clustering-based approach for discovering interesting places in trajectories. ACM Symposium on Applied Computing.

- 74 Chen, J., Wang, R., Liu, L., & Song, J. (2011). Clustering of trajectories based on Hausdorff distance. 2011 International Conference on Electronics, Communications and Control (ICECC), 1940-1944.
- 75 Guo, Y., Xu, Q., Li, P., Sbert, M., & Yang, Y. (2017). Trajectory Shape Analysis and Anomaly Detection Utilizing Information Theory Tools. *Entropy*, 19, 323.
- 76 Chen, H., Zhou, H., & Lin, P. S. (2014). Freeway deceleration lane lengths effects on traffic safety and operation. *Safety science*, 64, 39-49.
- 77 U.S. Department of Transportation. (2009). Manual on Uniform Traffic Control Devices (MUTCD) for Streets and Highways.

Appendix A: Average Speed Profile Results

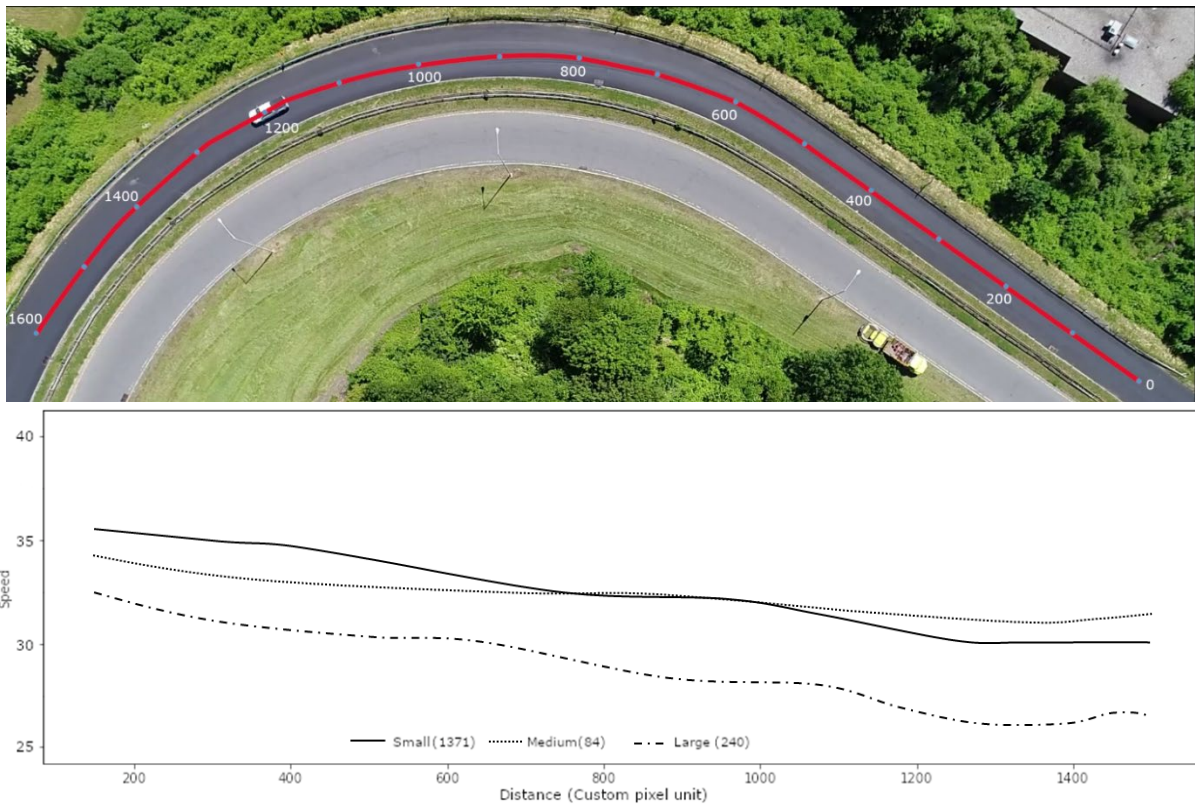


Figure 90. Average speed by category for West Springfield North

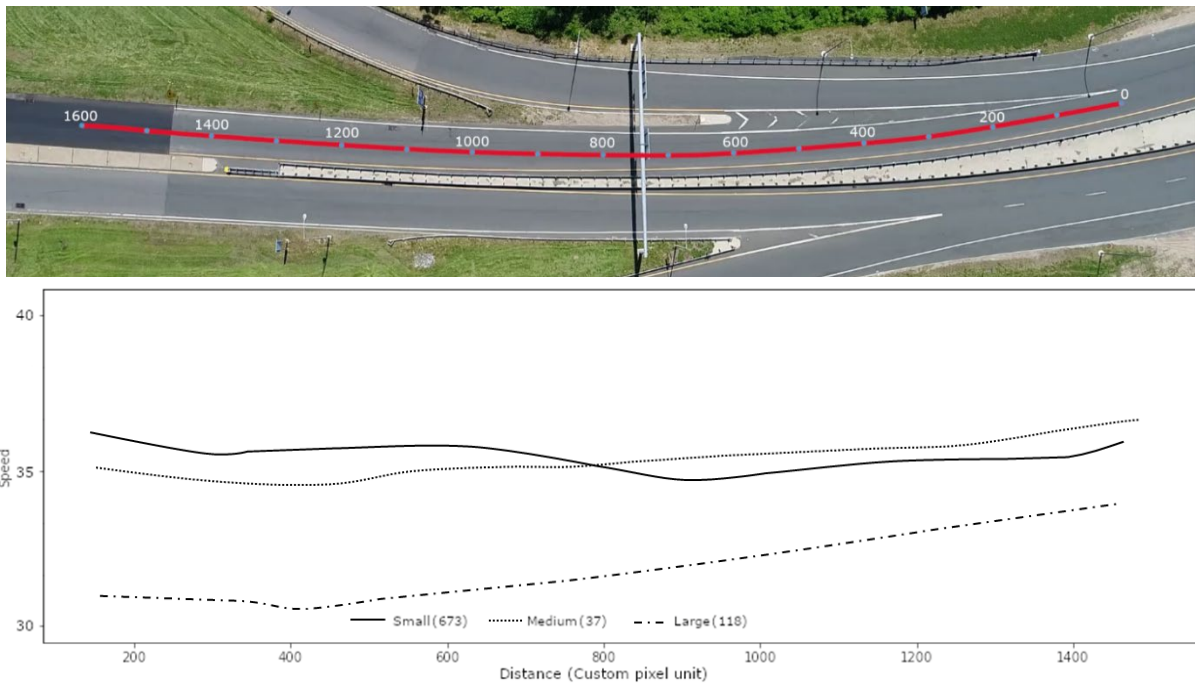


Figure 91. Average speed by category for West Springfield South

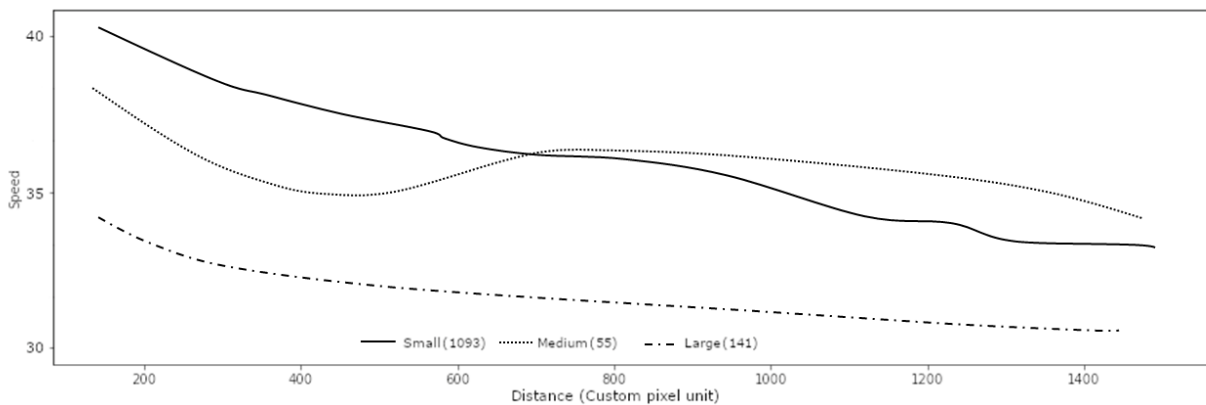


Figure 92. Average speed by category for West Springfield Old toll gate

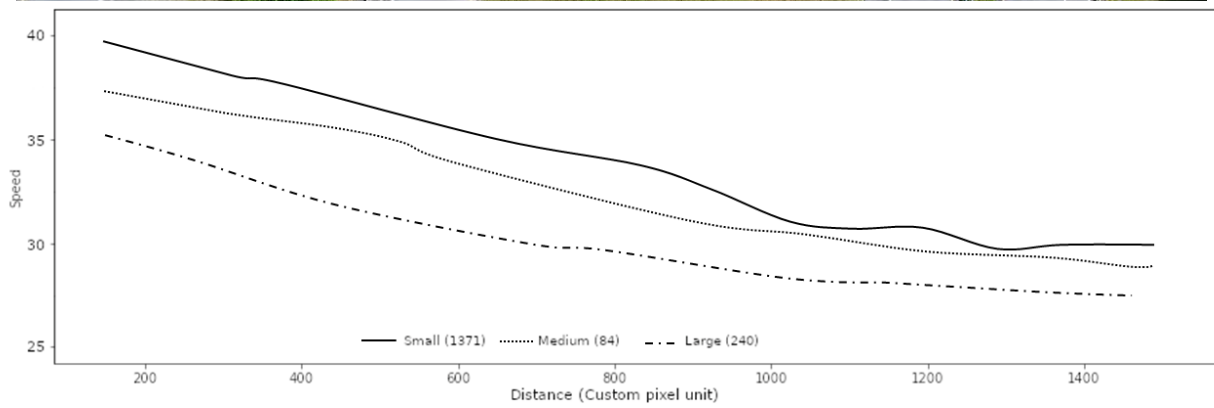


Figure 93. Average speed by category for Freetown North

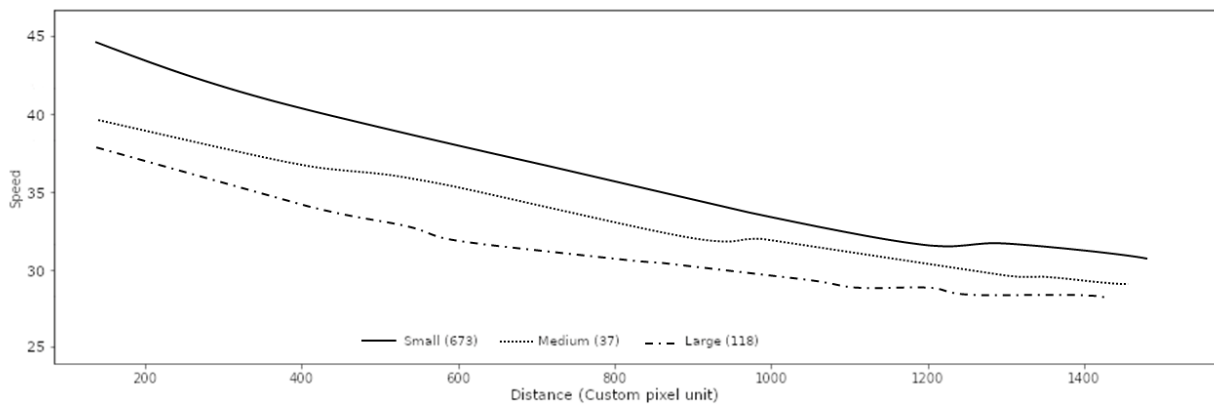


Figure 94. Average speed by category for Freetown South

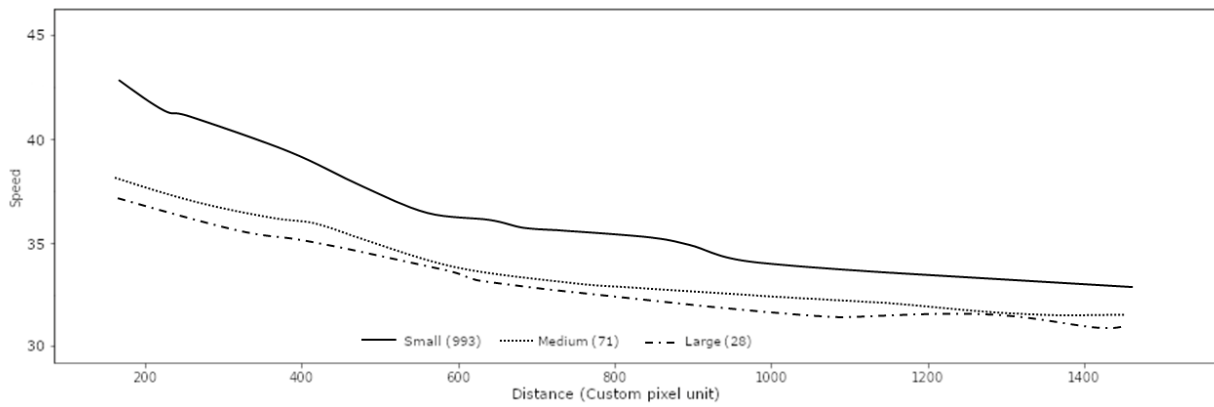


Figure 95. Average speed by category for New Bedford

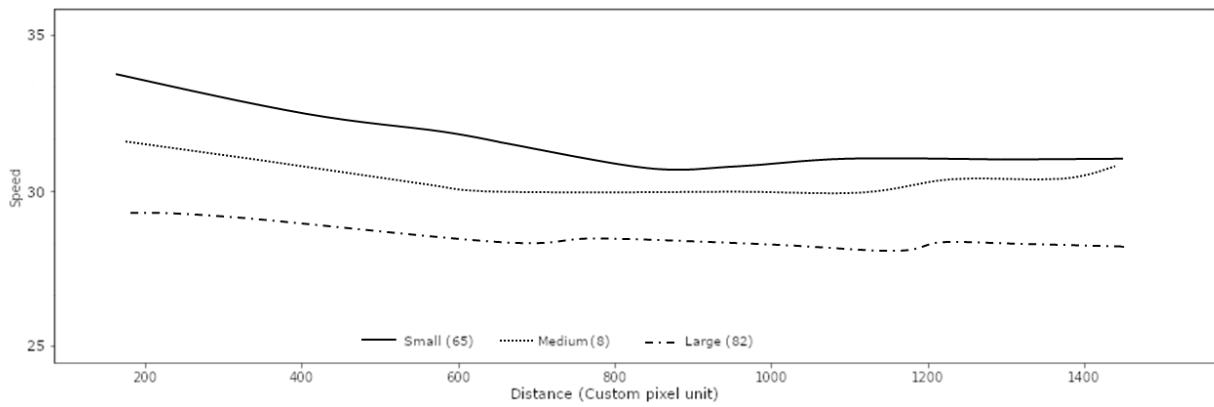


Figure 96. Average speed by category for Sturbridge

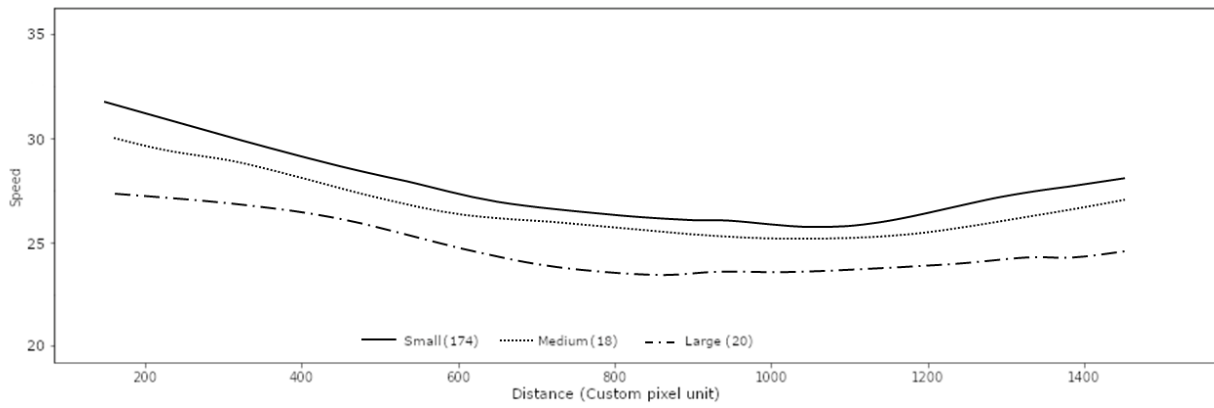
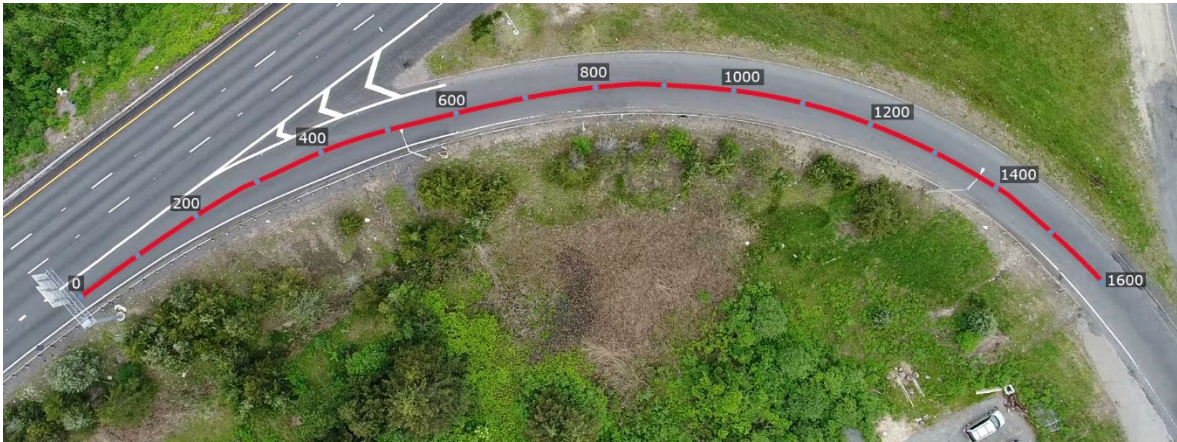


Figure 97. Average speed by category for Andover

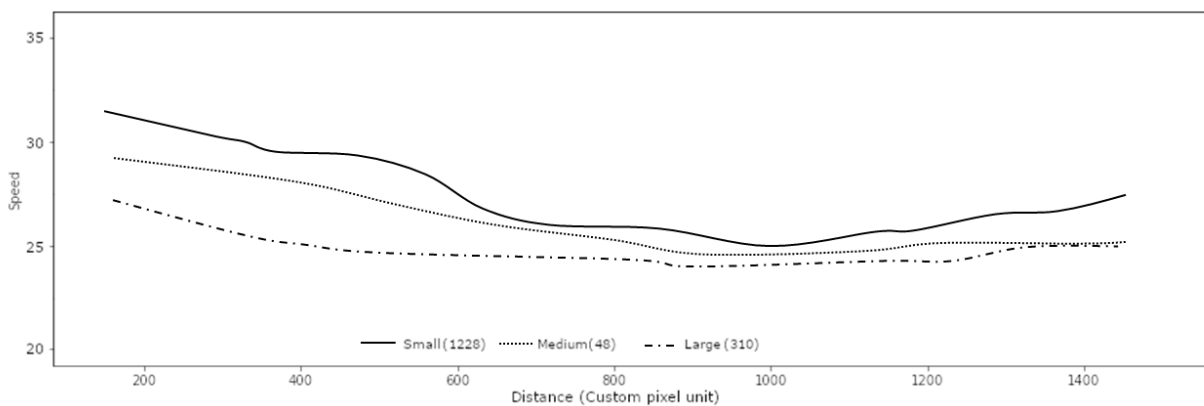


Figure 98. Average speed by category for Auburn